

NASA Contractor Report 3789

# Basic Experimental Study of the Coupling Between Flow Instabilities and Incident Sound

K. K. Ahuja

CONTRACT NAS3-23286  
MARCH 1984

**NASA**

NASA  
CR  
3789  
c.1

TECH LIBRARY KAFB, NM  
0062346

LOAN COPY: RETURN TO  
AFWL TECHNICAL LIBRARY  
KIRTLAND AFB, N.M. 87117



## NASA Contractor Report 3789

# Basic Experimental Study of the Coupling Between Flow Instabilities and Incident Sound

K. K. Ahuja  
*Lockheed-Georgia Company*  
*Marietta, Georgia*

Prepared for  
Lewis Research Center  
under Contract NAS3-23286



National Aeronautics  
and Space Administration

**Scientific and Technical  
Information Office**

1984



## FOREWORD

This report was prepared by Lockheed-Georgia Company, Marietta, Georgia, for NASA-Lewis Research Center, Cleveland, Ohio, under contract NAS3-23286, entitled "Basic Experimental Study of the Coupling Between Flow Instabilities and Incident Disturbances."

Dr. Allen Karchmer was the Project Manager for the NASA-Lewis Research Center. Lockheed's Program manager was Dr. H. K. Tanna.

Particular thanks are due to Mr. W. H. Brown for his help in designing the test facility.

Special thanks are due to Professor C. K. W. Tam of Florida State University for stimulating interest in the problem addressed herein. Frequent discussions with him during the course of this work proved to be extremely helpful.



## SUMMARY

The objective of the study described here is to determine whether or not a solid trailing edge is required to produce efficient coupling between sound and instability waves in a shear layer. The report starts out with a discussion on the differences found in the literature on the theoretical notions about receptivity and a need to resolve them by way of well-planned experiments. Instability waves in the shear layer of a subsonic jet, excited by a point sound source located external to the jet, were first visualized using an ensemble averaging technique. Various means were adopted to shield the sound reaching the nozzle lip. It was found that the low frequency sound couples more efficiently at distances downstream of the nozzle exit. To substantiate the findings further, a supersonic screeching jet was tested such that it passed through a small opening in a baffle placed parallel to the exit plane. The measured feedback or screech frequencies and also the excited flow disturbances were found to change drastically on traversing the baffle axially. As argued in the report, this provided strong indication that a trailing edge is not necessary for efficient coupling between sound and flow.



## TABLE OF CONTENTS

	PAGE
SUMMARY.....	v
1.0 INTRODUCTION.....	1
1.1 CURRENT CONTROVERSY.....	1
1.2 OBJECTIVE.....	3
1.3 BASIS OF THIS STUDY.....	4
1.4 REPORT OUTLINE.....	7
2.0 TEST FACILITIES AND EXPERIMENTAL PROCEDURES .....	11
2.1 AIR SUPPLY AND THE FLOW PLENUM.....	11
2.2 THE TEST NOZZLES.....	11
2.3 ACOUSTIC EXCITATION SOURCE.....	16
2.4 FLOW VISUALIZATION OPTICS.....	16
3.0 RESULTS FOR EXTERNALLY EXCITED JETS.....	21
3.1 FLOW QUALITY CALIBRATION.....	21
3.2 MODE OF OPERATION.....	24
3.3 ROUND JET RESULTS.....	26
3.3.1 Receptivity of a Bare Jet.....	26
3.3.2 Receptivity of a Baffled Jet.....	31
3.4 RECTANGULAR JET RESULTS.....	41
3.5 INSTABILITY-WAVE DATA.....	50
3.6 CONCLUDING REMARKS.....	59
4.0 RESULTS FOR SCREECHING SUPERSONIC JETS.....	61
4.1 PILOT EXPERIMENTS.....	63
4.2 FLOW VISUALIZATION.....	75
4.2.1 Test Configuration.....	75
4.2.2 Parallel Microphone Measurements.....	75
4.2.3 Results.....	80
5.0 CONCLUSIONS .....	93
APPENDIX I - TERMINOLOGY.....	95
REFERENCES.....	96



## 1.0 INTRODUCTION

In recent years, the problem of how external disturbances such as sound and free-stream turbulence excite the instability waves of a flow has become a subject of several investigations. The current interest in the so-called receptivity problem (refs. 1,2) is stimulated by the recent upsurge in research concerned with the development of Laminar Flow Control (LFC) concepts to reduce aircraft drag as well as by some jet-noise related problems that are still not completely understood after over 30 years of extensive research.

Receptivity refers to the means by which a particular forced disturbance enters a shear-flow boundary layer and to the effect it has on the development of this shear flow. The receptivity phenomenon differs from the instability phenomenon per se both physically and mathematically. Physically, it is the signature in the shear layer of some externally imposed disturbance. Mathematically, the problem is no longer one of homogeneous equations with homogeneous boundary conditions, but one where either the equation and/or the boundary conditions are nonhomogeneous (ref. 3). Hence, in contrast to the normal modes stability calculations, the receptivity phenomenon is not an eigenvalue problem. The stability theory alone is, thus, inadequate to solve receptivity problems. In fact, there is ample evidence (ref. 3) to show that under some circumstances, sound field incident upon a boundary layer can provide growing disturbances in a region that is stable according to the stability calculations.

The mechanisms by which instability waves are produced have received little attention because of the formidable theoretical and experimental difficulties. Little progress can be expected in predicting flow behavior until some way is found to deal with instability waves in terms of the disturbances that cause them. Before a detailed investigation is carried out to study receptivity, it is important to resolve the differences found in the literature on the theoretical notions about receptivity. A short description of these differences is given below.

### 1.1 CURRENT CONTROVERSY

The studies of Shapiro (ref. 4), Tam (ref. 5) and Murdock (ref. 6) were devoted primarily to the analysis of the excitation of Tollmien - Schlichting waves in a laminar boundary layer by external sound. This excitation process

is an important first step in the ultimate transition of a laminar boundary layer flow to turbulence. Investigations of the interaction of sound waves with free shear layers were carried out theoretically by Jones and Morgan (ref. 7), Crighton and Leppington (ref. 8), Munt (ref. 9), Tam (ref. 10), Tam and Block (ref. 11), Rienstra (ref. 12), Howe (ref. 13), and Tam (ref. 14). Although the aim, motivations, and techniques of these various, separate investigations were not the same, the question of how the passage of sound wave would excite the intrinsic instability waves of the shear layer was addressed in some way by all these authors. Unfortunately, there is no general agreement among the different theories, and in fact the practical implications of some of these works contradict one another. At the present time, if these contradictions remain unresolved, they would inevitably hinder further progress in our understanding of the receptivity processes.

The works of Munt (ref. 9), Rienstra (ref. 12), and Howe (ref. 13) were all concerned with the transmission of internally generated sound through the nozzle of a jet into the stationary ambient environment. These authors used the model of a cylindrical jet bounded by a vortex sheet. Because of the vortex sheet model, the solution was found to be generally singular at the nozzle exit. To remove the singularity, a form of Kutta condition was imposed at the trailing edge of the nozzle. Although it was not elaborated upon by all the authors, yet, as pointed out by Rienstra (ref. 12), all these analyses effectively made use of the instability wave eigensolution of the problem. In a nutshell, an appropriate amount of the eigensolution was added to the original singular solution so that the resulting total solution became regular at the nozzle trailing edge. Of course, in this case, the solution would grow without bound in the downstream direction, which is an inevitable outcome of the semi-infinite vortex sheet model.

With respect to the receptivity problem, a very important implication of the above-mentioned mathematical model and its solution is that the coupling between the sound wave and the instability wave is effectively localized solely at the trailing edge of the nozzle. There appears to be little interaction between the acoustic wave and the flow instability wave elsewhere.

On the other hand, Tam (refs. 10,14), in a recent investigation of the mechanism of broadband jet noise amplification by upstream acoustic tones, analyzed a similar physical problem, but by using an entirely different model and approach. In this study, the vortex sheet model was discarded, and, instead, the experimentally measured mean jet velocity profiles were used. One immediate consequence of this is that the instability wave will no longer become unbounded in the downstream direction.

In Tam's formulation of the receptivity problem, it was explicitly assumed that there was continuous coupling between the sound wave passing through the mixing layer of the jet and the excited instability wave. Furthermore, it was assumed that the amplitude of the instability wave was zero at the nozzle

exit. The reason for this appears to be that, right at the nozzle exit, the velocity profile is of the boundary layer type so that it will be stable (e.g. see Schlichting (ref. 15)), and would not support an inflexion instability of the Kelvin-Helmholtz type. This is also true behind the leading edge of a cavity (ref. 11). Only at a finite (but possibly small) distance downstream would the flow be able to adjust to the typical free shear-layer profile with an inflexion point near the center of the shear layer. According to Tam's modelling, strong coupling between the sound wave and the instability waves takes place over the distance of a few instability wave-lengths immediately downstream of the nozzle exit. In addition, because of the continuous change of the mean flow in the downstream direction, there is continuous excitation of the instability wave by the sound waves, although this process becomes increasingly ineffective towards the end of the potential core of the jet.

In summary, therefore, the model, approach, and results of the various investigators are very different. The question as to which theory corresponds to the physical reality can only be answered by delicate experiments.

The most important difference between the continuous interaction theory and the trailing edge interaction theory, as far as the excitation of the instability wave is concerned, is whether or not sound waves passing through the mixing layer of a jet can excite flow instability waves without the benefit of the assistance and coupling at the solid trailing edge. If it is conclusively shown that such a process is possible and is an effective means of exciting jet instability waves, then it would provide a strong experimental basis for the realistic model.

Clearly, a systematic research program - consisting of flow visualization experiments and instability wave measurements - is required to resolve the existing controversy about the coupling between instability waves and incident sound field.

## 1.2 OBJECTIVE

The major objective of this program is to increase our understanding of the coupling between incident sound and the associated flow instabilities. The specific objective is to conduct a basic and well-controlled experimental study to determine whether or not a solid trailing edge is required to produce efficient coupling between sound and instability waves.

### 1.3 BASIS OF THIS STUDY

At the time this study was initiated in 1982, some preliminary results had become available (ref. 16) that shed new light on this controversy. Using a unique laser schlieren system developed recently at Lockheed (refs. 17 and 18) and a process of photographic averaging, qualitative evidence was obtained that supported the contention that instability waves may be excited without the aid of coupling at a solid trailing edge. It is probably in order to present those preliminary results here.

In the preliminary experiments, an unheated jet was exhausted from a conical nozzle of 1.27-cm diameter. The area ratio between the plenum and the nozzle was 400 which provided a reasonably clean flow through the nozzle with insignificant velocities through the plenum chamber. All initial tests were obtained at a jet velocity  $U = 21$  m/sec.

A point sound source was used to excite the jet. The point source consisted of a commercially available 60-watt acoustic-driver unit coupled to a straight tube via an inverse conical horn section. The other end of the tube contained a smooth right-angle bend that terminated into a 0.64 cm diameter opening. The point sound source and the jet nozzle are shown in figure 1.1. The signals fed to the acoustic drivers were generated by an oscillator at fixed discrete-tone excitation frequencies,  $f$ . The point source was placed at various downstream distances ( $x$ ) from the nozzle exit plane such that the parameter  $fx/U = 0.4$ .

Helium was added to the flow to aid in the visibility of the air flow. A heated nichrome wire, stretched along one of the diameters of the nozzle exit (see figure 1.1), was used to help improve the visibility along a whole diametral plane. The optical setup was basically the same as that used by Whiffen and Ahuja (ref. 17). A continuous-wave laser was used as the light source. A Bragg cell was used as an electronic shutter, allowing the laser light through the system only over a specified length of time, then reflecting it off at an angle. The frequency of strobing the light was the same as that of the electronic signal. This was achieved by exciting the Bragg-cell by the same electronic signal that was used to excite the acoustic driver.

A typical schlieren photograph of an unexcited jet is shown in figure 1.2. The same jet when excited by the point sound source, with the source located at the exit plane and 0.125 cm above the lip line, is shown in figure 1.3. Here the jet was excited by sound at an excitation frequency of 500 Hz, and a given photographic plate was exposed synchronously 20 times. Clearly, a large-scale turbulence structure, also referred to here as an instability wave, has been excited within the jet. This instability wave appears to initiate near the nozzle lip, where the sound intensity is the maximum. It

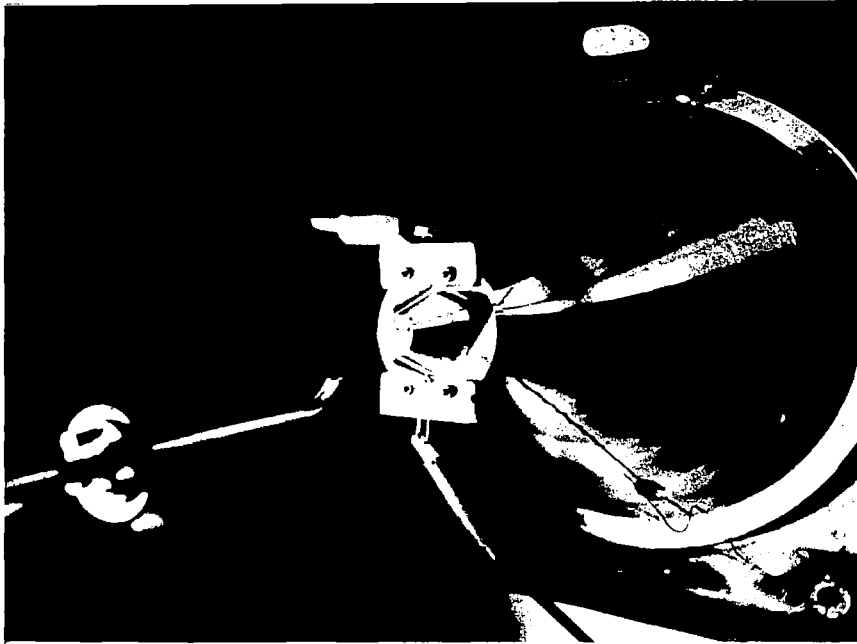


Figure 1.1 The point sound source and the test nozzle.



Figure 1.2 Schlieren photograph of an unexcited jet,  $U = 21$  m/s.

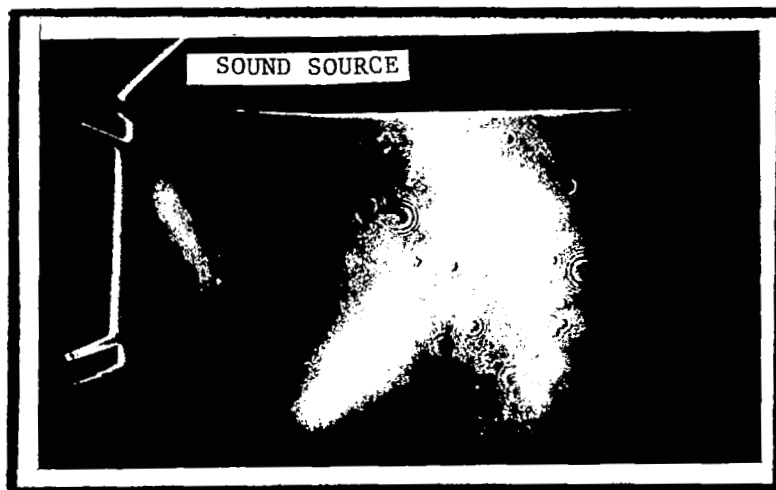


Figure 1.3 Schlieren photograph of an excited jet with the sound source located close to the nozzle lip. Excitation frequency = 500 Hz,  $U = 21$  m/s

was also found that this instability wave was predominantly in the mixing layer of the jet, and did not cross the center of the jet. This conclusion, although based upon limited observations, was reached by comparing the schlieren photographs of the excited jet once by making the flow visible with the heated wire, and another time by making the flow visible by seeding the flow with helium. Schlieren photographs with heated wire did not appear to show a dominant large-scale structure, but such structures were seen quite clearly with helium seeding. The photograph shown in figure 1.3 was obtained by seeding the jet with helium.

When the source of sound was moved away from the nozzle exit, however, the instability waves appeared to initiate some distance away from the nozzle lip from those flow regions near the sound source which were subjected to higher levels of sound. This is shown in figures 1.4(a), (b), (c), and (d). Here, the source was located only 1.5 jet diameters downstream of the jet exit, and the excitation frequency was 428 Hz. Each successive photograph represents a different time location of the large-scale structure, and was taken by shifting the timing of the light pulse relative to the phase of the acoustic excitation by 90 degrees. The four photographs shown here represent a complete 360 degrees of phase change, and thus provide a qualitative estimate of the extent of the region of the jet in which the excited instability wave is observed. In this case, the instability wave appears to initiate only beyond one diameter downstream (see figure 1.4(a)).

These and many other schlieren photographs, taken for other axial locations of the sound source, indicated that, at least qualitatively, the instability waves may not necessarily initiate at the nozzle lip. In fact, by assuming that there is a continuous coupling between the incident sound and the flow instabilities, a theoretical model has recently been developed at Lockheed by Tam and Morris (ref. 18) to predict the behavior of jet flows in response to a discrete tone excitation; the predictions provide excellent agreement with the measured data.

The preliminary optical data of 1982 described above were by no means conclusive about the ability of a flow instability to initiate in the absence of a solid edge, but they tended to point toward a need for further work to understand the receptivity phenomenon. It was to obtain further insight into this phenomenon and to substantiate the preliminary results that formed the basis of the study described in this report.

#### 1.4 REPORT OUTLINE

The report starts out, in section 2.0, with a description of the facilities and the experimental procedures. The next two sections describe the

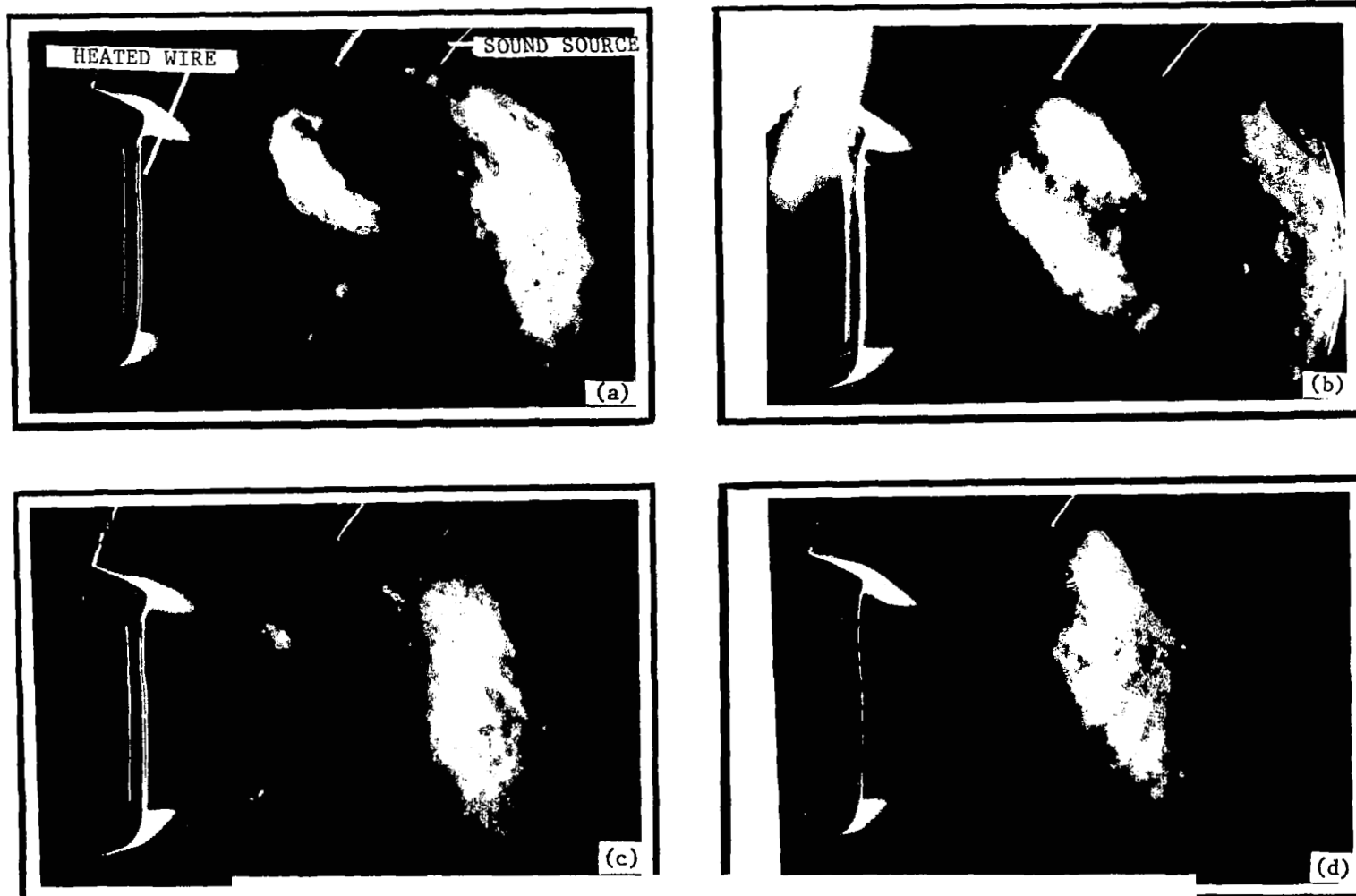


Figure 1.4 Schlieren photographs of an excited jet with the sound source located downstream of the nozzle lip. Each successive photograph (a)-(d) was taken by shifting the timing of the light pulse relative to the phase of the acoustic excitation by  $90^\circ$ . Excitation frequency = 428 Hz,  $U = 21$  m/s.



experimental results. The results described in section 3.0 are those for subsonic jets excited by an external sound source. As it will become clearer, the subsonic jet results made it extremely difficult to categorically conclude if regions downstream of the nozzle exit are locally receptive to the incident sound. New experiments were, therefore, conducted in which supersonic jets were used such that the screech produced by them could be used as the source of sound. The rationale behind using the supersonic jets and the results obtained from these experiments are presented in section 4.0. This is followed by a summary of important conclusions from this study in section 5.0.



## 2.0 TEST FACILITIES AND EXPERIMENTAL PROCEDURES

Most of the measurements described in this report were made in the optics laboratory located in the Lockheed Research Building. Limited measurements with the supersonic jet were made in a larger flow facility (described separately later).

### 2.1 AIR SUPPLY AND THE FLOW PLENUM

The 689000 Newton/Square meter (100 psia) shop air was used for the tests in the optics laboratory. The shop air was supplied to the jet plenum by a 5.08-cm (2.0-in) diameter pipe as shown schematically in figure 2.1. The air into the plenum enters and exits through 20.32-cm (8.0-in) diameter sections. The intermediate section has a diameter of 45.72 cm (18 in). This plenum chamber, shown photographically in figure 2.2, was manufactured by Industrial Acoustics Company, and was originally intended to be used as an acoustic muffler. In the present arrangement, it served both as an acoustic absorber (of noise emanating from upstream) as well as a large area contractor. To make the flow smoother one step further, honeycomb and screen sections were installed in the 20.32-cm diameter section at the downstream end.

### 2.2 THE TEST NOZZLES

The majority of the tests were conducted using a 2.80-cm (1.1-in) diameter, contoured convergent nozzle shown mounted on the plenum chamber in figure 2.2. A cross-sectional view of this nozzle is shown in figure 2.3. The contraction ratio with this nozzle was 53.

For limited tests, a plane jet nozzle was also used. This nozzle (see figure 2.4) had a slot width of 12.3 mm (0.48 in) and an aspect ratio of 8.25 : 1. The contraction ratio for this nozzle was 10.3.

Finally, majority of the supersonic jet experiments were conducted using a 1.27-cm (0.5-in) diameter conical nozzle, which provided a contraction ratio of 256.

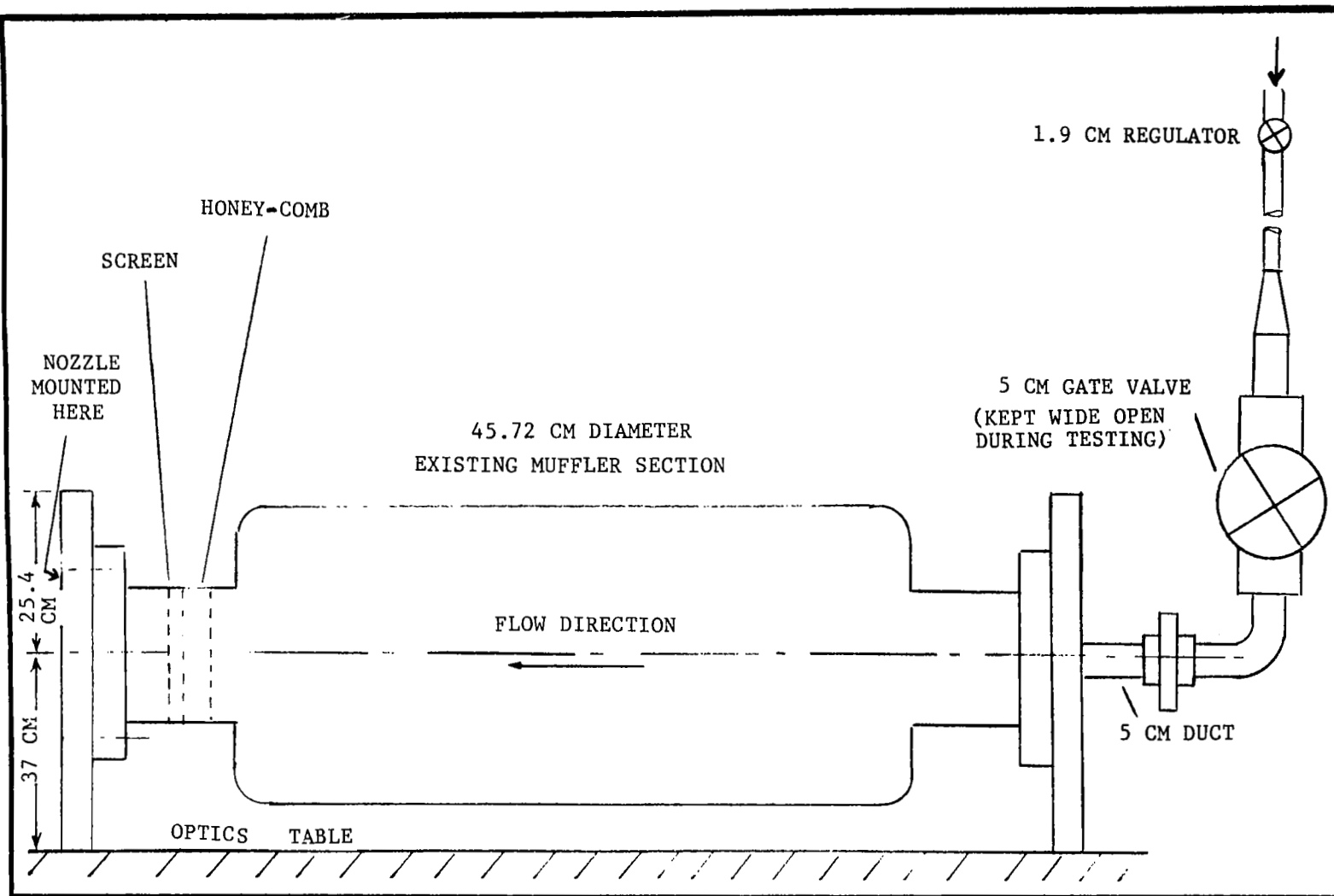


Figure 2.1 Schematic of the jet plenum and the air-supply ducts.

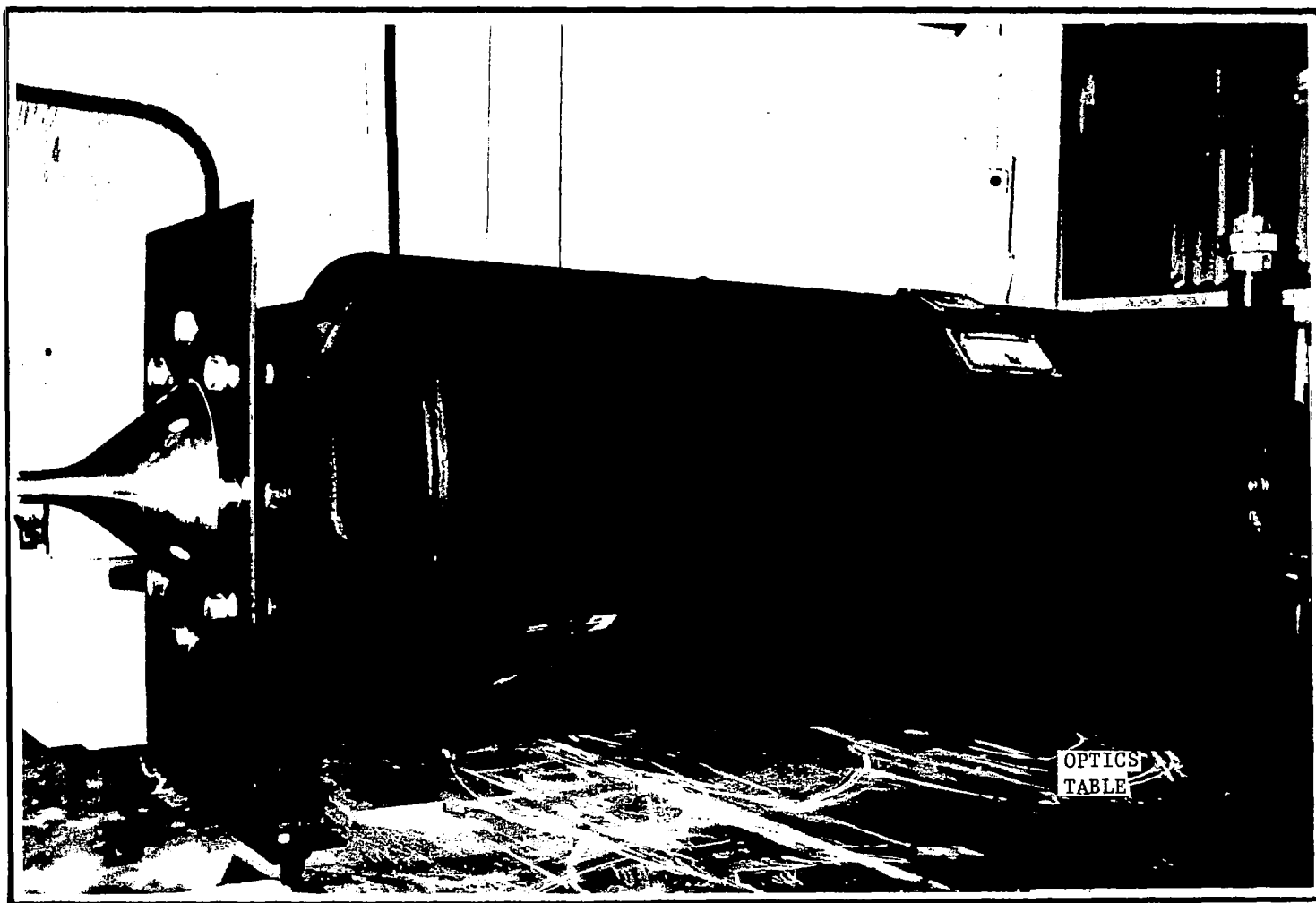


Figure 2.2 The plenum, the 2.8-cm diameter nozzle, and the optics table.

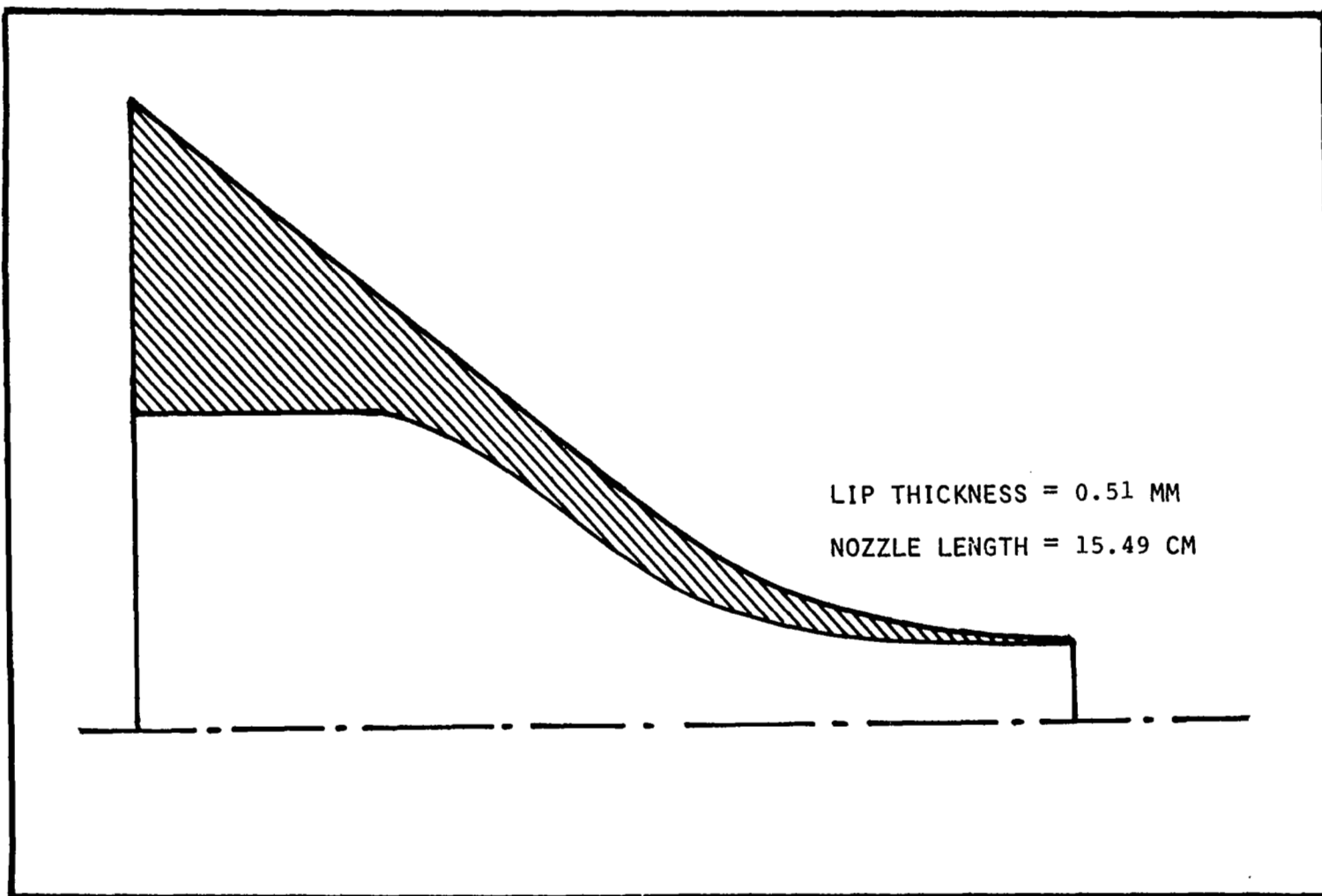


Figure 2.3 Cross-sectional view of the contoured 2.8-cm nozzle.



Figure 2.4 The rectangular nozzle.

The rationale behind using a given nozzle for a given test is given in the subsequent text at the appropriate places.

### 2.3 ACOUSTIC EXCITATION SOURCE

When this program was begun, an acoustic source was designed and assembled to simulate a point-dipole source for use in the planned experiments. It consisted of two identical point monopole sources that can be operated out-of-phase. One end of these point sources consisted of a commercially available 100-watt acoustic driver unit coupled to a straight tube via an inverse conical horn section. The other end contained a right angled-bend terminating into a 0.635-cm diameter opening, as shown schematically in figure 2.5.

Unfortunately, after the initial use of this unit, it was found that the dipole unit was much more cumbersome to use, and that the levels generated by this unit were not high enough to serve the need of the present program. Only a single point monopole source unit was, therefore, used for the majority of the tests, involving external acoustic excitation of jets.

The above unit was used only for the round jets. For the plane jet, on the other hand, a two-dimensional horn was used. This horn unit had an opening of 3.2 mm by 63.5 mm and was connected to the exit of the point monopole source described above (figure 2.5) through a flexible plastic tubing.

The acoustic drivers connected to these sound sources were driven by a commercially available sine wave generator and a power amplifier.

### 2.4 FLOW VISUALIZATION OPTICS

Most shadowgraphs and schlieren photographs, particularly those for axisymmetric flows, display a certain degree of confused detail resulting from small-scale turbulence in the jet, and from thermal convection in the ambient air. A method of removing these sometimes unwanted details, and thereby highlighting essential characteristics, is the application of a photographic averaging technique [for example see Moore (ref. 19) and Whiffen and Ahuja (Ref. 17)]. This is an effective method for revealing large-scale structure in a jet. The method involves repeated triggering of a light source and



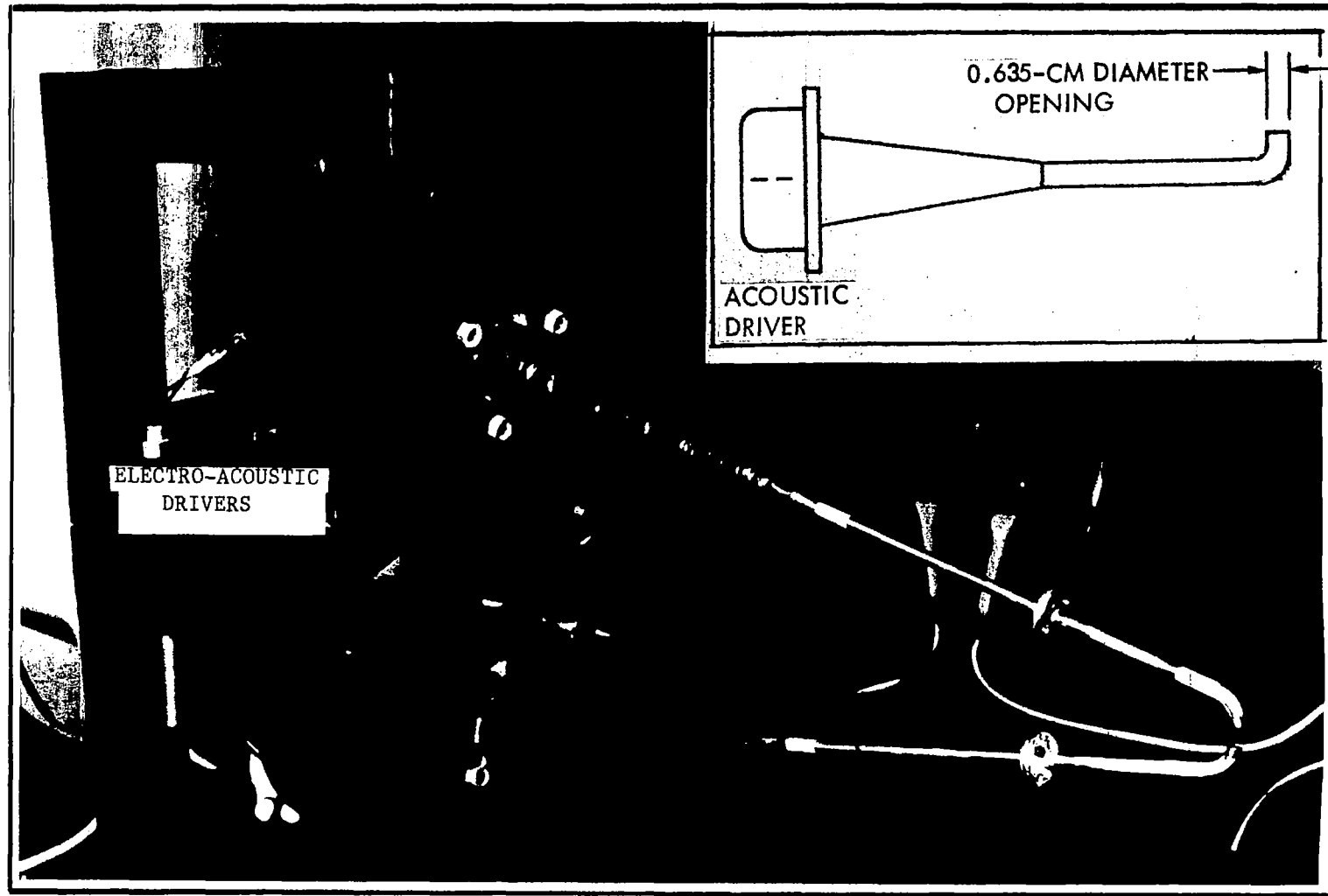


Figure 2.5 The dipole point sound source.

superposition of all the schlieren images on a single photographic film. By this means, the images of the coherent structure associated with the trigger signal are reinforced, and those from the random turbulence tend to cancel.

The above method was used in the present experiments, but a new and a very simple method of synchronizing the source of light was used (ref. 17). The laser beam passing through a Bragg cell was the source of light. The Bragg-cell shutter was synchronized with the excitation signal itself, thus the strobe frequency was the same frequency as that of the acoustic signal used to excite the jet.

A block diagram of the optical facility is shown in figure 2.6. Part of the optical components used can be seen photographically in figure 2.4. It features a Bragg cell that pulses the light beam from a Continuous Wave Argon laser. The combination of the spatial filter and the first lens forms a collimated beam through the jet flow. The second lens focuses the collimated light at the knife edge, and images the flow area on the film plane, as in the conventional schlieren arrangement. Since the laser-light source is coherent, a graduated knife edge consisting of a reflection coating on glass, is used to avoid image degradation by diffraction. It was found subsequently that the edge of a front coated prism (figure 2.7) worked even better, and was used for the bulk of the experiments. An on-axis type camera shutter is placed at the film plane to obtain the final schlieren photographs.

In operation, the Bragg cell acts as a shutter blocking the laser beam. In this application, when the cell is excited by a known frequency signal, the light beam is deflected, and thus aligned with the schlieren optics. A pulsed shutter is obtained by using a diode switch to interrupt the excitation except when activated by the pulse generator.

The Bragg cell could be operated either in the multi-pulse mode or in the single-pulse mode. In the multiple-pulse mode, the Bragg cell is continually pulsed by the acoustic signal, and the camera shutter is adjusted to average the light from several pulses to illuminate the large-scale structure. In the single-pulse mode, the camera shutter is used to limit exposure to background light (some residual light comes through the selecting aperture), and the shutter strobe opens a latch that allows the next audio trigger to pulse the Bragg cell.

The power level of the laser-light source was adjustable up to several watts, and this provided excellent film exposure control.

For the low velocity jets, the air density variations were too small to be recorded. Therefore, helium was used to produce the refraction changes necessary to make the flow visible.

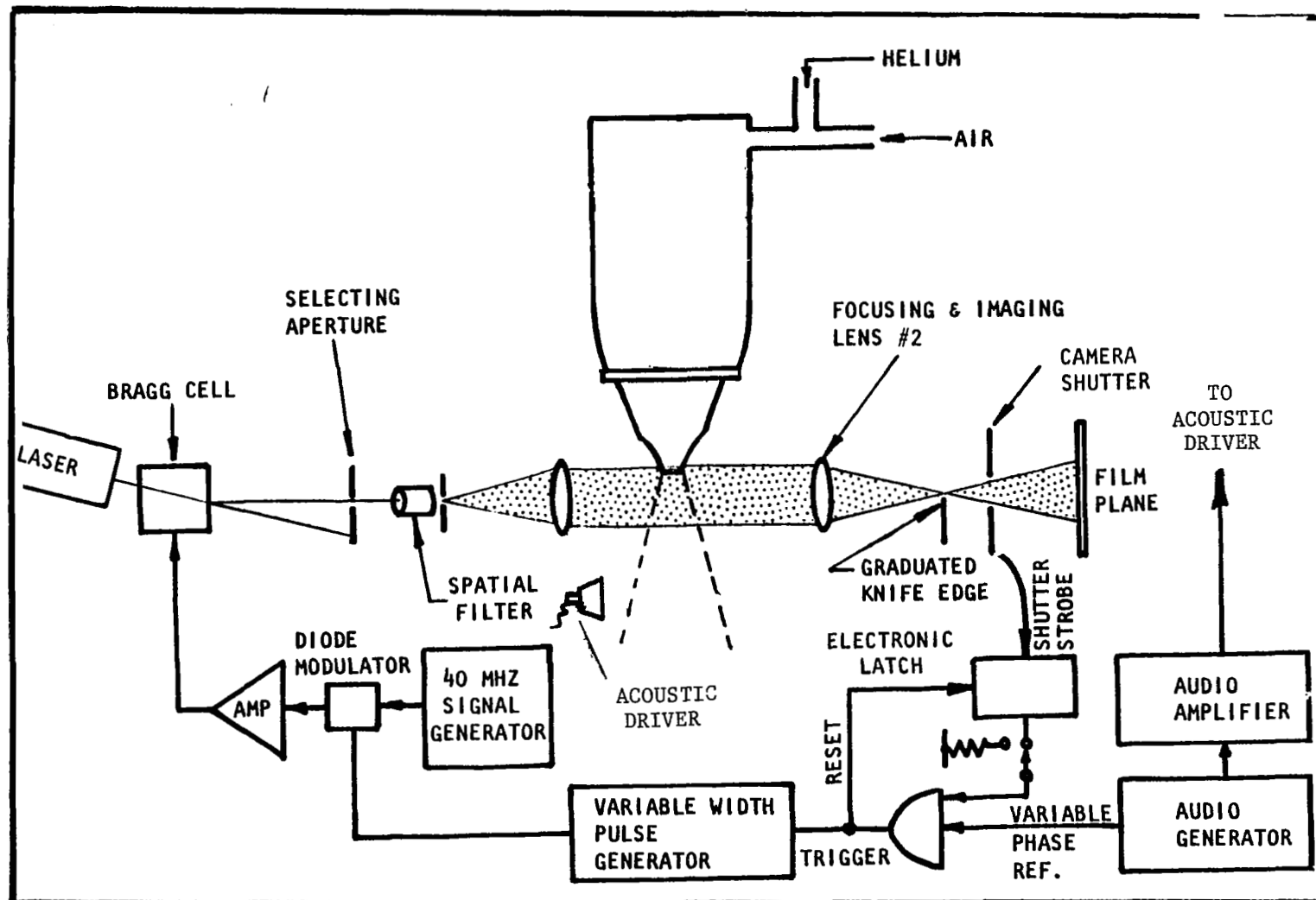


Figure 2.6 Schematic of the flow-visualization set up and the associated electronics.

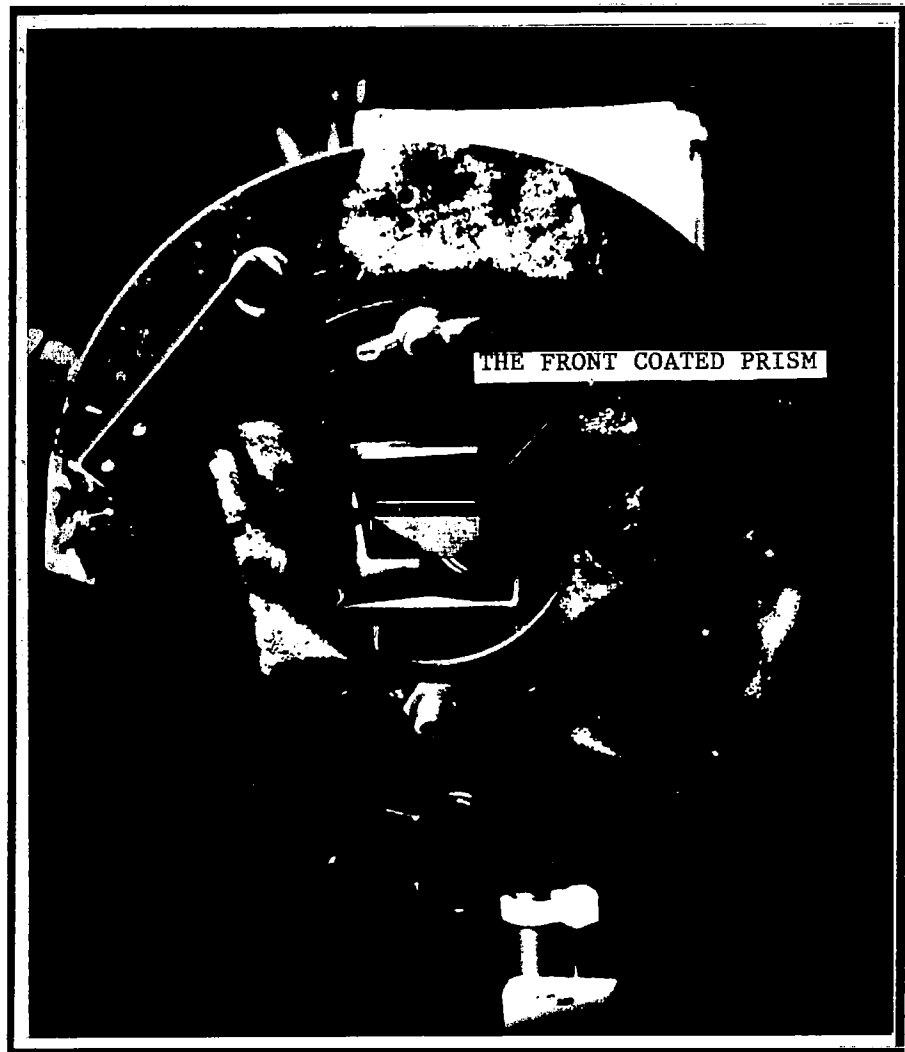


Figure 2.7 The prism knife edge.  
(view from the camera.)

### 3.0 RESULTS FOR EXTERNALLY EXCITED JETS

In this section are described the results pertaining to the coupling between shear-layer instability and the sound generated by a point sound source located external to the jet nozzle. Most of the results consist of flow visualization of the jet as obtained by the photographic or phase averaging method as described in the previous section. Where possible, whenever the photographs of the excited jets are presented, corresponding photographs, or a typical photograph, of the unexcited jets are also provided for comparison.

Results for the round convergent nozzle are presented first. Effects of placing different types of barriers between the lip of this nozzle and the source of sound on the flow-sound receptivity are then described. These barriers were used to decrease the sound levels reaching the nozzle exit. Their description is given later together with the results.

Results for the rectangular nozzle are described in section 3.4. Finally, the instability-wave data acquired for both the round as well as the plane jet are presented in subsection 3.5.

#### 3.1 FLOW QUALITY CALIBRATION

Before describing the main results, it is worth pointing out that prior to obtaining them, the jet facility was thoroughly checked out for its aerodynamic quality. The velocity profile at the 2.8-cm diameter nozzle exit was found to be almost square at all flow velocities of interest as shown in figure 3.1, thus indicating a thin boundary layer. The velocity decay along the axis (see figure 3.2) also was consistent with similar data on larger nozzles from our other facilities and those available in the open literature.

The optics room, where most of the experiments were conducted, was also calibrated for its reflection characteristics. With the sound source turned on, the noise levels at the nozzle exit were measured by placing 5.08 cm (2.0-in) thick polyurethane foam on various room surfaces that were thought to be possible dominant reflectors of sound. Reductions of 2 to 3 decibels were achieved by placing the foam on the two walls closest to the nozzle exit and also on most surfaces in the immediate vicinity of the nozzle exit. This arrangement was used for the majority of the experiments.

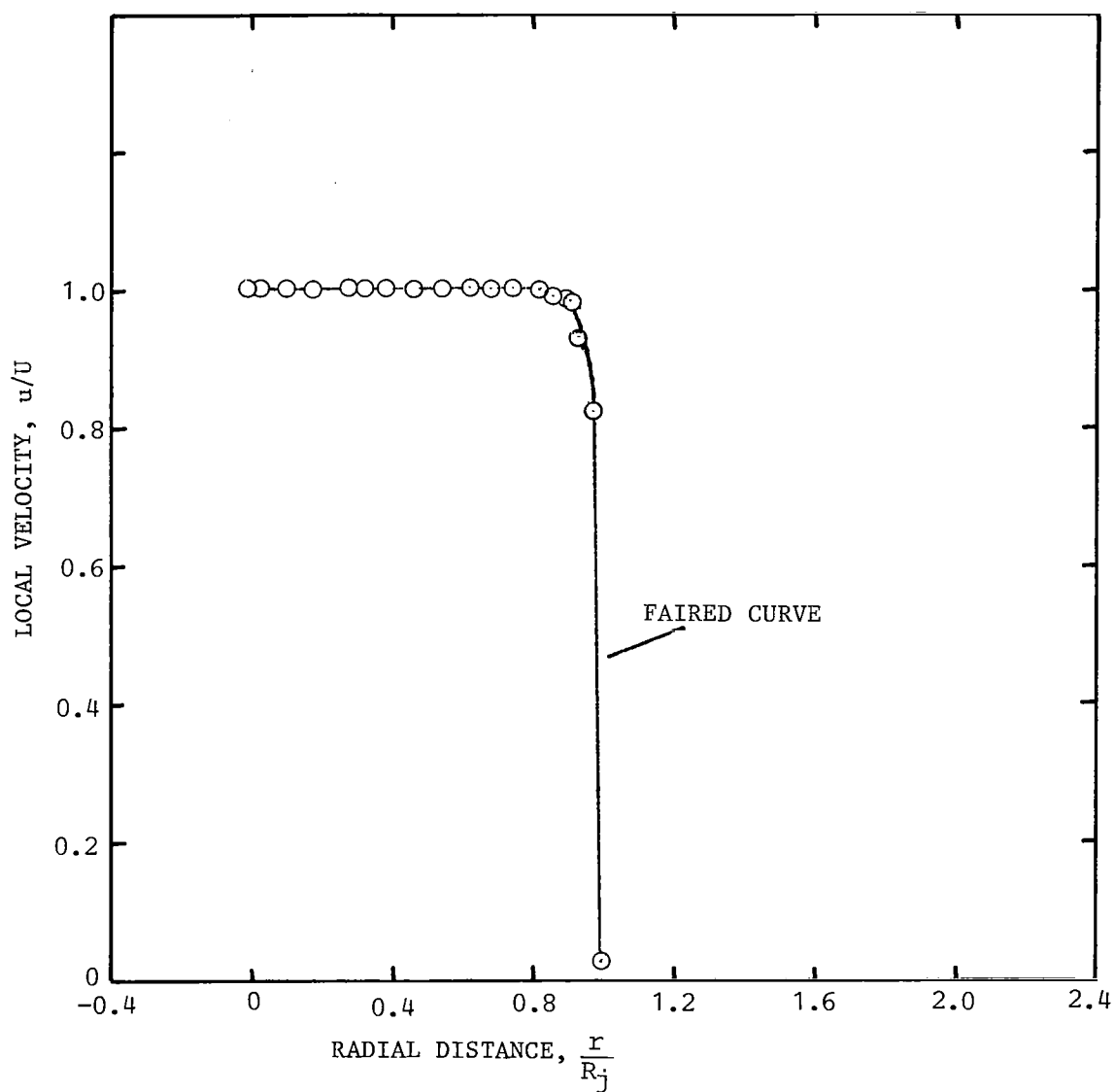


Figure 3.1 Mean velocity profile at the exit plane for the round convergent nozzle.  
( $U = 80$  m/s)

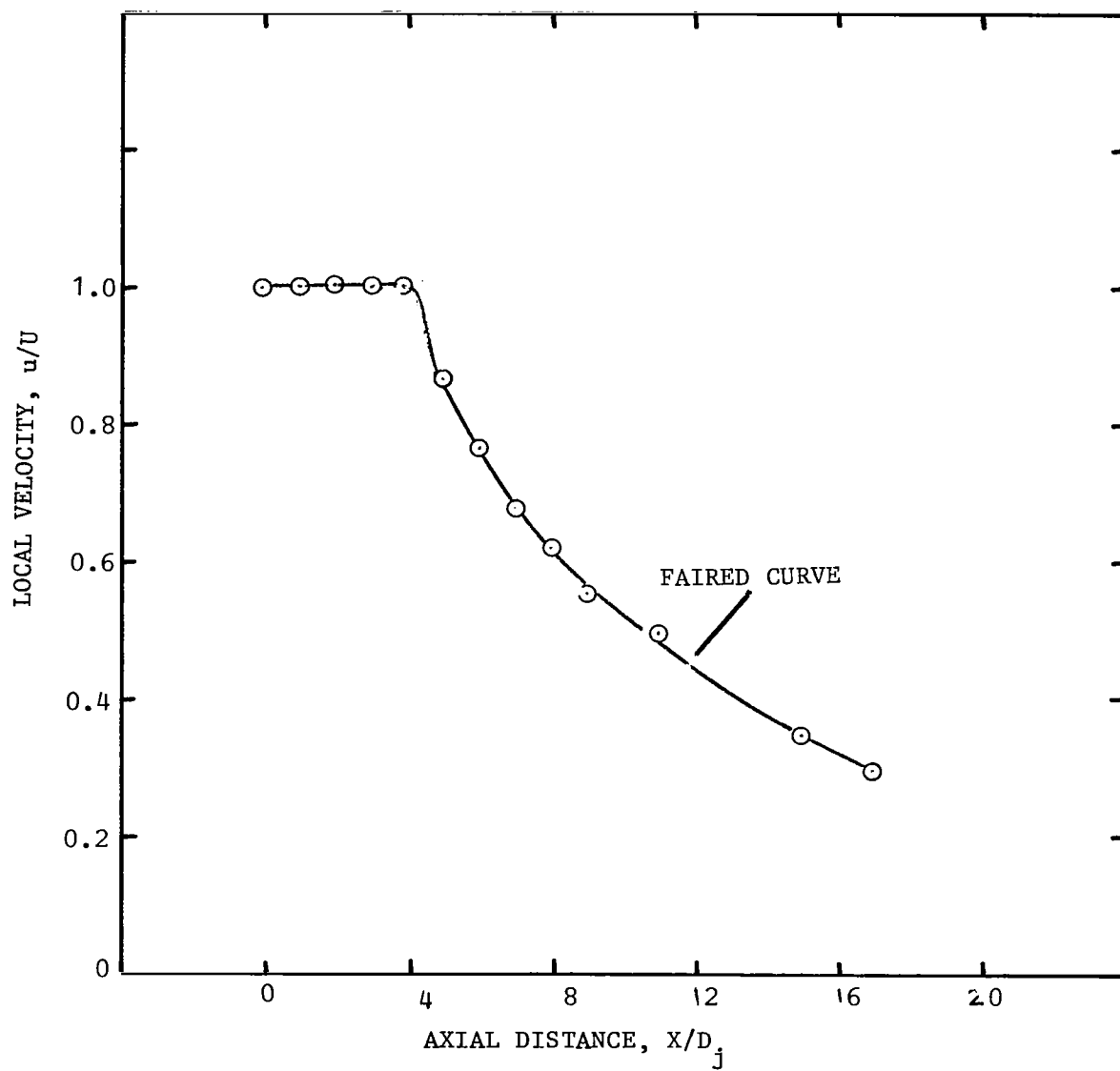


Figure 3.2 Centerline mean velocity distribution for the round convergent nozzle.  
( $U = 80$  m/s)

### 3.2 MODE OF OPERATION

#### Dipole Source Replaced by a Point Monopole Source

As pointed out in subsection 2.3, initial tests were done with the dipole source shown in figure 2.5. It was, however, found that it was not the most suitable source for the bulk of this program. This source was found to be effective only at high frequencies, while at low frequencies, it suffered from two critical problems: (1) it did not generate high enough levels and, (2) it was difficult to simulate dipole noise source directivity. Based upon limited understanding of the coupling between flow and sound source (ref.10), it was expected that if local coupling downstream of the nozzle takes place, it will most likely take place at lower frequencies. With the dipole source, it would have been possible to investigate the effects of sound only at high frequencies, but not at low frequencies. Flow visualization results depicting this are shown in figure 3.3 for a frequency of 1127 Hz (fig. 3.3b) and also 500 Hz (fig. 3.3c). For comparison a photograph of the unexcited jet is also presented (fig. 3.3a).

An additional problem associated with the dipole setup was the inability in positioning the point opening of the source close to the shear layer of the jet, because of the physical mounting of the sound carrying tubes. Keeping these problems in mind, the bulk of the initial tests were conducted with sound radiated through only one opening as shown in figure 3.3 (d). Through this arrangement, it was possible to bring the source opening closer to the jet shear layer and also to generate high enough levels at all frequencies of interest.

#### Both Excited and Unexcited jets Visualized in the Phase Averaging Mode

It should be noticed that all four photographs shown in figure 3.3 are phase averaged, and were obtained by strobing the light at a frequency equal to that of the acoustic excitation frequency and by exposing the photographic film repeatedly. This procedure was adopted for both the excited and the unexcited jets, except that for the unexcited conditions, the strobe frequency was adjusted to that equal to the frequency used for excitation. It was necessitated by the fact that this was the only way to maintain similar lighting conditions for both the excited and the unexcited jets, if a proper comparison was to be obtained for the two cases. It is for this reason that the photographs of the same unexcited jet taken at different frequencies and presented in various parts of the report may not always appear to be identical.



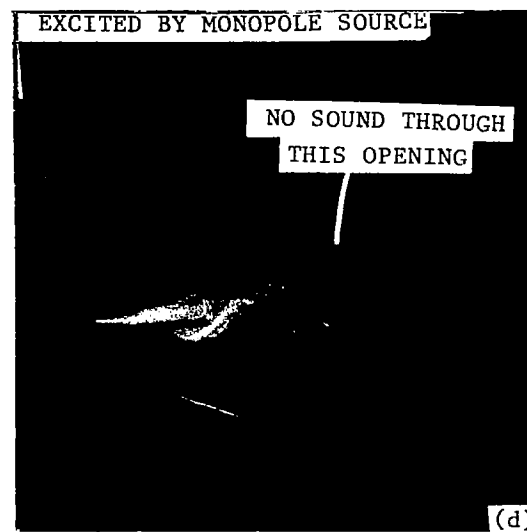
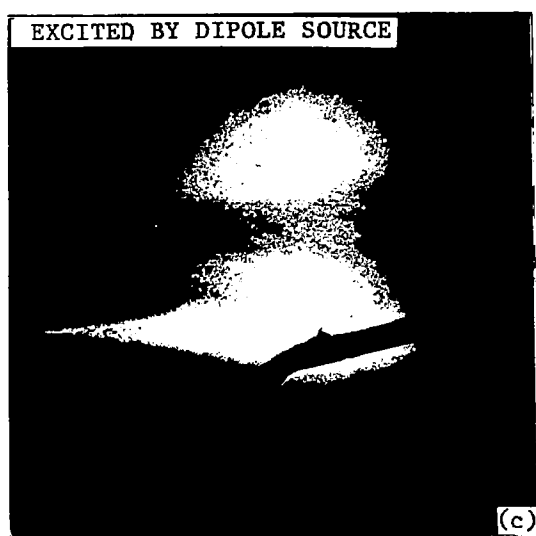
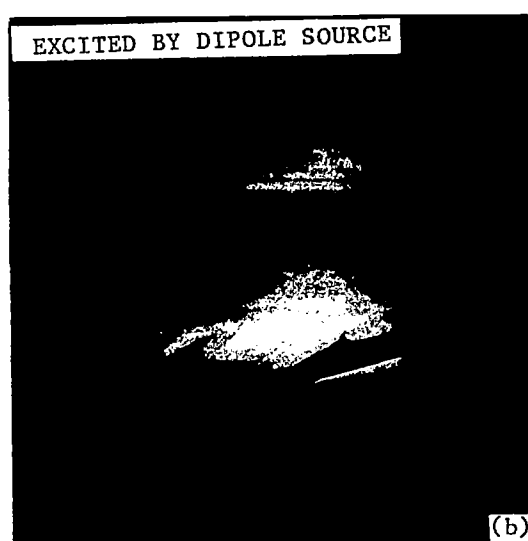
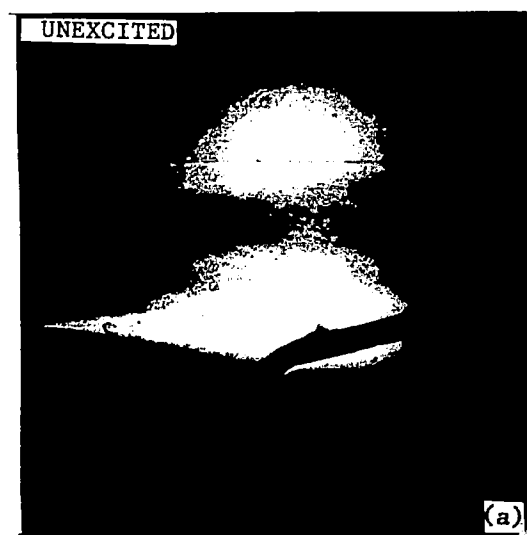


Figure 3.3 Effectiveness of the dipole versus the monopole sound source with the acoustic drivers operated at their peak voltages:  
 (a) unexcited, (b) excited,  $f_e = 1127$  Hz, (dipole), (c) excited,  $f_e = 500$  Hz (dipole), and (d) excited,  $f_e = 500$  Hz (monopole).

### Flow-Visualization Data Presented at Various Strobe Phases

In order to trace the initiation point of an instability in the flow, it was necessary to obtain flow visualization photographs at various phase delays between the sound and the strobe frequency. This enabled us to freeze the large-scale structure or the instability waves at various spatial locations. Invariably, the data presented are only for equally spaced phase delays, e.g., 0, 90, 180, and 270 degrees. But where considered necessary, a narrower interval of phase delay has been used to highlight the point being made. It should be noted that these phase values are arbitrary, and merely represent that a change of 180 degrees in phase implies that the large-scale structure has moved by half its wave length in space. In many parts of this report, the flow visualization data are presented starting with the photograph taken at that phase which shows a given peak of the instability farthest from the nozzle exit. In the subsequent photographs of the same jet, the phase of the strobe has been varied such that the instability peak moves upstream towards the nozzle so that its starting point can be traced back.

The avid reader is, therefore, warned that if he finds the quantity of photographs rather overwhelming, he should focus his attention primarily on the location of the large-scale structure with respect to the nozzle exit as he progresses from photographs of one strobe-phase to another.

A side note : with a few exceptions, in each group of photographs, the last photograph is that of the unexcited jet obtained at the same lighting and strobe frequency conditions as those used for the excited jet.

### "Instability Waves" and "Large-Scale Structures" Used Interchangeably

To avoid confusion, it is appropriate to state at this time that throughout the text of this report the terms "instability waves" and "large-scale structures" will be used interchangeably to refer to the same physical entities.

## 3.3 ROUND JET RESULTS

### 3.3.1 Receptivity of a Bare Jet

### Real Time Data Used to Optimize Excitation Frequencies and Levels

Before acquiring still photographs of the jet flow under the influence of external acoustic excitation, real time flow visualization was examined in great detail to determine the range of excitation frequencies and levels for which the jet was visually receptive to the external sound. Frequencies in the range of 200 Hz to 8 KHz were used, whereas the the acoustic driver was operated from its threshold level of noise production to its upper limit. Without exception, it was found that, for a given frequency, the higher the excitation level, the better defined was the excited large-scale structure in the jet. For this reason, the majority of the photographs presented here were taken with the driver operated at its maximum response condition. These levels were different for different frequencies and were measured by a microphone both directly under the source opening and also at the nozzle exit.

#### Low Frequency Sound Appears to Couple Further Downstream than the High Frequency Sound

In so far as the effect of changing the frequencies is concerned, it was found that for a given source location, low frequency tended to excite large-scale structure farther from the nozzle exit than did the high frequency. Typical results alluding to this effect are shown in figure 3.4 for a low frequency of 428 Hz and in in figure 3.5 for a high frequency of 2410 Hz. In each figure, the last photograph is that for the unexcited jet, and photographs (a) thru (e) in figure 3.4 and (a) thru (d) in figure 3.5 are for the excited jet. The successive photographs for the excited condition in each figure were taken with the strobing phase delayed by an amount so as to cover a complete period of the excited large-scale structure.

The successive locations of the excited large-scale structure for the complete period are denoted by a '+' sign in each figure. As one examines successive photographs, the instability wave appears to move towards the nozzle. It is difficult to conclude categorically from these photographs whether the instability is actually initiating right at the exit or close to the acoustic source itself. It is clear, however, that high frequency excitation is more effective near the nozzle exit than is the low frequency excitation.

#### Receptivity May Be Source Location Dependent

The sound source in figure 3.4 was located about 1.0 cm downstream of the nozzle exit. It was found that if the source is moved further downstream, and the jet is excited by low frequency sound, the excited large-scale structure is different in nature compared to that excited by the source located closer to the nozzle exit. This is shown in figure 3.6 for the same conditions as those of figure 3.4, but this time the source is moved downstream to a distance of one nozzle diameter. The region of the jet affected by the excitation is now more spread out, and the dominant large-scale structure

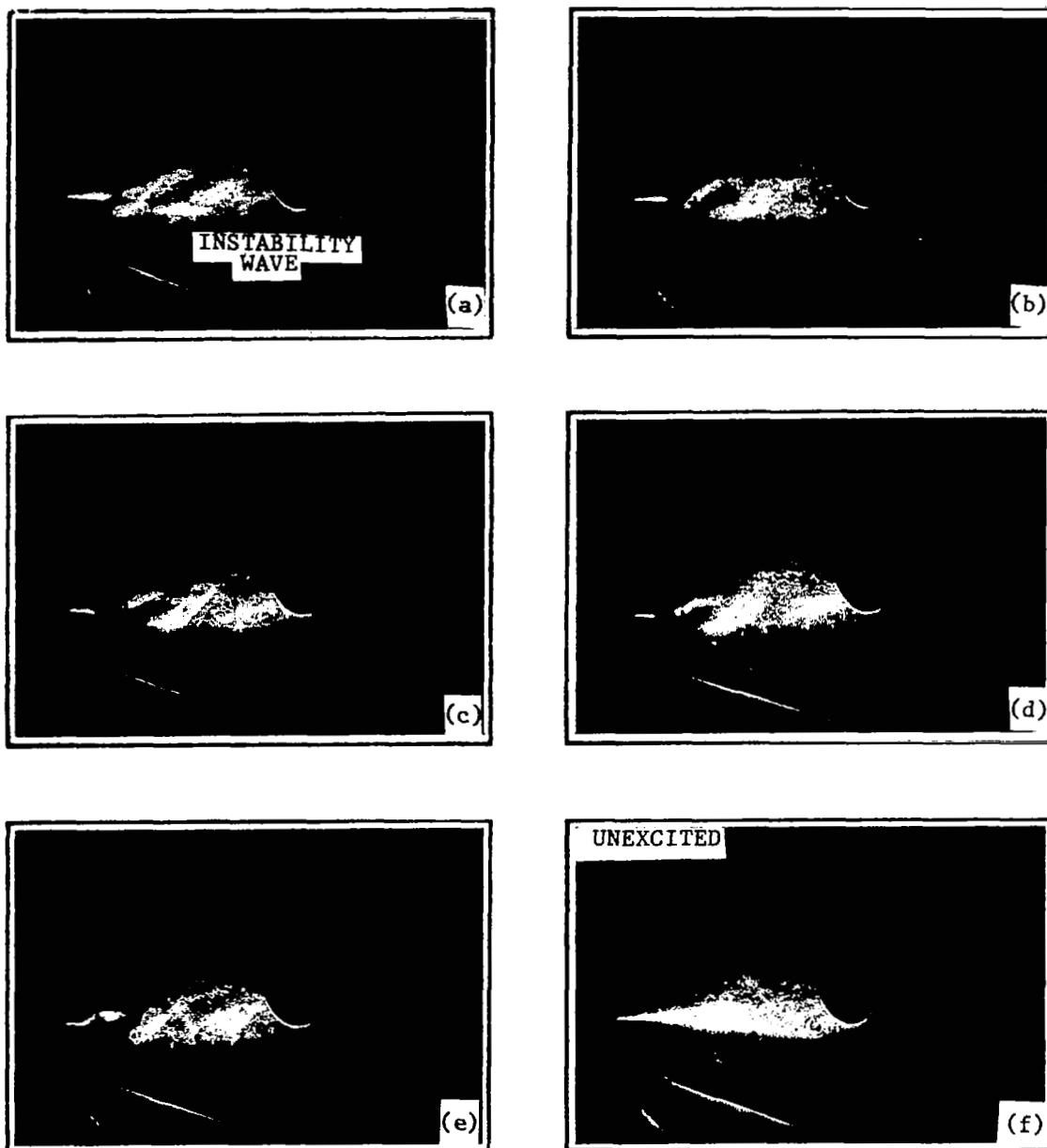


Figure 3.4 flow-acoustic coupling at low frequency,  $f = 428$  Hz.  
 $\phi$  : (a)  $270^\circ$ , (b)  $180^\circ$ , (c)  $130^\circ$ , (d)  $90^\circ$ ,<sup>e</sup> (e)  $0^\circ$ , and  
 (f) Unexcited.

(Knife edge: horizontal,  $U = 20$  m/s,  $L_e = 118$  dB,  
 $L_s = 132$  dB)

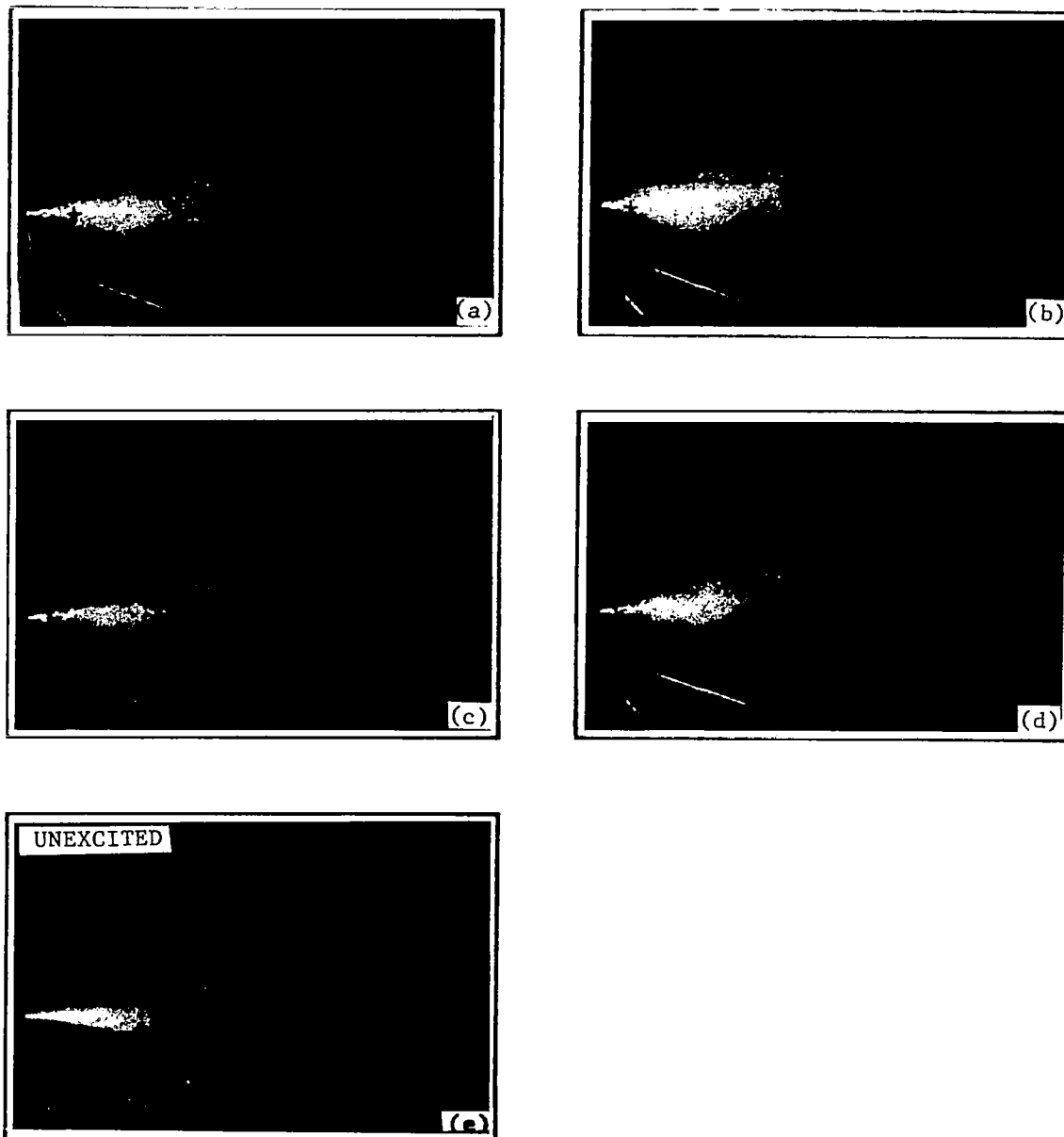


Figure 3.5 Flow-acoustic coupling at high frequency,  $f_e = 2410 \text{ Hz}$ .  
 $\phi$  : (a)  $0^\circ$ , (b)  $90^\circ$ , (c)  $180^\circ$ , (d)  $270^\circ$ , and  
 (e) unexcited.  
 (Knife edge: horizontal,  $U = 20 \text{ m/s}$ ,  $L_e = 126 \text{ dB}$ ,  
 $L_s = 142 \text{ dB}$ )

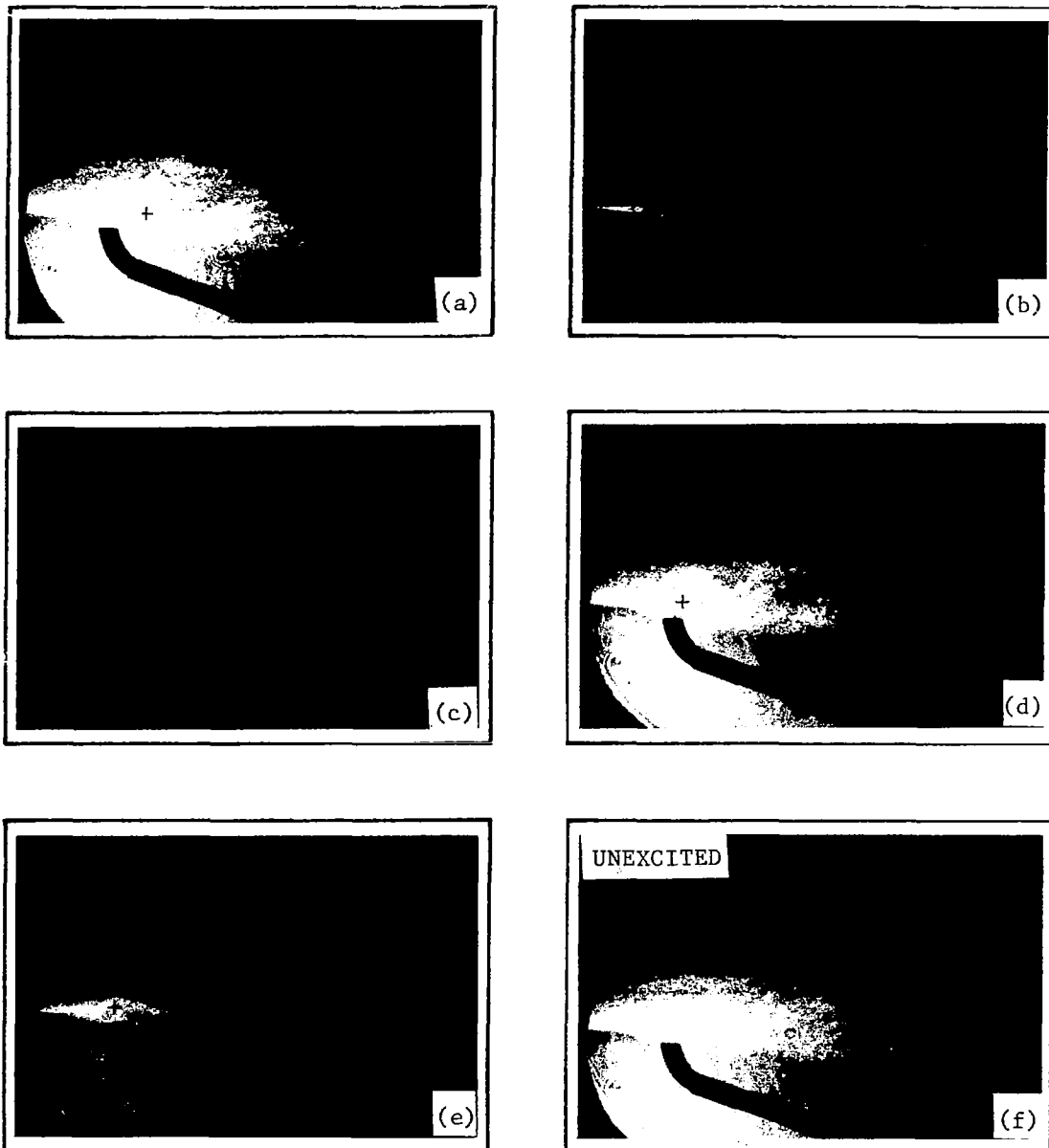


Figure 3.6 Flow-acoustic coupling at low frequency  $f_e = 428$  Hz with the source located downstream of the jet exit. (Compare with figure 3.4.)  $\phi$  : (a)  $300^\circ$ , (b)  $270^\circ$ , (c)  $180^\circ$ , (d)  $90^\circ$ , (e)  $0^\circ$ , and (f) unexcited. (Knife edge: horizontal,  $U = 20$  m/s,  $L_e = 110$  dB,  $L_s = 133$  dB)

appears to be located downstream of the sound source just as it did when the source was closer to the nozzle as shown in figure 3.4. Does it indicate that the sound reaching the nozzle may be coupling there and may also be coupling near the source, where the sound levels are relatively stronger?

To probe the above posed question further, additional flow visualization data were obtained for two configurations of the sound source. In the first configuration the source was located right at the exit, whereas in the second configuration, it was located 2 cm downstream of the nozzle exit. But for both configurations, the sound levels were adjusted to be the same at the nozzle exit plane. Typical results depicting this effect are shown in figure 3.7 for an excitation frequency of 428 Hz. Each column of photographs represents one strobe phase. The photographs captioned (a) in each column is for the unexcited jet, whereas the remaining two photographs captioned (b) and (c) are for the two locations of the sound source. These results clearly show that the instability or large-scale structures excited in the jet are not similar for the two configurations, thus fortifying the suspicion that, when the source is located downstream, we may be seeing the results of coupling at the nozzle lip as well as that at or near the noise source. And although it does not categorically prove that the flow downstream is locally receptive to the incident sound, it certainly points in that direction.

The results presented above formed the backbone of the experiments conducted subsequently. It was clear that if the objective is to obtain a clear-cut answer to the problem addressed in section 1, experiments must be designed to isolate the nozzle from sound reaching the nozzle exit. Although it is realized, that it may be an impossible task, it was hoped that if the sound could be attenuated considerably before it reaches the nozzle exit, and maintained dominant at some point downstream, the results may be more definitive. Keeping this in mind, new experiments were performed that consisted of placing barriers between the sound source and the nozzle exit. These results are described in the next subsection.

### 3.3.2 Receptivity of a Baffled Jet

For the experiments described in this section, the concept of reducing sound by placing a barrier between the nozzle and the sound source was utilized to reduce the sound levels reaching the nozzle exit. Although majority of these tests were conducted using lead baffles with the jet passing through a small opening in the baffle, the concept was first tested out by placing a simple one-sided aluminum plate barrier as shown schematically in figure 3.8. For this configuration, calculations from barrier theory (e.g., see Maekawa, ref. 20) indicate that reductions of up to eight decibels can be obtained between the source and the observer (nozzle in this case). These reductions can be expected to be higher at higher frequencies.

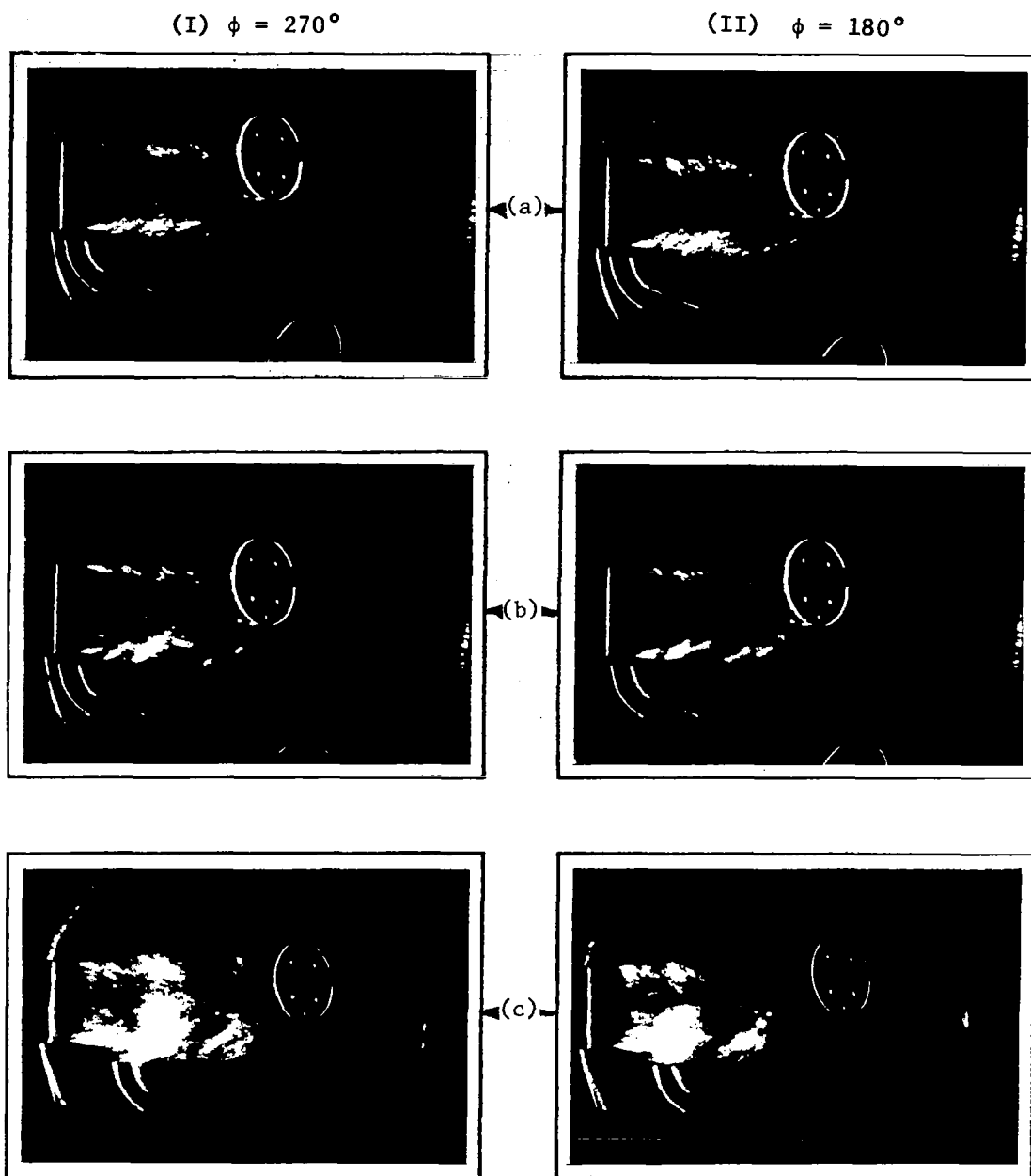


Figure 3.7 Different type of flow-acoustic coupling for different source locations for a fixed sound pressure level at the exit plane,  $L_e = 110$  dB. (a) Unexcited, (b) excited, source at nozzle exit, (c) excited, source at  $x = 2$  cm. (Knife edge: vertical,  $U = 20$  m/s,  $f_e = 428$  Hz)

(Continued on next page)



(III)  $\phi = 90^\circ$

(IV)  $\phi = 0^\circ$

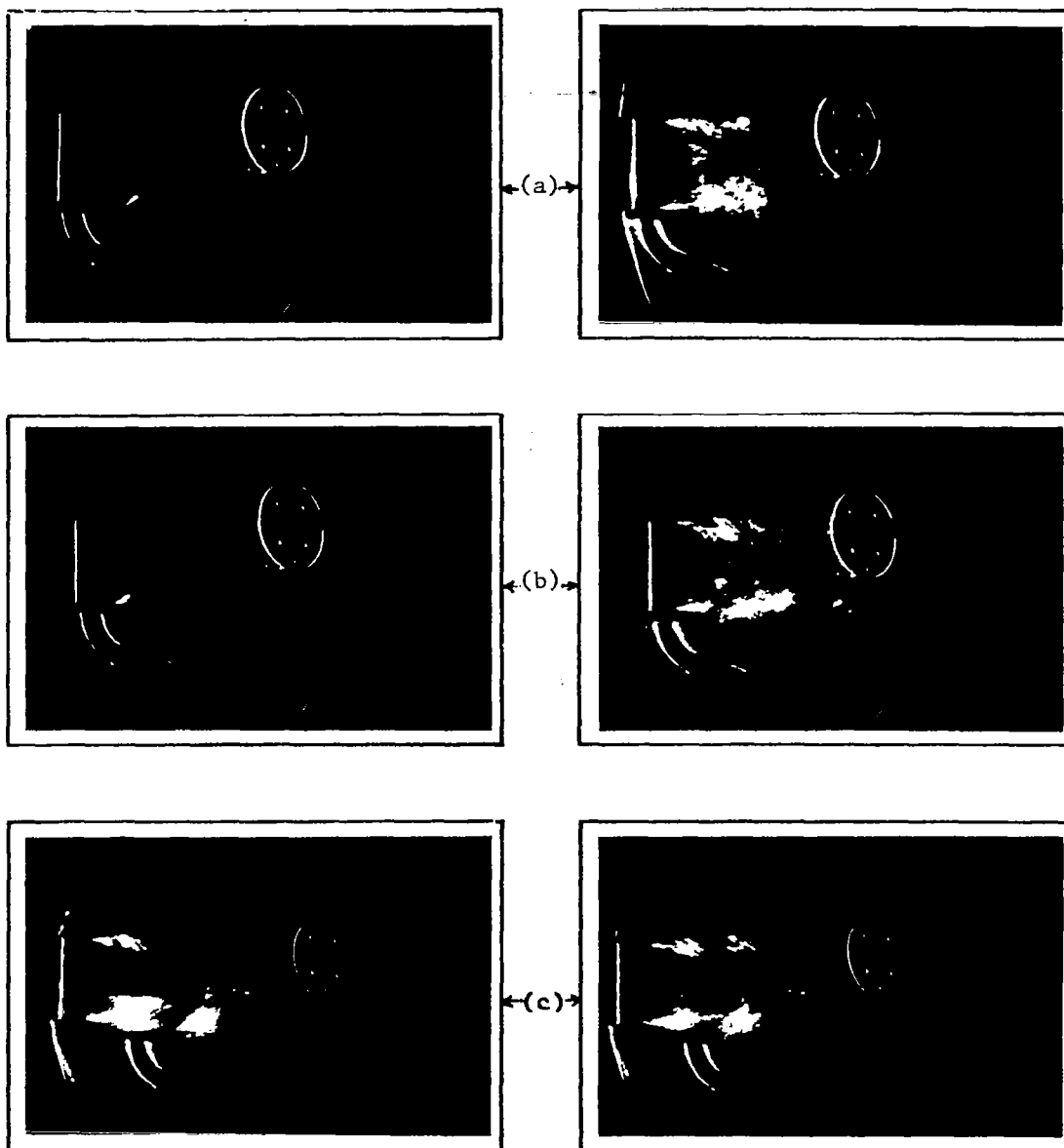


Figure 3.7 (Continued from the previous page)

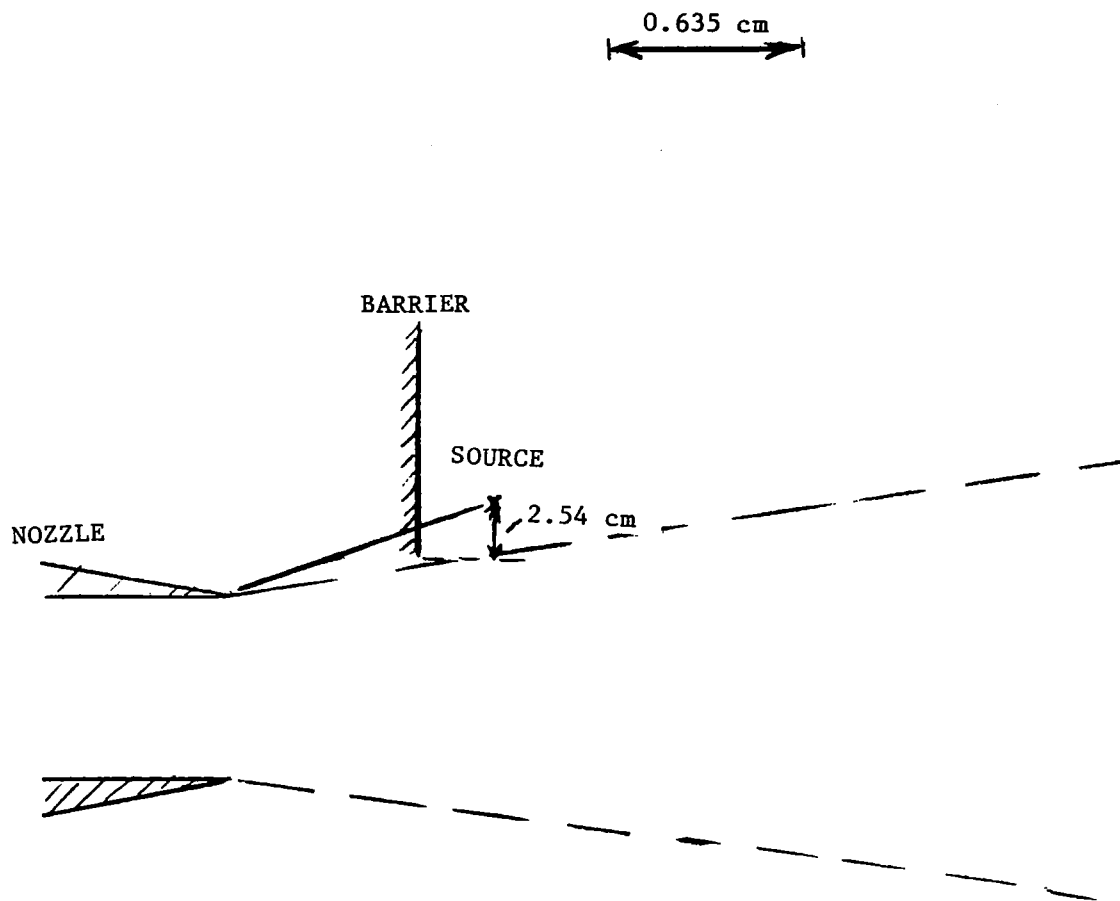


Figure 3.8 Schematic of the barrier configuration to reduce the SPLs at the nozzle exit

The preliminary results for a 1.875-cm thick barrier placed between the source and the nozzle exit are shown in figure 3.9. As before, these photographs have been phase-averaged to highlight the excited large-scale structures, and each successive photograph represents a shift in the strobe phase of 90 degrees. Thus the four photographs cover the total extent of the structure denoted in the figure by a ' + ' sign during its repeatable time period ("life cycle" : so to say !). When these results are compared with similar photographs for the unexcited jet, which are shown in figure 3.10, it appears that the large-scale structures in this case are initiating somewhere under the barrier, and away from the nozzle exit plane.

To further reduce the noise levels reaching the nozzle exit, the one-sided barrier seen in figures 3.8 thru 3.10 was replaced by a 5.08-cm (1.0-in) thick barrier made out of lead with a center opening of 7.62 cm (3.0 in). The baffle was placed about 1.27 cm (0.5 in) downstream of the nozzle exit. The test configuration is shown in figure 3.11, and the corresponding results are presented in figure 3.12. Photographs (a) thru (d) are for the excited case and photograph (e) is for the unexcited case. It should be noted that, to maximize the effectiveness of the baffle, the sound source was also moved in this case to a radial distance of 5 cm (2.0 in) from the lip line. Compared to the results shown in figure 3.10 for the one sided barrier, for which the sound source was closer to the lip line, the nature of instability waves is somewhat different, but the instabilities appear to initiate downstream of the nozzle and from close to the plane in which the sound source is located.

These flow visualization data were obtained with a vertical knife edge at an excitation frequency of 428 Hz. It is interesting to notice that, in the region close to the nozzle exit and upstream of the baffle, there are no signs of density gradients perpendicular to the vertical knife edge (i.e., along the axial direction). In fact, the flow in this region, in so far as the presence of large-scale structures is concerned, is identical for both the excited and the unexcited jet.

The results for the high frequency excitation, however, showed a different trend as shown in figure 3.13 for an excitation frequency of 1275 Hz. Here the instability waves can be seen to be excited closer to the nozzle as also seen earlier.

#### Optics Realigned to Examine the Excited Structure Near the Nozzle Exit

The flow visualization photographs taken by a vertical knife-edge thus indicated that the higher frequency sound excited large-scale structure closer

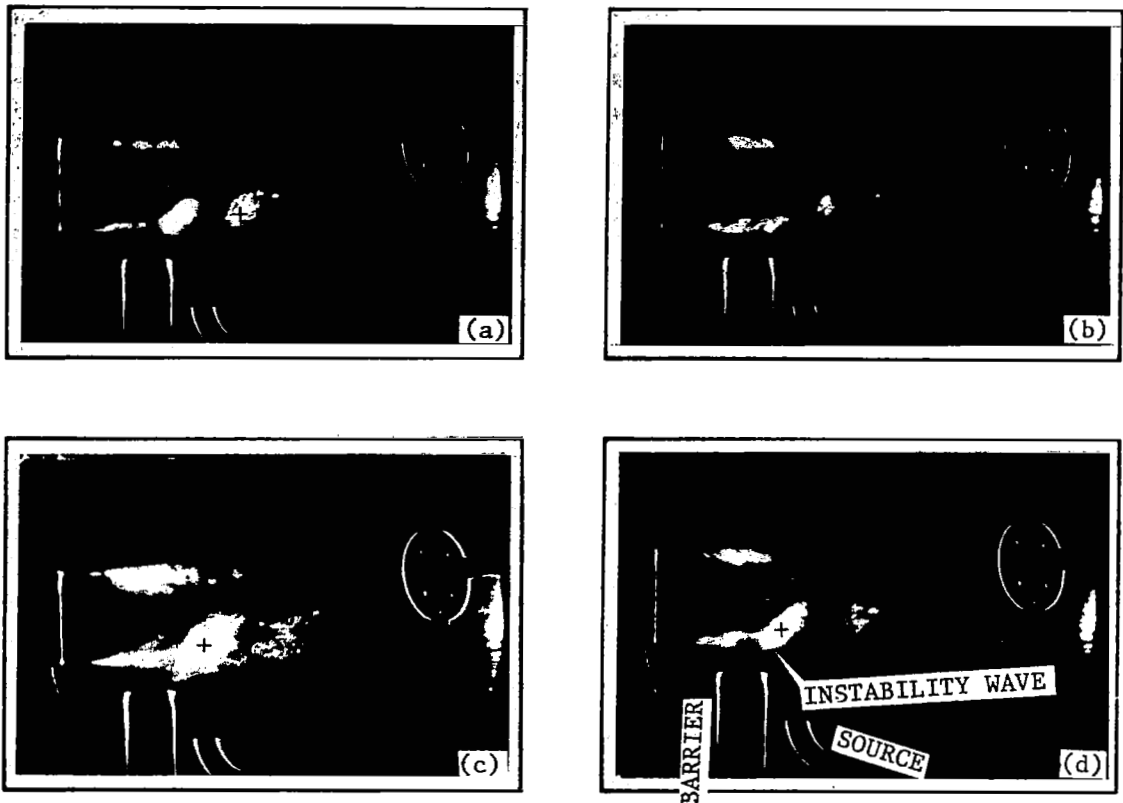


Figure 3.9 Preliminary results with the 1.875-cm thick aluminum barrier placed between the nozzle lip and the sound source.  
 $\phi$  : (a)  $270^\circ$ , (b)  $180^\circ$ , (c)  $90^\circ$ , (d)  $0^\circ$ .  
 (Knife edge: vertical,  $U = 20$  m/s,  $f = 428$  Hz,  $L_e = 108$  dB,  $L_s = 134$  dB, Level at the shear layer<sup>e</sup> = 127 dB)

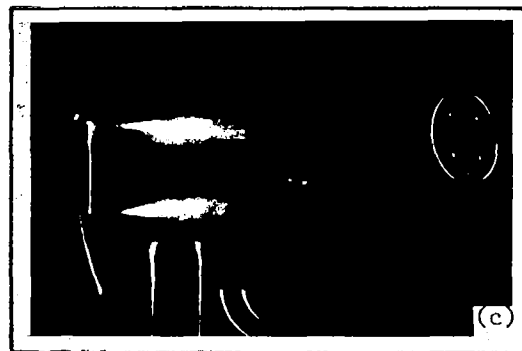
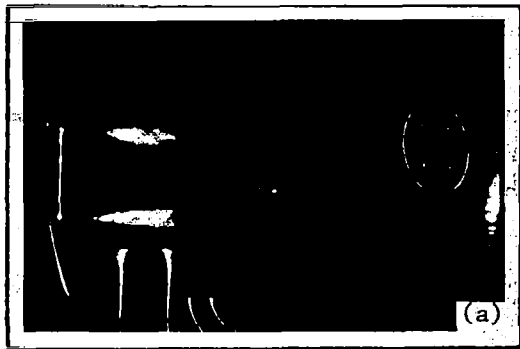


Figure 3.10 Unexcited jet for conditions corresponding to those of figure 3.9. (Here the laser was strobed at a frequency of 428 Hz.)  $\phi$  : (a)  $270^\circ$ , (b)  $180^\circ$ , (c)  $0^\circ$ .



Figure 3.11 Test configuration with the lead barrier

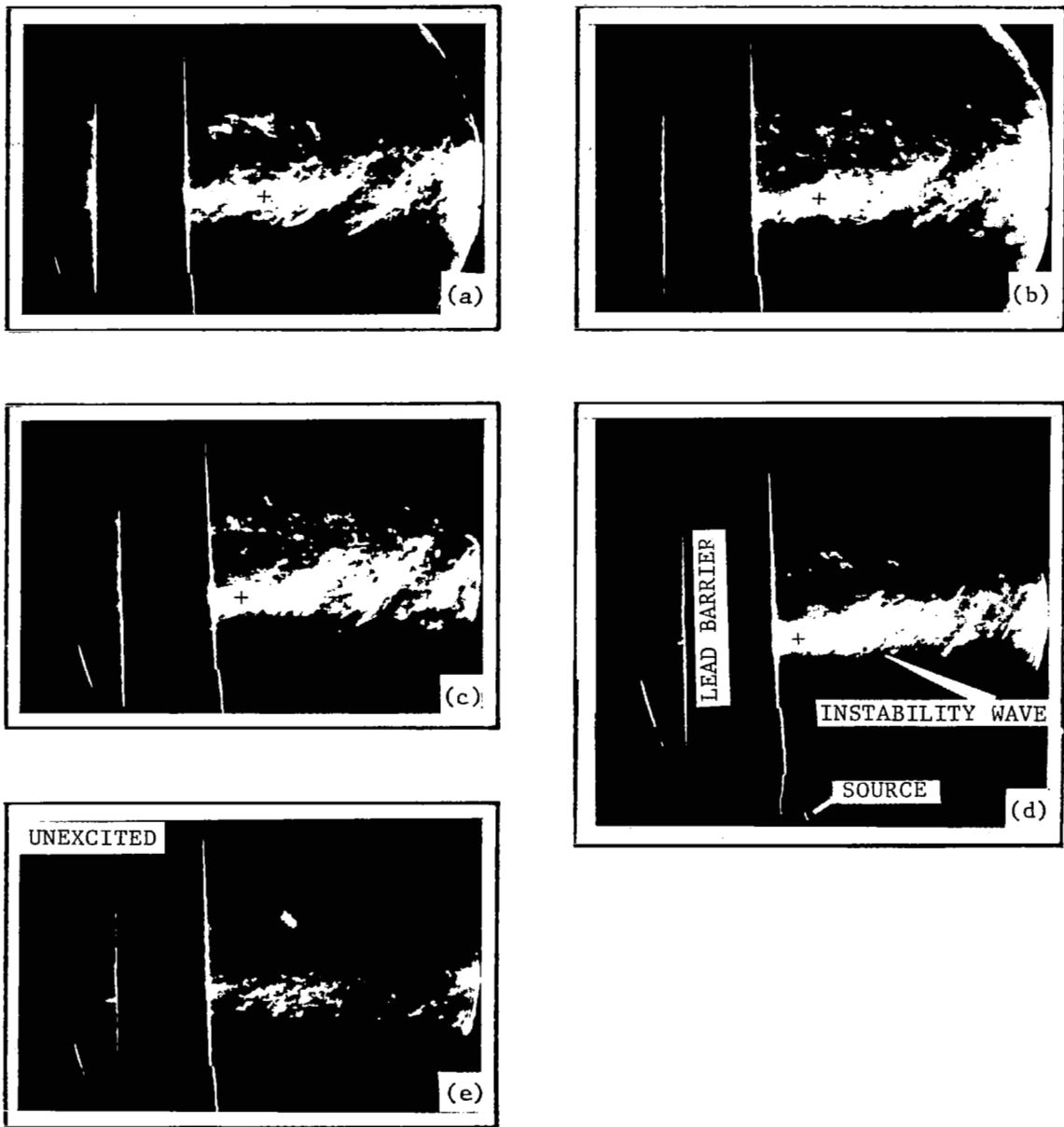


Figure 3.12 Low-frequency flow-acoustic coupling with the lead barrier between the sound source and the nozzle lip.  $\phi$  :  
 (a)  $270^\circ$ , (b)  $180^\circ$ , (c)  $90^\circ$ , (d)  $0^\circ$ , and (e) unexcited,  
 $\phi = 90^\circ$ . (Knife edge: vertical,  $U = 20$  m/s,  $f_e = 428$  Hz,  
 $L_e = 99$  dB)

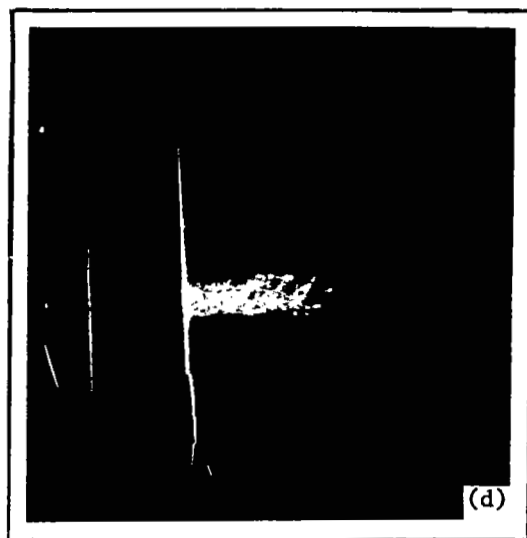
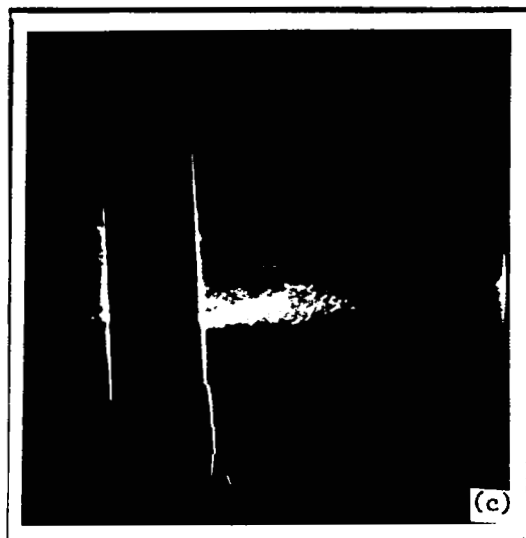
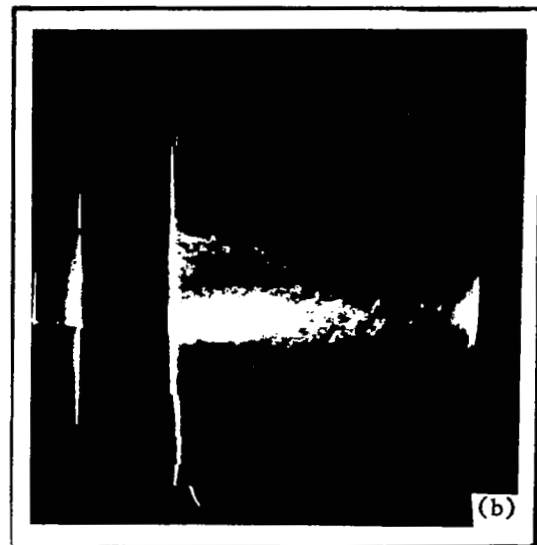
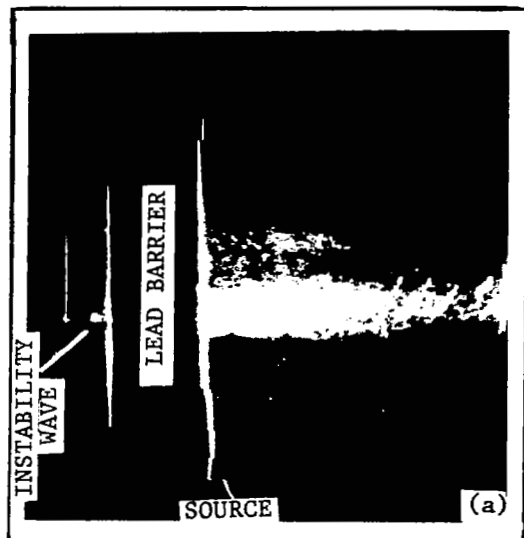


Figure 3.13 High-frequency flow-acoustic coupling with the lead barrier between the sound source and the nozzle lip.  
 $\phi$  : (a)  $0^\circ$ , (b)  $90^\circ$ , (c)  $180^\circ$ , (d)  $270^\circ$ .  
 (Knife edge: vertical,  $U = 20$  m/s,  $f_e = 1275$  Hz,  
 $L_e = 110$  dB)



to the nozzle exit than the lower frequency excitation. However, since the optical set up was arranged to cover the region of the jet almost up to the potential core of the jet, it was necessary to obtain the flow visualization presented above at a low image/object magnification. For this reason, the instability waves near the nozzle exit were not well defined, although their presence was noticeable.

The optical setup was realigned to flow-visualize only the region close to the jet exit. The image/object magnification of 0.5 was increased to 2.0. In addition, the knife edge was changed to horizontal (from one that was vertical) to highlight density variations in the direction perpendicular to the jet axis.

Typical results from the new set up also indicate that at higher frequencies the instability waves start close to the nozzle exit, but still not at the exit. Optical results for an excitation frequency of 1275 Hz are shown in figure 3.14 for the lead-barrier configuration described above. Typical photograph for the corresponding configuration and operating condition for the unexcited jet is shown in figure 3.15. Here, only the shear layer between the nozzle lip and the lead barrier is visible. To highlight the motion of the instability wave, photographs taken at smaller increments of the strobe phase have been presented here. The presence of the excited large-scale structure upstream of the baffle is quite clear here, but all of it is still located downstream of the nozzle exit. Similarly, photographs for a different but higher frequency of 2550 Hz are shown in figure 3.16, whereas the data for the lower frequency of 428 Hz is shown in figure 3.17. It appears from all these optical results that a much higher-frequency sound will be required to initiate the instability right at the exit.

### 3.4 RECTANGULAR JET RESULTS

#### Why A Rectangular Jet?

During the course of this work, a rectangular nozzle that fitted the plenum exit in the optical facility became available. Opportunity was, therefore, taken to obtain some flow visualization results using this nozzle also. Even though the extent of the data acquired with this nozzle was not as large as that for the round nozzle, the results obtained proved quite useful.

#### Only Bare Jet Studied

Since the findings from the round jet tests indicated that the location of the

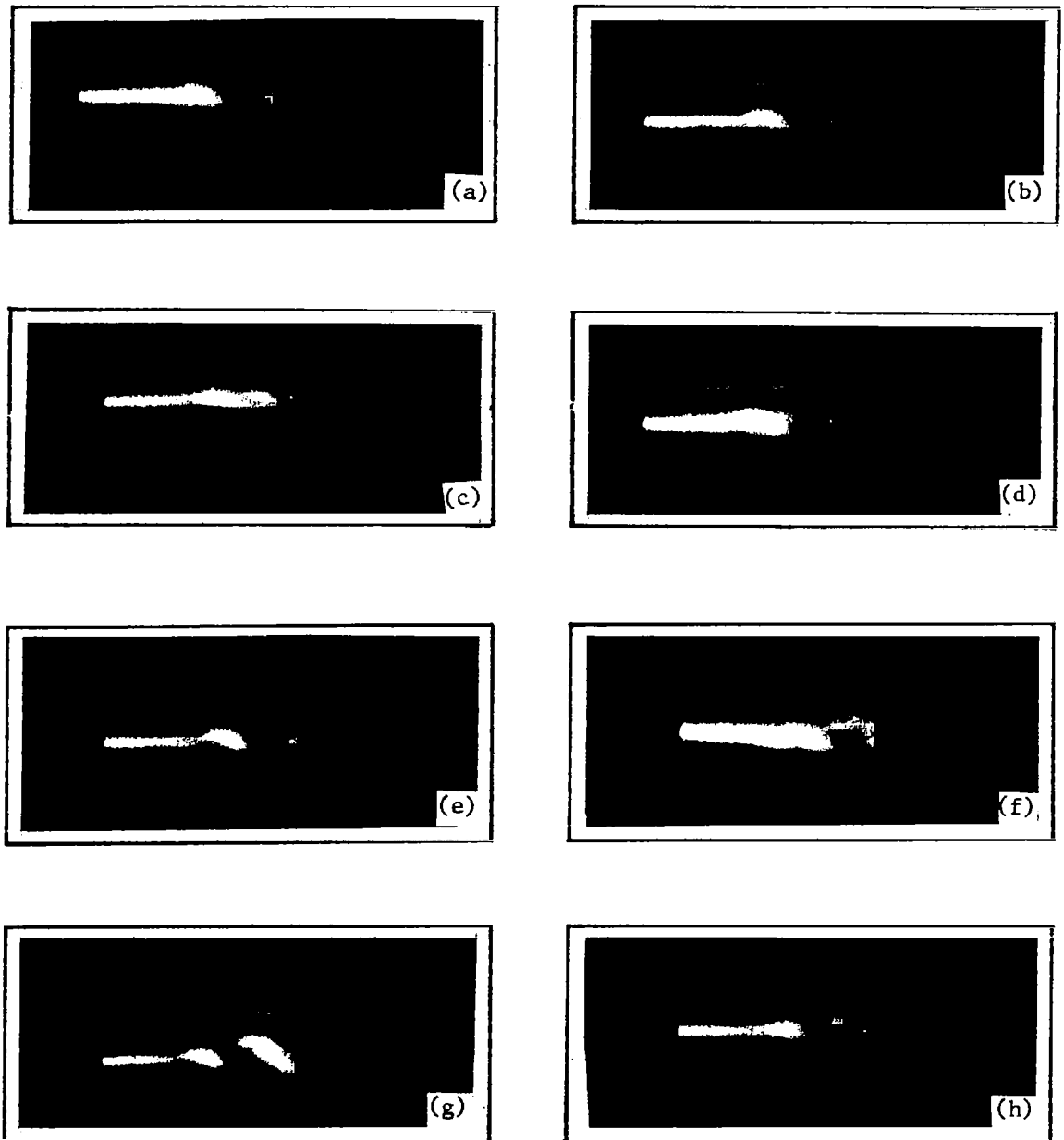


Figure 3.14 Magnified views of the instability wave between the nozzle lip and the lead barrier for test conditions of figure 3.13.  $\phi$  : (a)  $0^\circ$ , (b)  $8^\circ$ , (c)  $30^\circ$ , (d)  $90^\circ$ , (e)  $185^\circ$ , (f)  $260^\circ$ , (g)  $270^\circ$ , and (h)  $300^\circ$ .

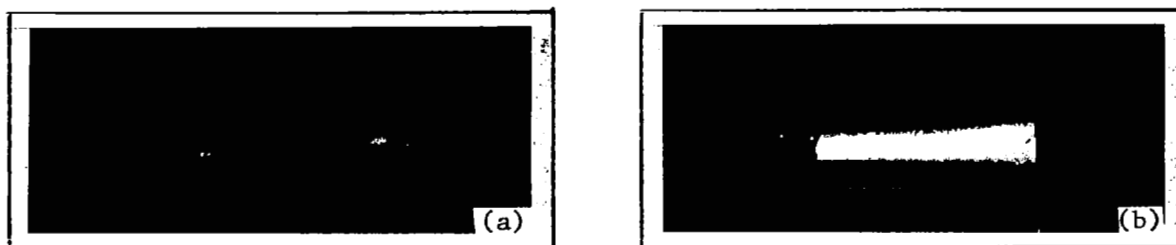


Figure 3.15 Unexcited jet data to compare with excited jet data of figure 3.14.  
 $\phi$ : (a)  $0^\circ$  and (b)  $270^\circ$ .

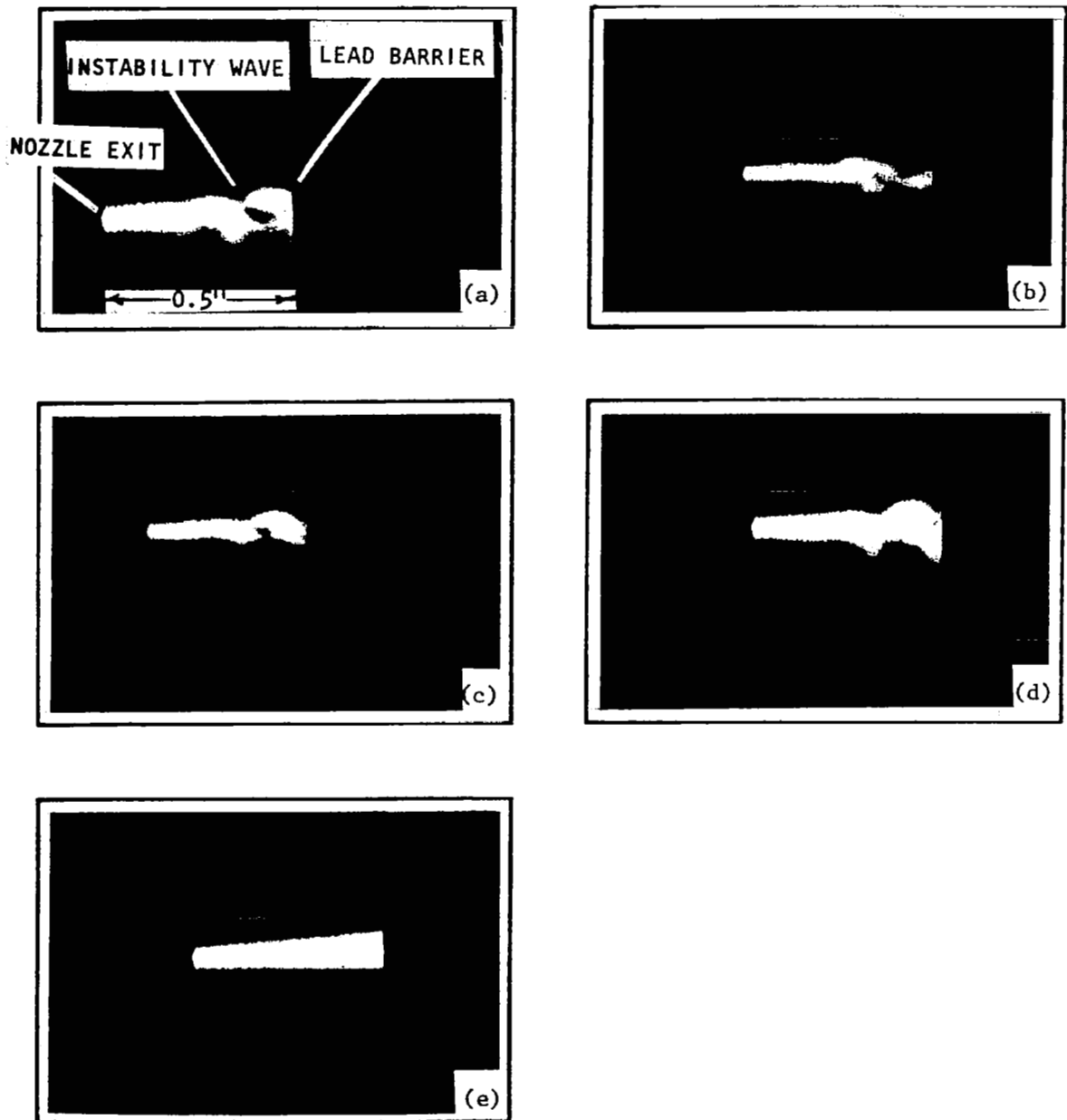


Figure 3.16 Higher-frequency flow-acoustic coupling with the lead barrier between the sound source and the nozzle lip.  
 $\phi$ : (a)  $0^\circ$ , (b)  $90^\circ$ , (c)  $180^\circ$ , (d)  $270^\circ$ , and (e) unexcited,  $\phi = 0^\circ$ .  
 (Knife edge: vertical,  $U = 20$  m/s,  $f_e = 2550$  Hz,  $L_e = 99.6$  dB)

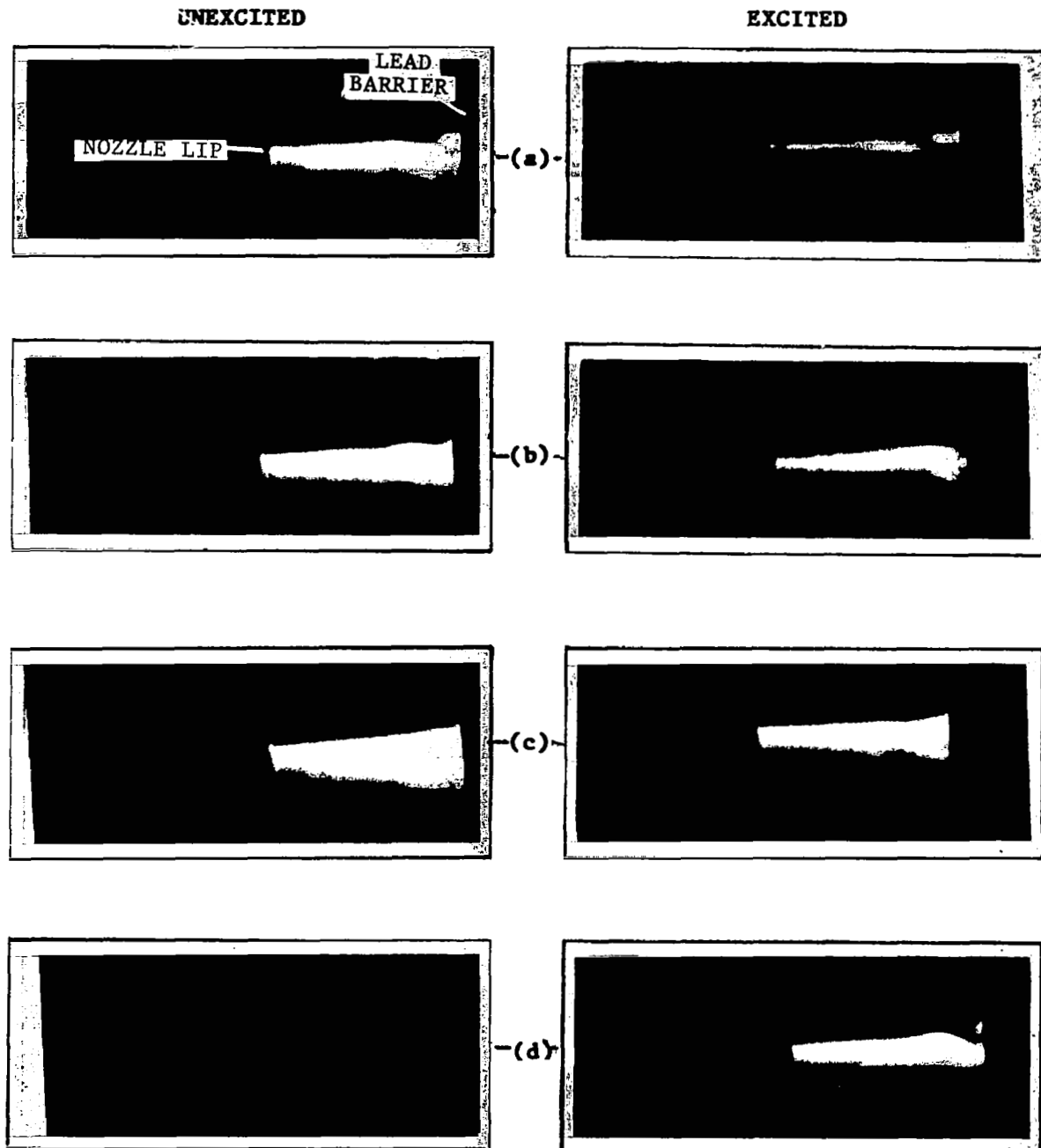


Figure 3.17 Low-frequency flow-acoustic coupling with the lead barrier between the sound source and the nozzle lip.  
 $\phi$  : (a)  $0^\circ$ , (b)  $90^\circ$ , (c)  $180^\circ$ , and (d)  $270^\circ$ .  
 (Knife edge: vertical,  $U = 20$  m/s,  $f_e = 428$  Hz,  
 $L_e = 100$  dB)

initiation of the excited instability is a function of both the excitation frequency and localized sound pressure levels, data were acquired with the bare jet only.

#### Two-Dimensional Sound Source Used

The excitation sound in these tests emitted from a two-dimensional slit of an exponential horn described earlier. The configuration of the source with respect to the nozzle used for flow visualization is shown in figure 3.18.

#### Two Dimensionality of the Jet Improves the Flow Visibility

The laser light used to visualize the flow was passed through the larger dimension of the two-dimensional jet. This large travelling length, together with the two-dimensionality of the flow, enabled us to visualize the flow without always seeding the jet air with helium as done for the round jet. And as seen below, the quality of the schlieren photographs also improved considerably.

#### Low-High Frequency Coupling Found Similar to That for the Round Jet

The coupling between flow and sound for the rectangular jet was found to be similar to that for the round jet at both the high as well as the low values of excitation frequencies. The coupling at the low frequencies appeared to take place farther from the nozzle exit, whereas the instability waves excited by the high frequency sound could be seen very close to the nozzle lip. Typical results depicting this are shown in figure 3.19.

#### High Frequency Coupling Traced as Far Back as the Nozzle Lip

Excitation of the rectangular jet from one side of the shear layer appeared to affect the shear layer closest to the sound source more strongly than the shear layer on the opposite side. This is shown in figure 3.20. The round jet, on the other hand, was found to be affected throughout its perimeter equally strongly, particularly at the high frequencies.

An additional but unusual feature of the results shown in figure 3.20 is that the starting point of the instability in the shear layer on the other side of the sound source does not appear to change with the changing phase of the strobe, and remains some distance from the nozzle exit. The tip of the instability wave with this behavior is indicated by inverted triangles in the figure.

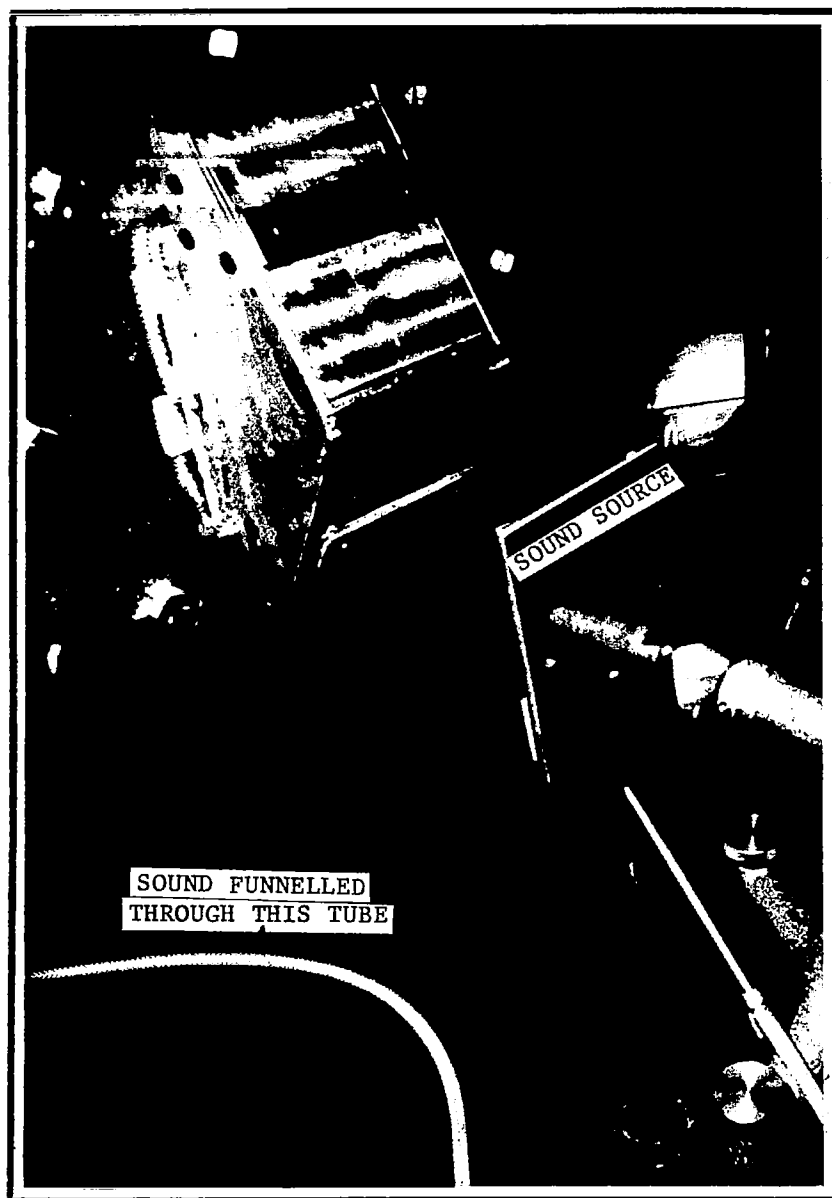


Figure 3.18 The rectangular nozzle and the sound source

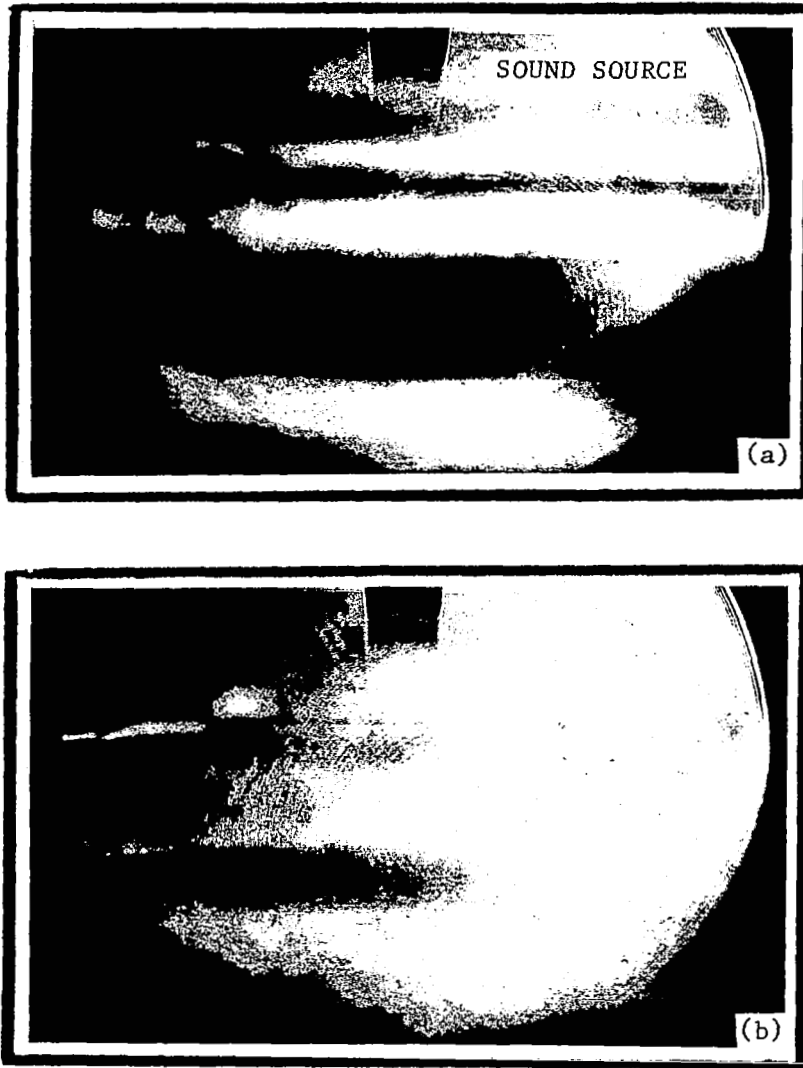


Figure 3.19 Low and high frequency coupling for the planar jet  
 $f$ : (a) 557 Hz (b) 1115 Hz  
(Knife edge: horizontal,  $U = 40$  m/s)





Figure 3.20 Dominant effect of acoustic excitation on the shear layer closer to the sound source.

$\phi$ : (a)  $0^\circ$ , (b)  $90^\circ$ , (c)  $180^\circ$ , and (d)  $270^\circ$ .

(Knife edge: horizontal,  $U = 40$  m/s,  $f_e = 1115$  Hz)

The situation is quite different in the shear layer closer to the sound source. Since this shear layer is not as clear in the photographs of figure 3.20, which were taken without seeding the air flow with foreign gases, additional photographs were taken by injecting helium in the same flow. As seen in figure 3.21, this made the details of the upper layer much clearer. Now as one proceeds thru these photographs in a decreasing order of the strobing phase (which is an indication of the location of the in space of a convecting or propagating instability wave) and follows the movement of the structure marked "+" in each photograph, it leaves no doubt in establishing that this structure definitely initiated at the nozzle lip.

All phase-averaged photographs obtained for the low frequency excitation and examined in the same detail as those in figure 3.21 somehow always failed to show a dominant structure right at the lip. Typical low-frequency results are shown in figure 3.22.

Taken together, these results are very similar to those obtained for the round jet. This concludes the presentation of the flow visualization data for the externally excited jets.

### 3.5 INSTABILITY-WAVE DATA

To understand the physical processes involved in the receptivity somewhat better, instability-wave data were acquired in the jet, both along the lip-line and also along the jet center line. These data were obtained by a 0.318-cm (1/8-in) diameter Bruel and Kjaer microphone fitted with a nose cone. The instability-wave pressure amplitude values were derived by measuring the cross-power spectra between the microphone signals and the electronic signal that was used to generate the excitation sound. This technique has been used by others (refs. 16 and 19) for such measurements.

These results, however did not prove to be too useful, since it was found that for all cases studied the pressure amplitudes at the exit were found to be dominated by the sound levels reaching the nozzle exit plane. This was found to be true even for those cases where lead baffles were used to attenuate sound reaching the exit plane. Some of such results are shown in figures 3.23 and 3.24. Thus over the whole potential-core region of the jet, the sound appeared to be dominant over the instability-wave pressures, and little use was foreseen in acquiring further instability-wave data. However, as described below, these results were instrumental in dictating the direction of some important new experiments.

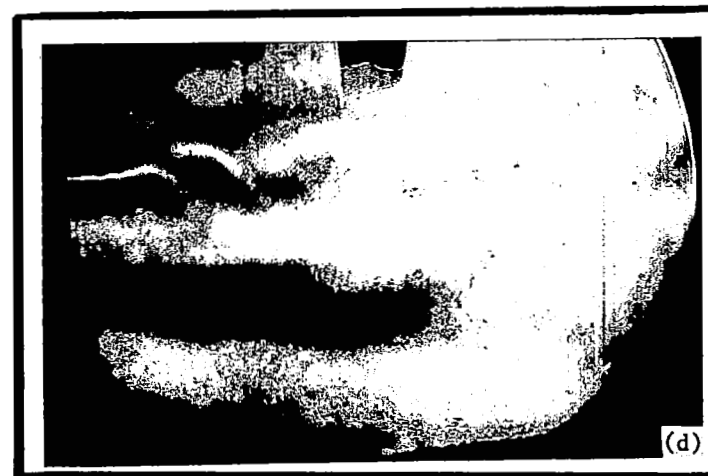
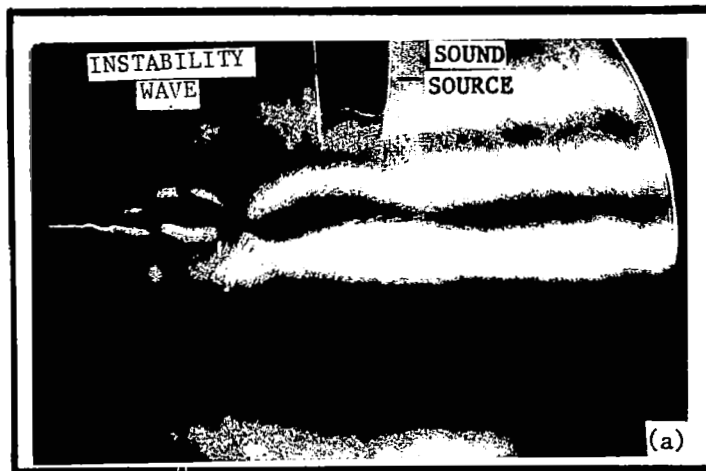


Figure 3.21 Tracing the origin of the instability wave by fine-tuning the strobe phase.

$\phi$ : (a)  $290^\circ$ , (b)  $280^\circ$ , (c)  $270^\circ$ , (d)  $250^\circ$ , (e)  $230^\circ$ , (f)  $210^\circ$ , (g)  $180^\circ$ ,  
 (h)  $160^\circ$ , (i)  $120^\circ$ , (j)  $110^\circ$ , (k)  $90^\circ$ , (l)  $60^\circ$ , (m)  $40^\circ$ , (n)  $20^\circ$ , (o)  $340^\circ$ ,  
 (p)  $320^\circ$ , (q)  $320^\circ$ , (r)  $310^\circ$ , (s)  $300^\circ$ , and (t)  $290^\circ$ .

(Knife edge: horizontal,  $U = 40$  m/s,  $f_e = 1115$  Hz). (Continued on next page)



Figure 3.21 (Continued from last page)

(Continued)

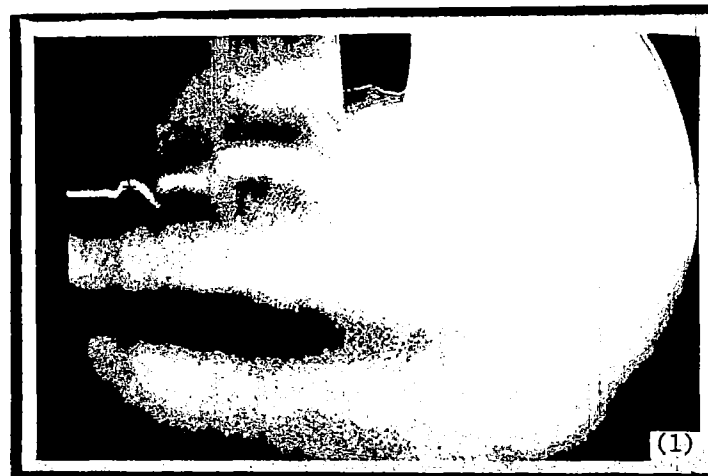


Figure 3.21 (Continued from last page)

(Continued)



Figure 3.21 (Continued from last page)



Figure 3.21 (Continued from last page)

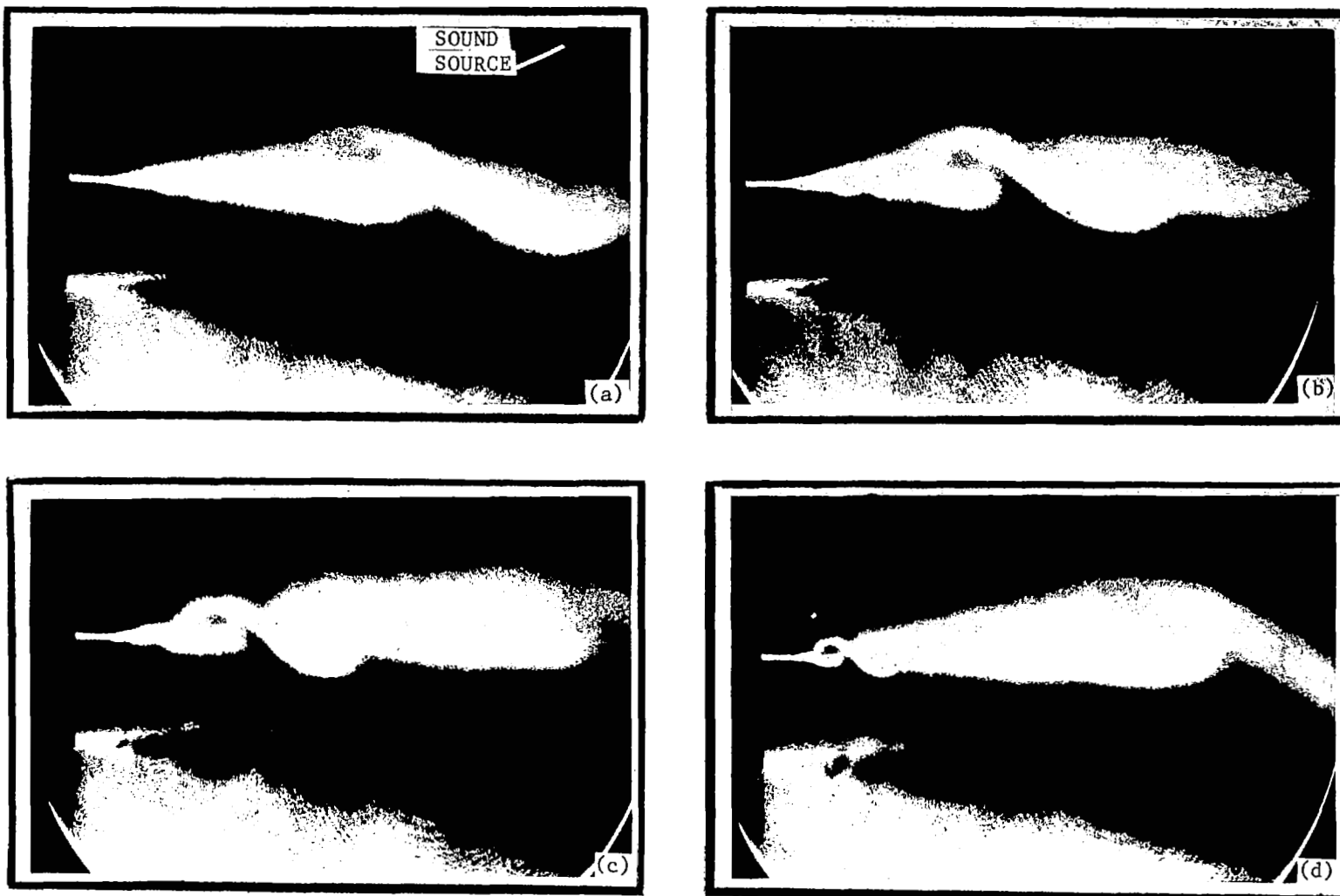


Figure 3.22 Low-frequency excitation of the planar jet.  
 $\phi$ : (a)  $270^\circ$ , (b)  $180^\circ$ , (c)  $90^\circ$ , and (d)  $0^\circ$ .

(Knife edge: horizontal,  $U = 54$  m/s,  $f_e = 578$  Hz)



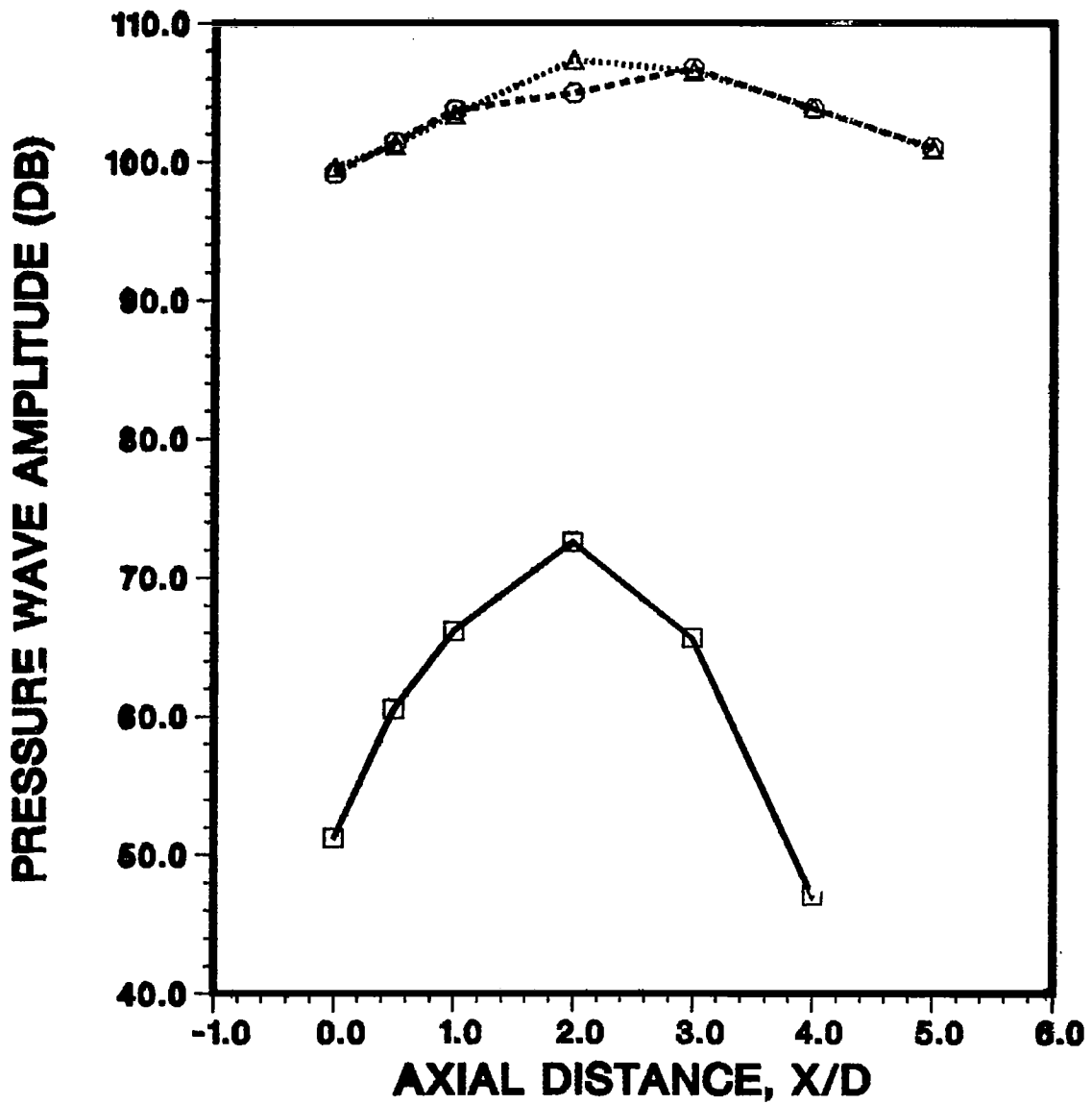


Figure 3.23 Instability-wave pressure distribution along the lip line for the data shown in Figure 3.12.

□ : Unexcited,    ○ : excited ( $U = 20$  m/s,  
 $f = 428$  Hz);    △ : sound alone (no flow,  
 $f_e = 428$  Hz)

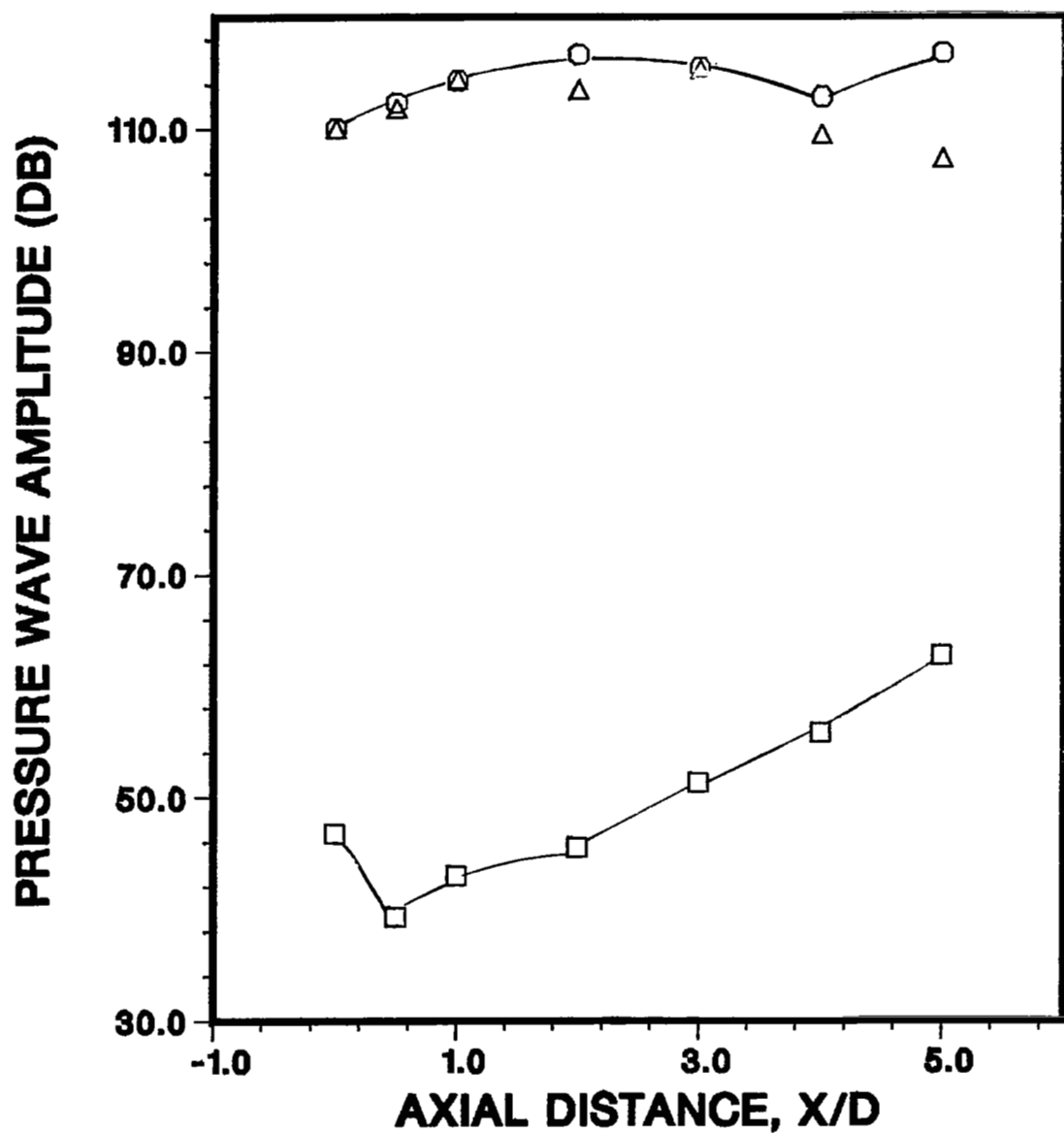


Figure 3.24 Instability-wave pressure distribution along the jet center line for the data shown in Figure 3.13.  
 □ : Unexcited; ○ : excited ( $U = 20$  m/s,  $f_e = 1275$  Hz); △ : sound alone (no flow,  $f_e = 1275$  Hz).

### 3.6 CONCLUDING REMARKS

The results described above can be summarized as follows:

#### Externally Incident Sound Does Couple with the Jet Shear Flows

Instability waves are excited in the jet when sound of suitable level and frequency is incident upon the shear layer of the jet, even when the sound is generated by sources located external to the jet.

#### Flow-Acoustic Coupling Found to depend Upon the Source Location

The nature and the extent of the spatial developments of the excited instability waves were found to be different for the different locations of the sound source, each operated such that the noise levels measured at the nozzle exit were same for each case. These were the first set of results in favor of the concept of local receptivity, indicating that the assistance of the trailing edge may not be necessary for an incident sound to couple with the shear-layer flow. Instead, the coupling may be controlled by the localized levels of sound.

#### Higher the Frequency, The Closer to the Jet Lip the Receptivity Location

When excited by high frequency sound, the excited instability waves appeared to initiate at the nozzle lip. At lower frequencies, the instability waves initiated downstream of the nozzle lip. Invariably, this point was found to be at or just downstream of the the separation of the shear layer from laminar to turbulent.

#### Categorical Conclusions About Local Receptivity Not Possible Without Further Experiments

The results of the experiments described above, both for the round jet as well as a rectangular jet, make it extremely difficult to conclude categorically if the regions downstream of the nozzle exit are locally receptive to the incident disturbances. This is especially difficult since, for all configurations examined, it was not possible to isolate the jet exit from incident sound. Thus, even though there is strong indication that local receptivity may occur, these results fail to provide a positively convincing

proof that it definitely does. To further substantiate the results described above, new experiments had to be devised and conducted. These new experiments are described in the next section.

#### 4.0 RESULTS FOR SCREECHING SUPERSONIC JETS

As concluded in the previous section, the results described so far dictated that different experiments be planned, if the objectives of this project were to be accomplished successfully, accompanied by firm conclusions. After due deliberation, it was decided that new experiments be conducted wherein the jet be operated under those conditions wherein the feedback phenomenon is present and is, as a result, producing an intense tone, and use this tone as the source of sound. (This experiment was suggested by professor C. K. W. Tam of Florida State University, Tallahassee.)

Both the edgetone and the screech phenomena fall in this category. In both cases, the tones are a result of the back reaction of the sound on the flow. This results in the generation of flow disturbances in the shear layer, which are phase-locked to the feedback sound that they produce on interacting with shock waves (for screech) or the impingement surface (for edge tone). A similar phenomenon is observed when the jet impinges directly onto a plate. The feedback phenomenon is observed for both the subsonic and the supersonic jets (ref. 21). The major difference, however, is that the feedback sound travels within the jet for subsonic jets, whereas, for supersonic jets the path of sound is exterior to the jet. For a given jet velocity, the feedback frequency is a function of the distance between the sound source and the nozzle exit.

The technical approach for the new experiments consisted of placing a hard baffle with an opening just larger than the nozzle diameter perpendicular to the axis of an underexpanded supersonic jet as shown in figure 4.1. For a given axial position of the baffle, the feedback frequency was then recorded. The baffle was then moved back and forth to see if the feedback frequency had changed. It was expected that if changes in the feedback frequency are observed, it may be suggestive of changes in the point of receptivity between the flow and the incident sound, which should be confirmed by optical means.

Thus, if the concept of local coupling has any merit, a new "embryo" eddy should start near the baffle opening to complete a new path-length for feedback, and hence a different frequency. Even if sound is reaching the nozzle exit and initiating a feedback eddy there, it is expected that an additional feedback tone due to the excited eddy near the baffle opening will be seen. This is illustrated in figure 4.1 under the title "expected

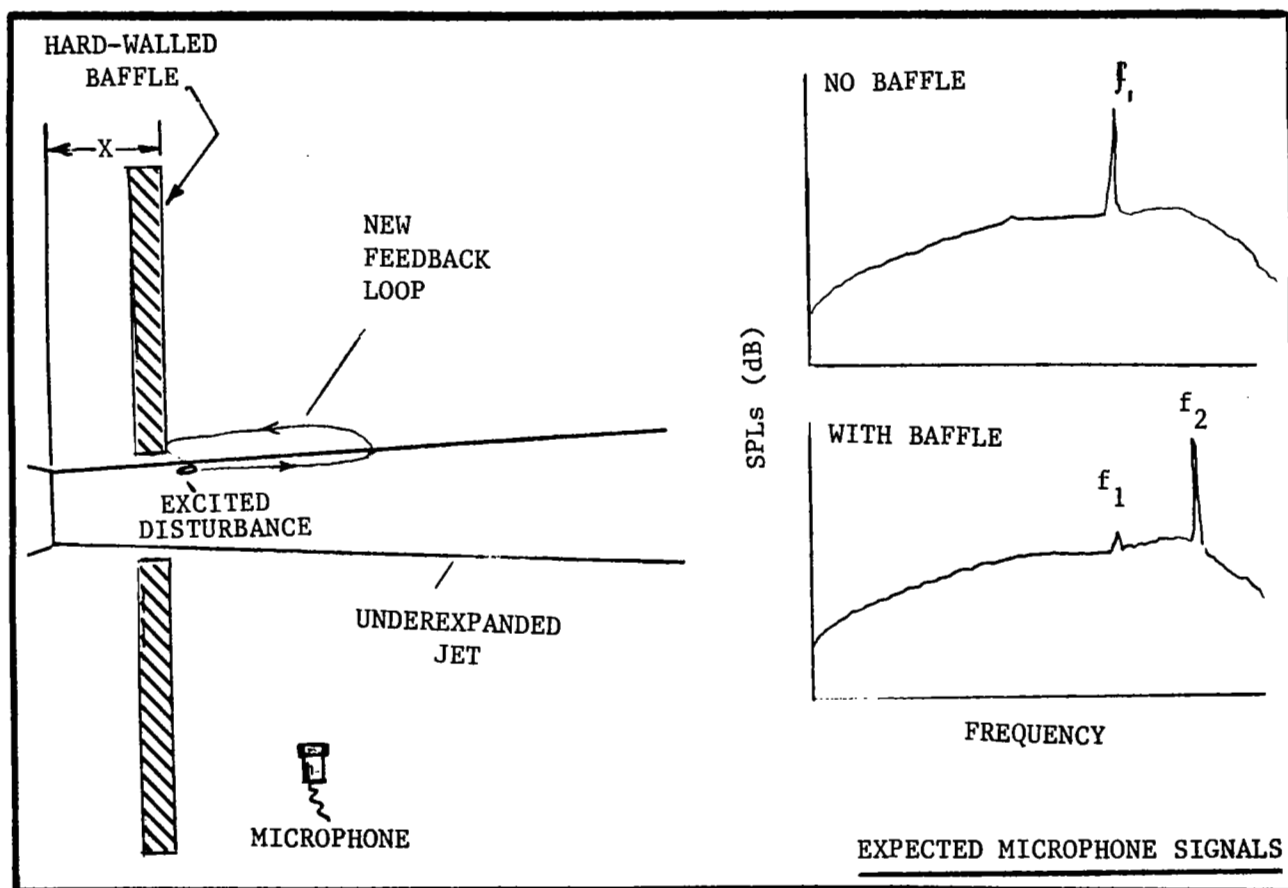


Figure 4.1 Traversing baffle arrangement for the experiments with the screeching supersonic jet to modify the feedback frequency.

(Frequency  $f_2$  produced through the new feedback loop and, if observed, should change with changing axial location of the baffle)

microphone signals."

An alternate experiment along the same lines would be to use either an impingement plate or an impingement wedge. The advantage of this set up is that the feedback frequency due to the interaction at the nozzle exit will be absolutely fixed, and will not be a function of the shock cell location. This set up was also tried out.

A high velocity jet is desirable for these tests. This is because the high velocity jets have thinner shear layers, which permit larger growth rates of the instability waves. In addition, since these jets have larger core lengths, it permits a larger axial movement of the baffle with a relatively smaller opening in it.

#### 4.1 PILOT EXPERIMENTS

Preliminary experiments were carried out to check out the feasibility of this concept in our jet-flow laser velocimeter facility, where the baffle was mounted on one of the traversing frames of the facility. The nozzle diameter was 5.08 cm (2.0 in). Screech frequencies of the jet operated at a pressure ratio of 2.95 were measured by moving a 2.54 cm (1.0 in) thick plywood baffle axially (see figure 4.2). Results were obtained for two separate baffles, with opening diameters of 5.72 cm (2.25 in) and also 6.99 cm (2.75 in), respectively. No flow-visualization results were obtained. Typical results, showing the changes in the screech frequency, as the baffle was moved downstream of the nozzle exit, are shown in figure 4.3 and 4.4 for two pressure ratios and baffle openings indicated in the figure captions.

The screech or feedback frequency clearly increases with increasing baffle distance, implying that the length of the feedback loop is somehow decreasing. And as seen in the sound pressure spectra measured at about 100 degrees with respect to the exhaust exit and shown in figure 4.5, there are drastic changes in the discrete-tone noise levels as a result of traversing the baffle away from the nozzle exit. In fact, as seen in this figure, not only did the screech frequency disappear for certain baffle locations, more than one discrete tones were produced at others. Although it was too premature to draw any conclusions about the receptivity point by examining these preliminary results, they certainly pointed to the merit of this exercise and indicated a need for further measurements, which were carried out subsequently, and are described below.

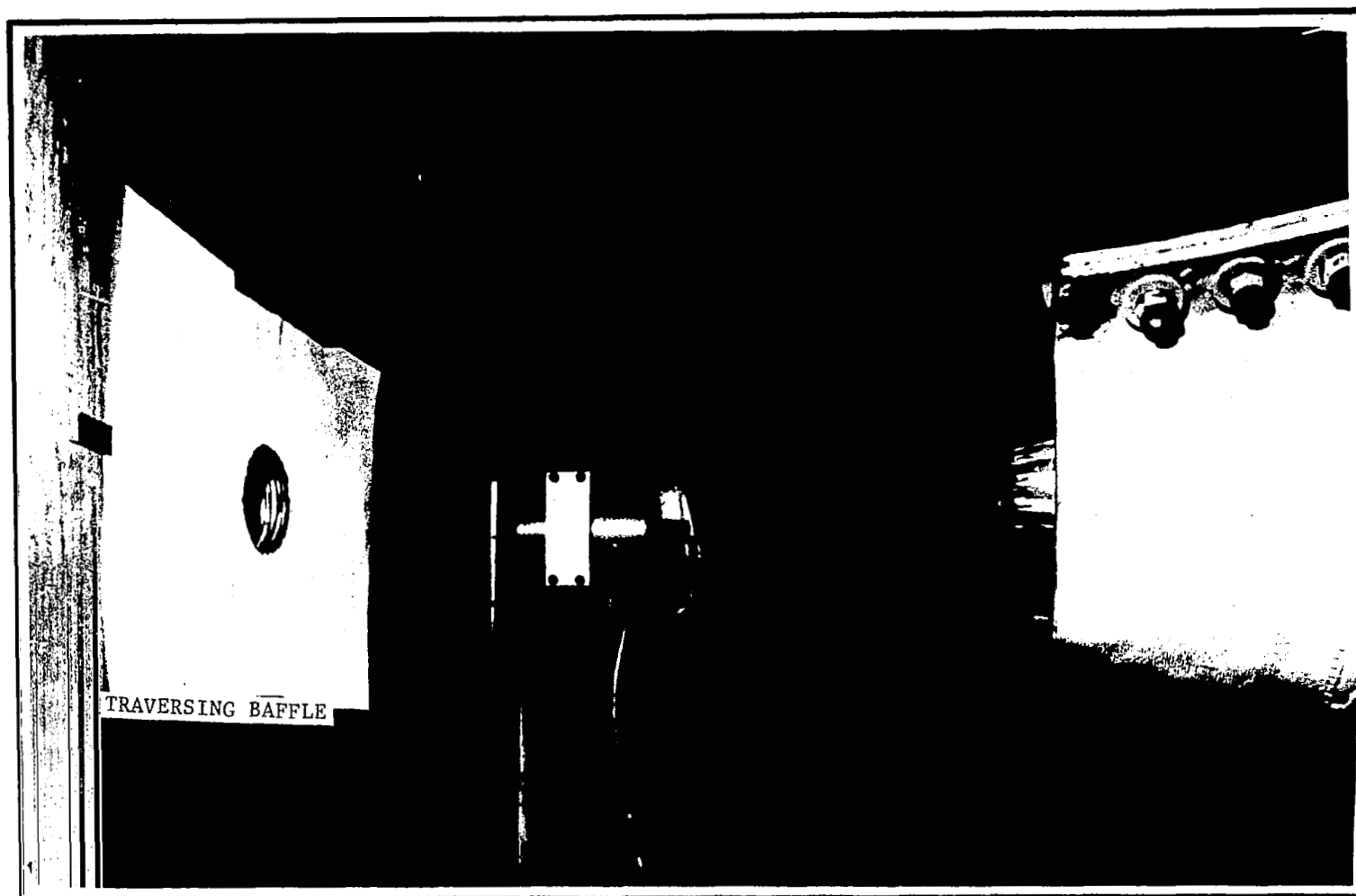


Figure 4.2 View of the baffle mounted on a traversing frame.  
(Only the inner nozzle used for the present  
experiments.)



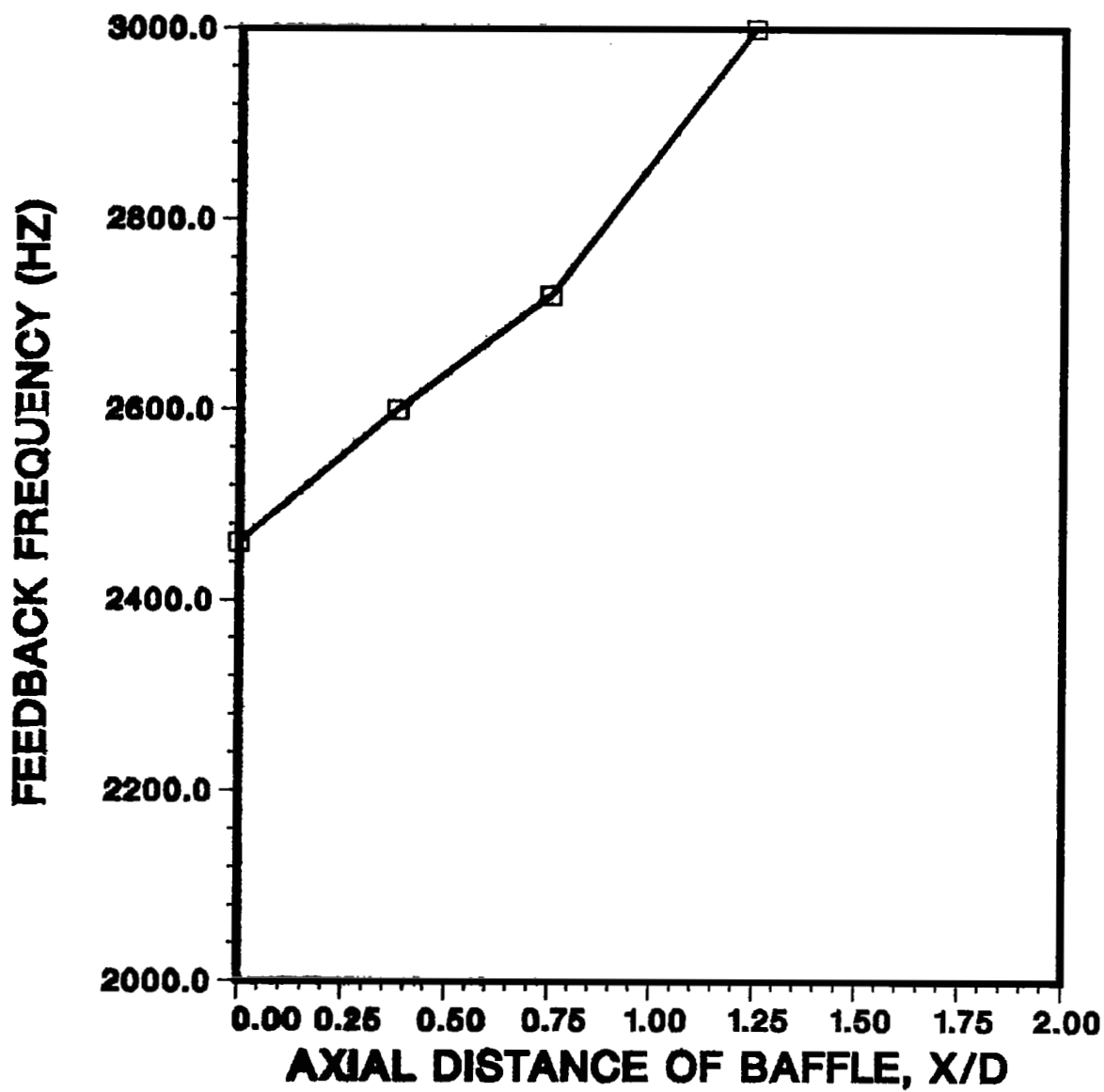


Figure 4.3 Increasing feedback frequencies with increasing axial distance of the baffle from the nozzle exit.  
(Jet operating pressure ratio = 2.95; baffle opening diameter = 5.72 cm)

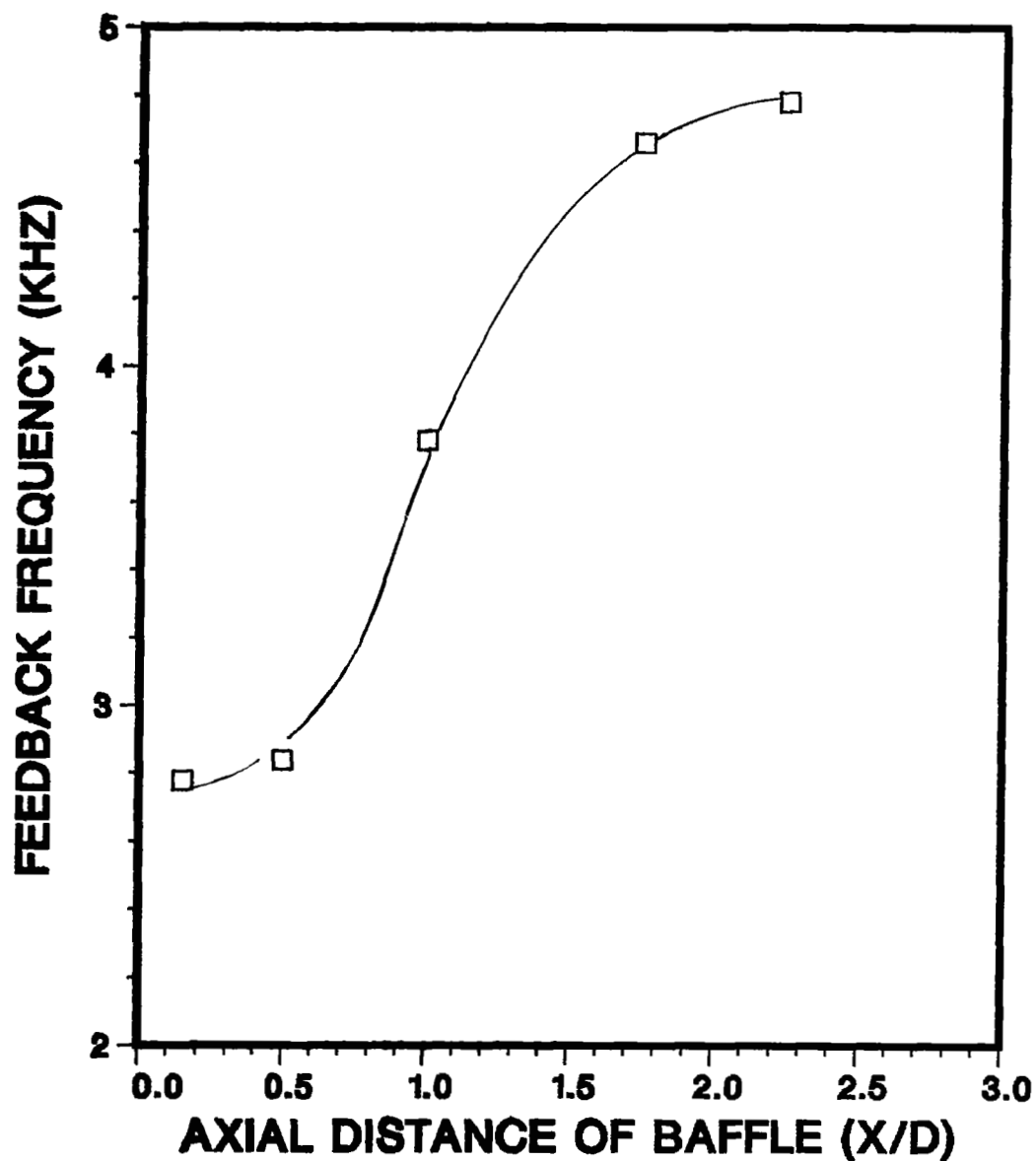


Figure 4.4 Increasing feedback frequencies with increasing axial distance of the baffle from the nozzle exit.  
(Jet operating pressure ratio = 2.51; baffle opening diameter = 5.72 cm)

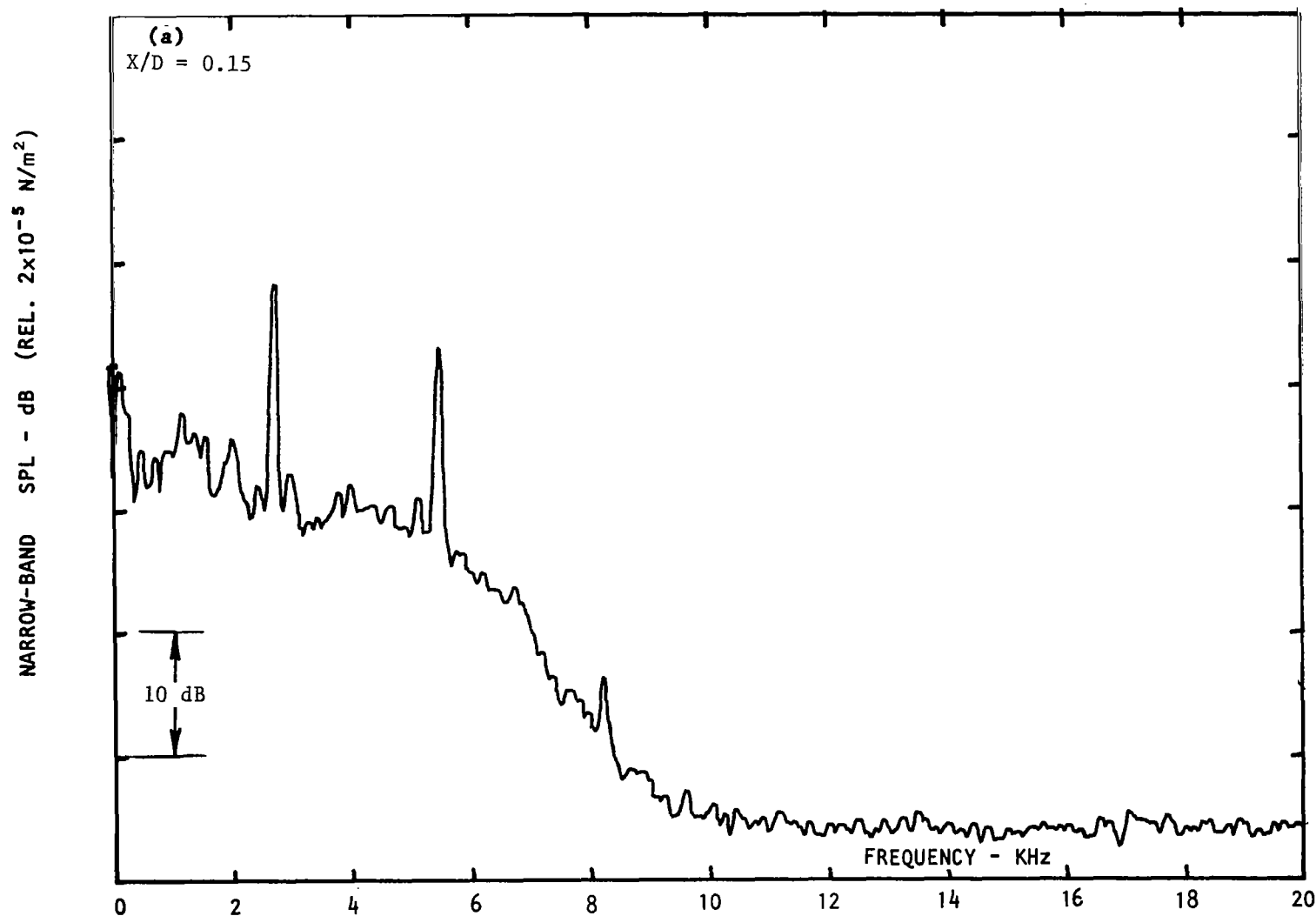


Figure 4.5 Noise spectra showing changes in the feedback frequencies as a function of the baffle location,  $X/D$ : (a) 0.15, (b) 0.5, (c) 1.0, (d) 1.5, (e) 1.75, (f) 1.875, (g) 2.0, and (h) 2.25.

(Jet operating pressure ratio = 2.51, baffle opening diameter = 5.72 cm)

(Continued on the next page)

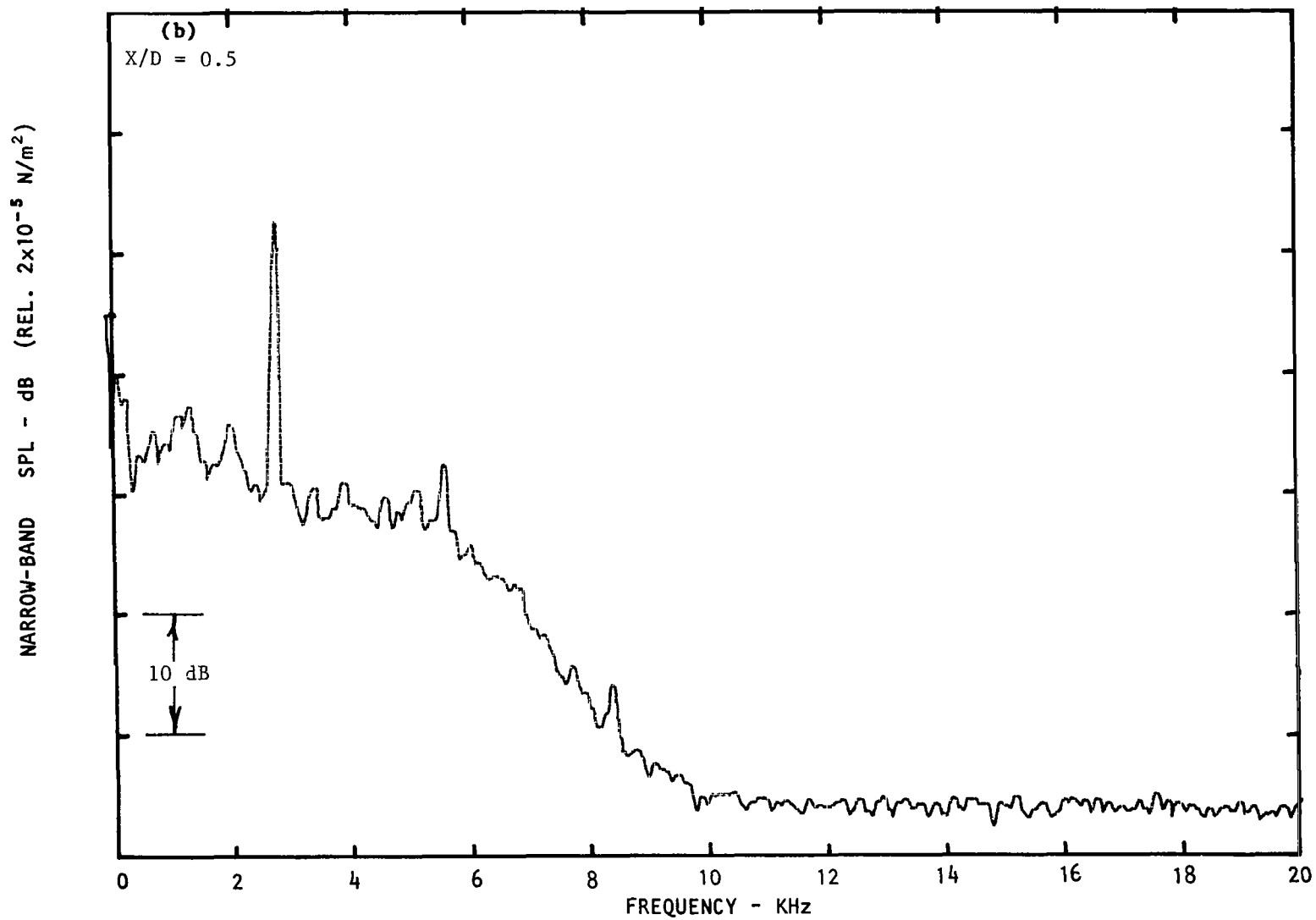


Figure 4.5 (Continued from the previous page)

(Continued on the next page)

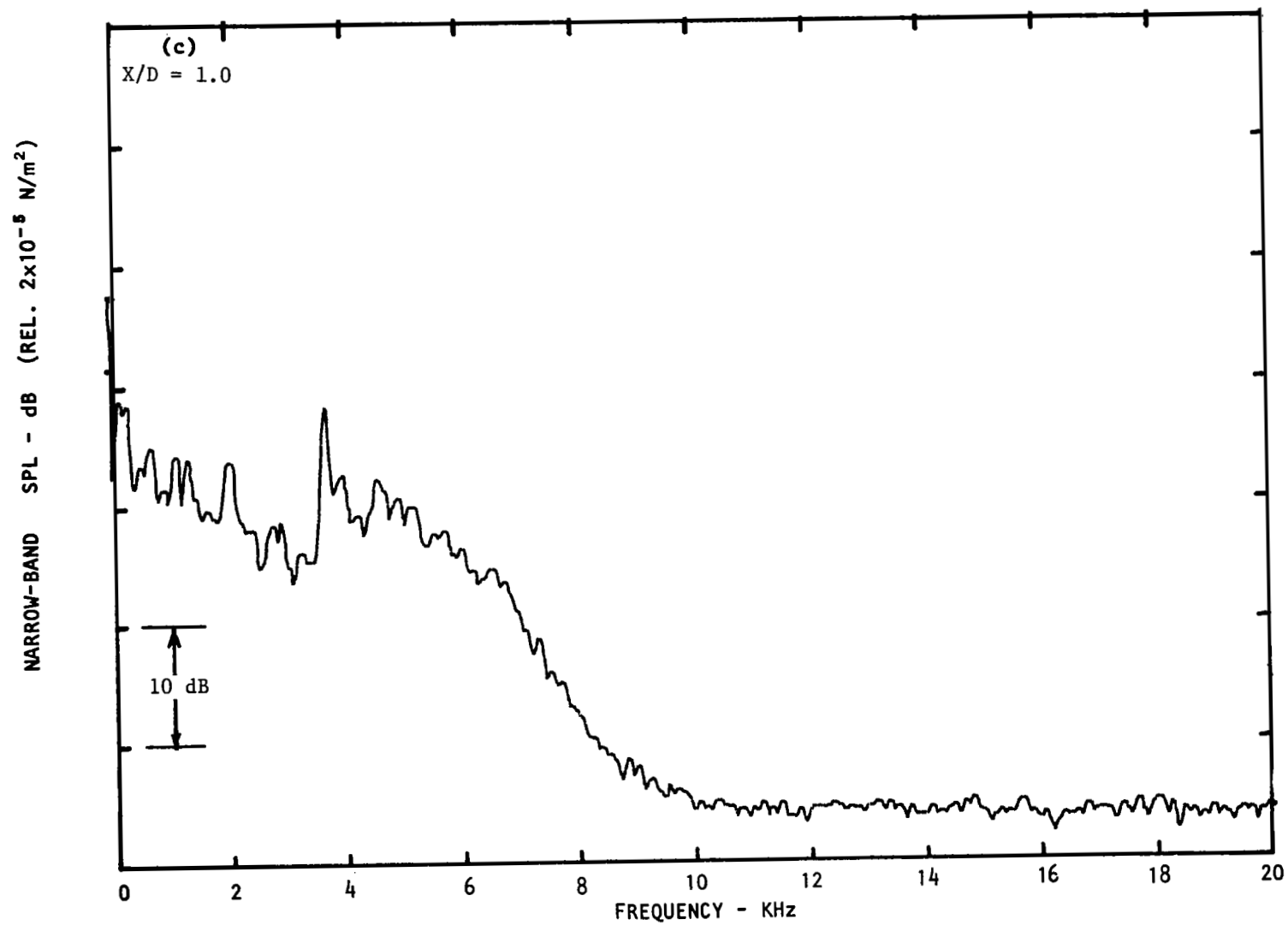


Figure 4.5 (Continued from the previous page)

(Continued on the next page)

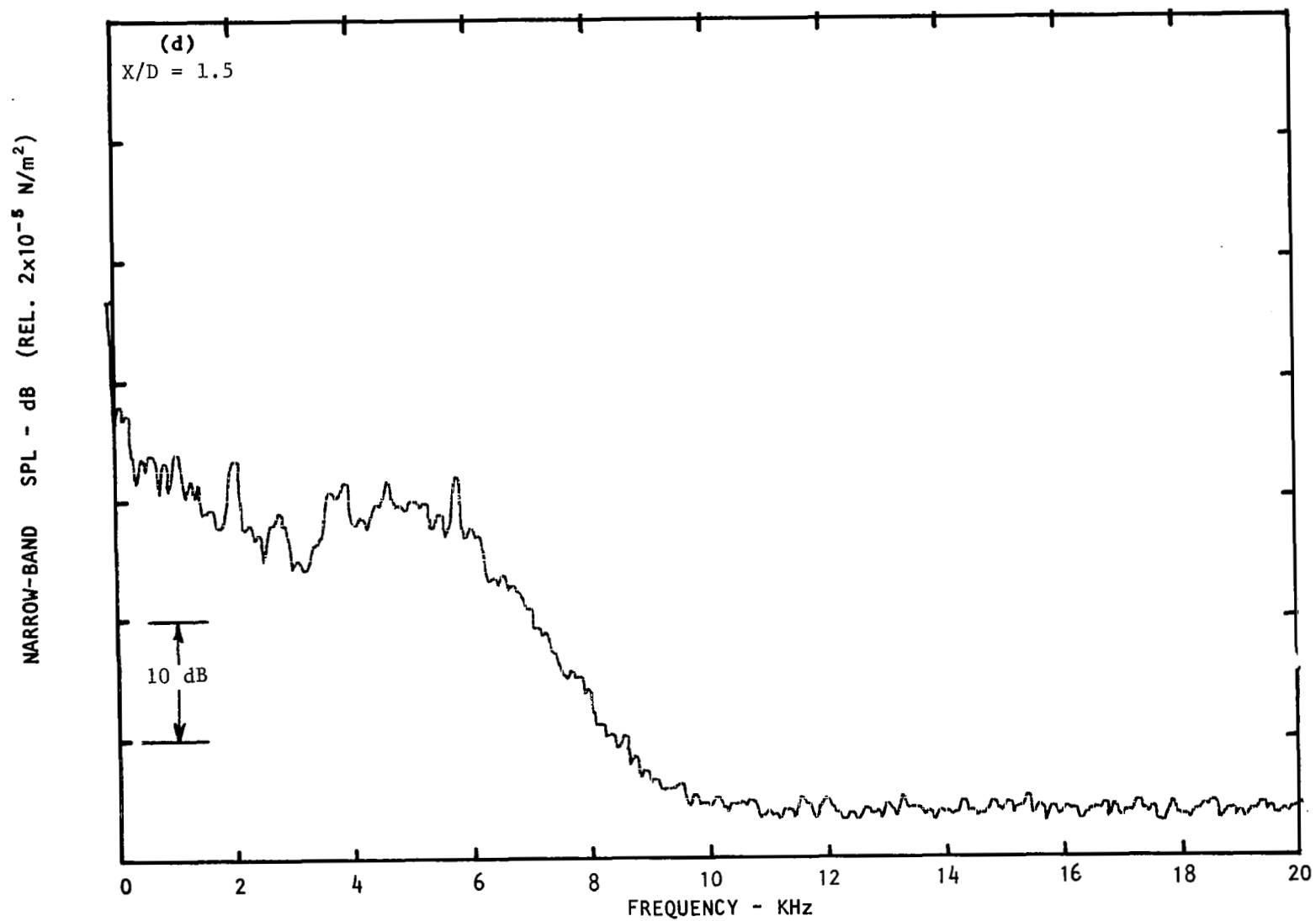


Figure 4.5 (Continued from the previous page)

(Continued on the next page)

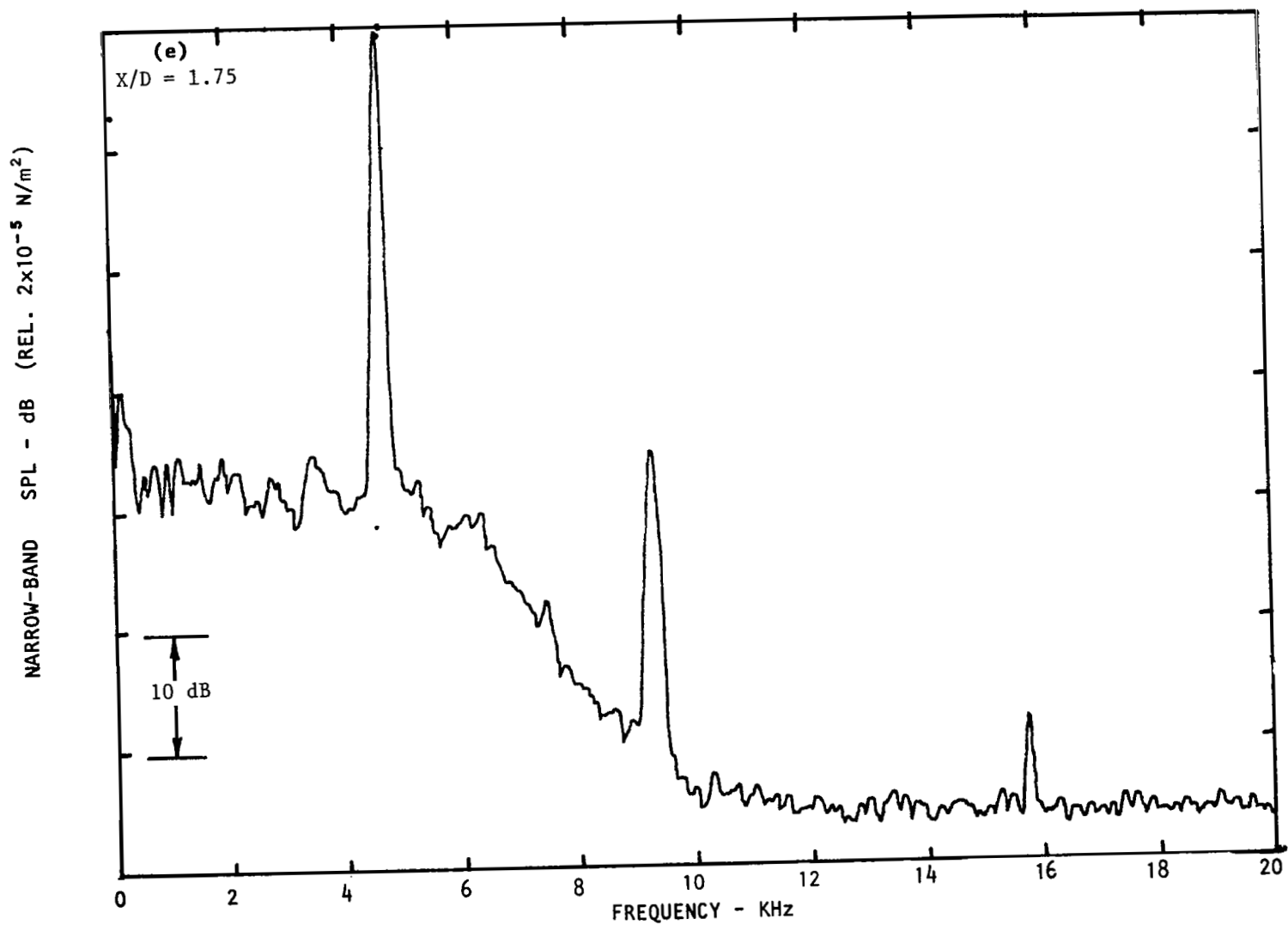


Figure 4.5 (Continued from the previous page)

(Continued on the next page)

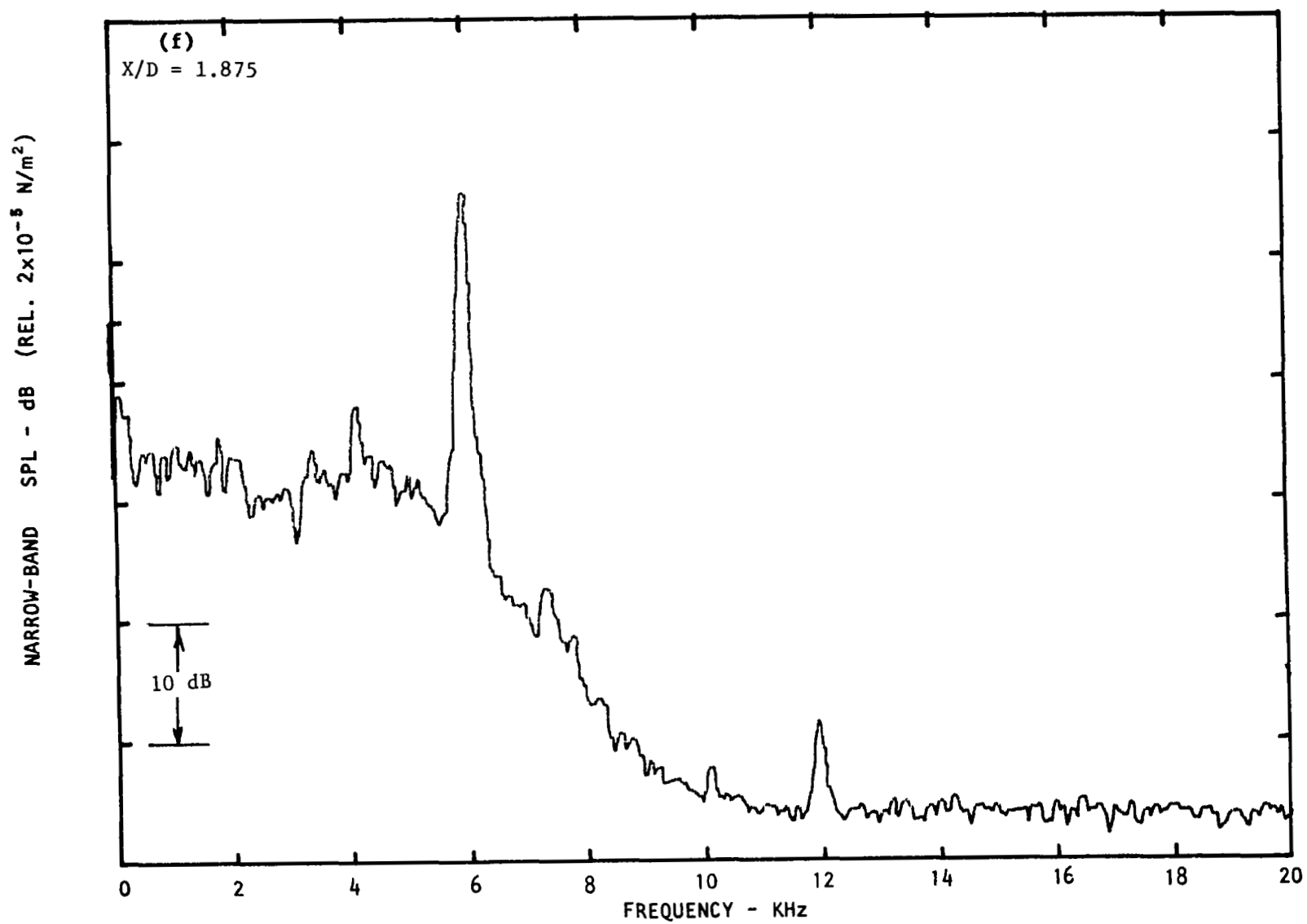


Figure 4.5 (Continued from the previous page)

(Continued on the next page)



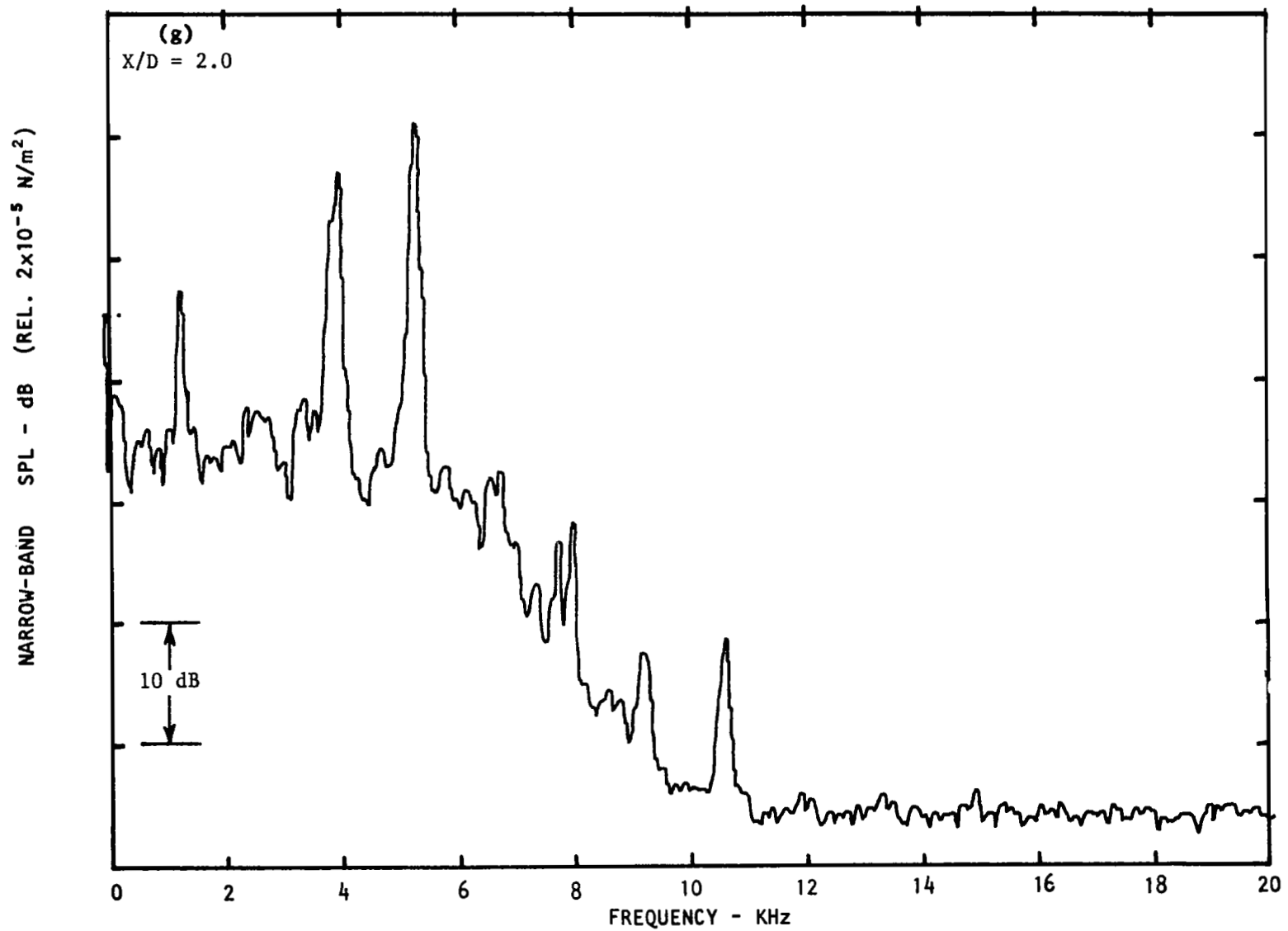


Figure 4.5 (Continued from the previous page)

(Continued on the next page)

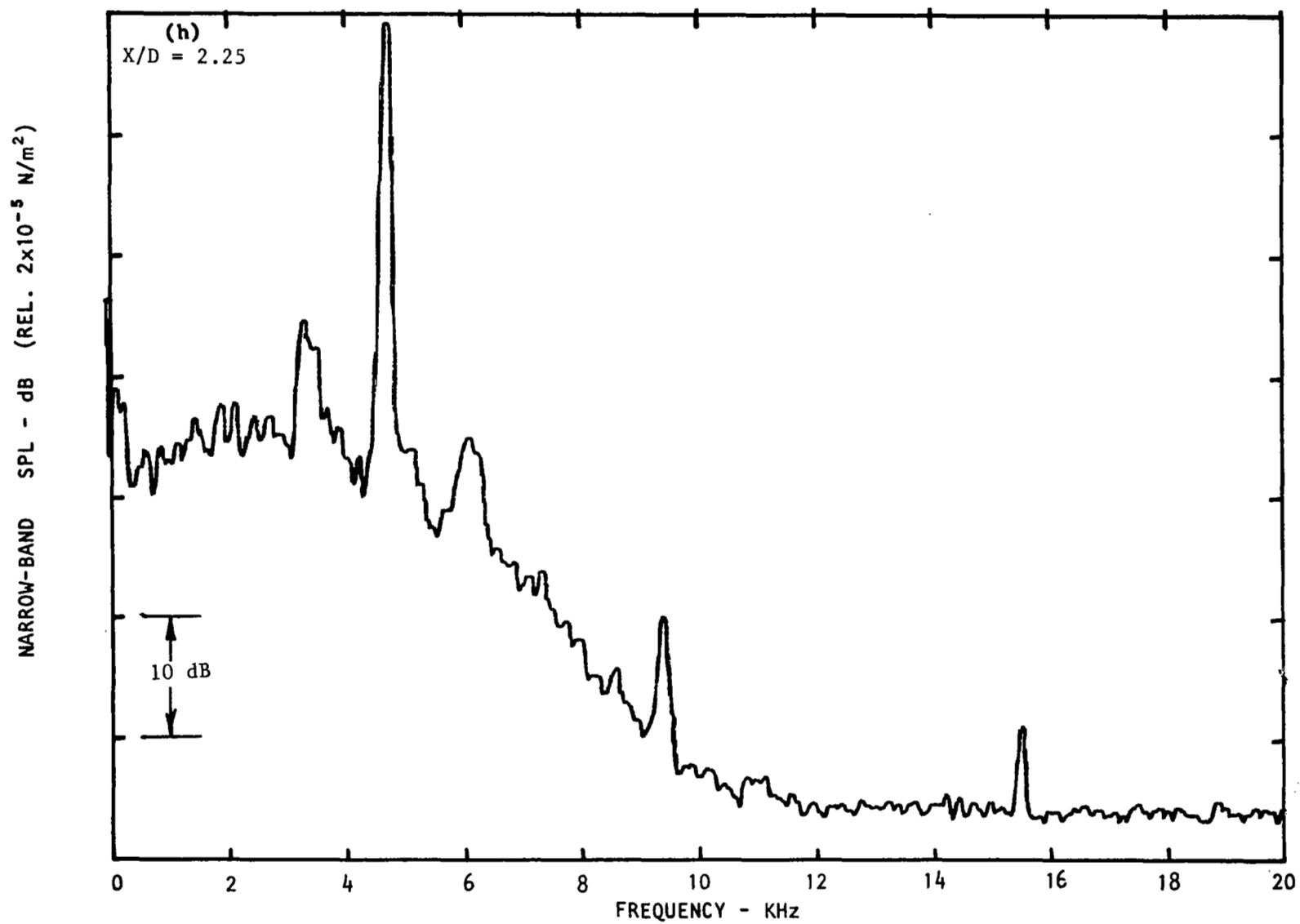


Figure 4.5 (Continued from the previous page)

(Last)

## 4.2 FLOW VISUALIZATION

### 4.2.1 Test Configuration

After having completed the pilot study in a facility that already had a built-in traversing frame, and having determined that this new exercise was worth pursuing further, a new traverse was designed for the optics facility (see figure 4.6). Since the shop air supply is used in this facility, a smaller diameter (1.27 cm (0.5 in)) jet was installed for these tests (see figure 4.7) to accommodate the high mass flow requirements of supersonic jets. Baffles with opening diameters of 1.905 cm (0.75 in), 2.54 cm (1.0 in), and 3.810 cm (1.5 in) were tested. A half circle baffle was also used for some of the tests described later. The baffle shown in figure 4.6 has an opening of 3.810-cm diameter. To test the baffle with other diameter openings, the orifice plates shown in figure 4.8 were mounted on the baffle shown in figure 4.6, by using the four bolt holes seen in the figure.

As seen below, these results still left a certain element of doubt about the certainty with which firm conclusions could be derived. Additional tests were, therefore, conducted by positioning an impingement plate downstream of the traversing baffle as shown in figure 4.9. This plate was in fact the 1.905-cm (0.75-in) diameter plate shown in figure 4.8. The purpose of this plate was to ensure that the noise for the feedback loop was being generated at a fixed point instead of possibly different locations for the other configurations tested for screeching jets. This plate is referred to as the "impingement plate" in the text below. The traversing baffle used for these tests was the one with a 2.54-cm (1.0-in) opening.

### 4.2.2 Parallel Microphone Measurements

For this test series, sound pressure levels were measured both upstream and downstream of the baffle, and the results similar to those observed from the pilot study were obtained. Large changes in the screech frequency were obtained in these tests also.

The signals from these microphones were used to trigger the laser strobe to freeze the excited large-scale structure in the jet that was coherent with the acoustic signal. And in order to visualize the frozen structure at various spatial locations, the changes in the strobing phase were achieved by simply traversing a microphone just outside the jet parallel to the axis of the jet.

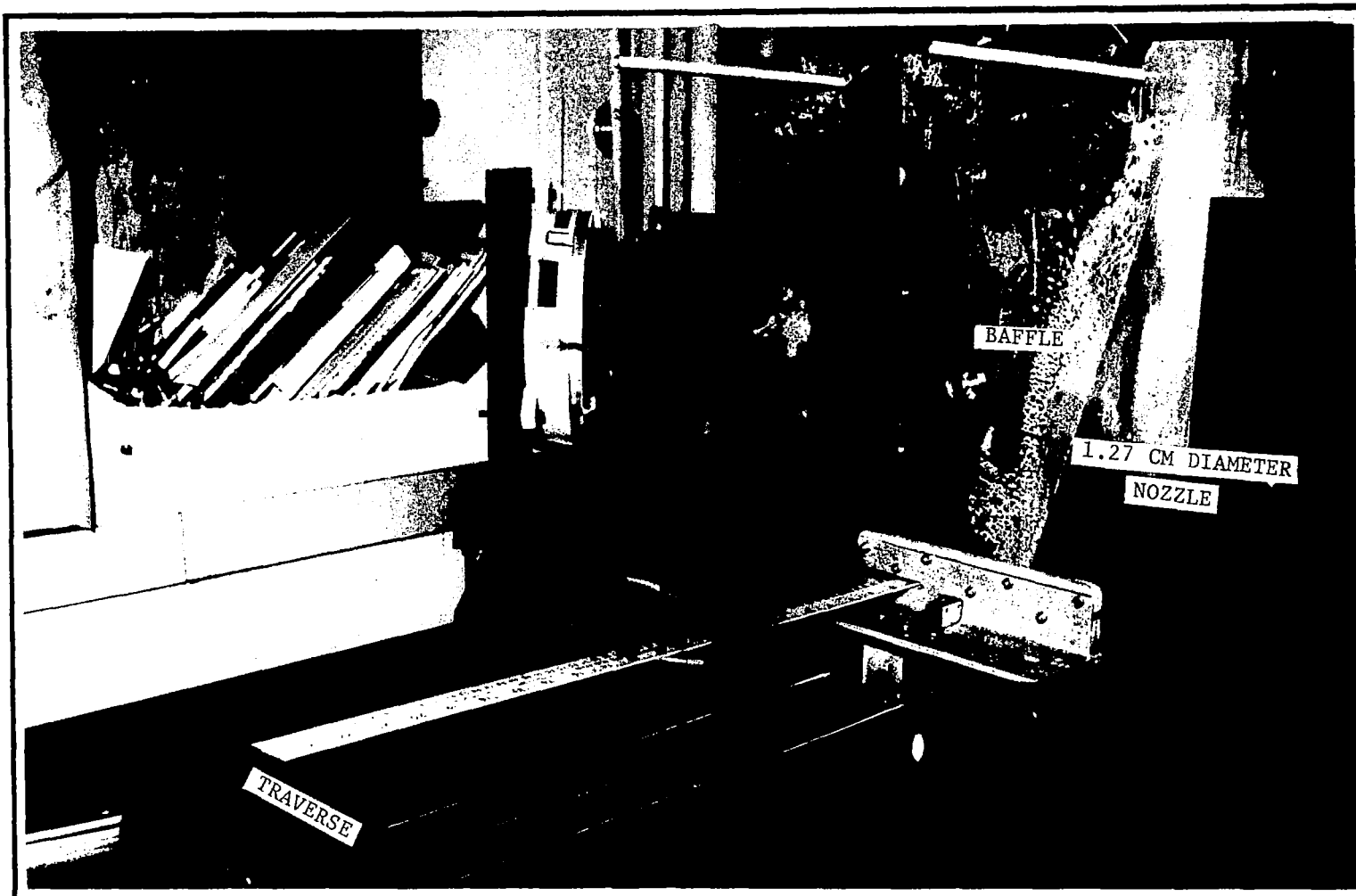


Figure 4.6 Traversing baffle arrangement in the optics facility.

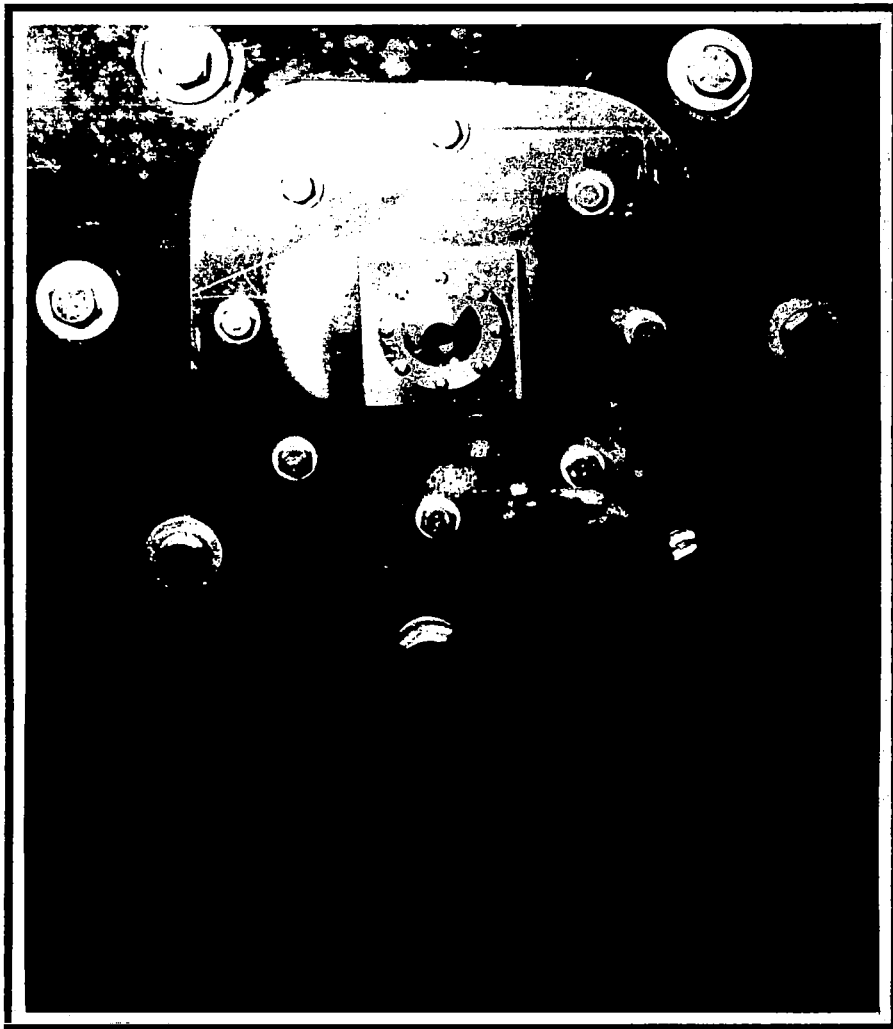
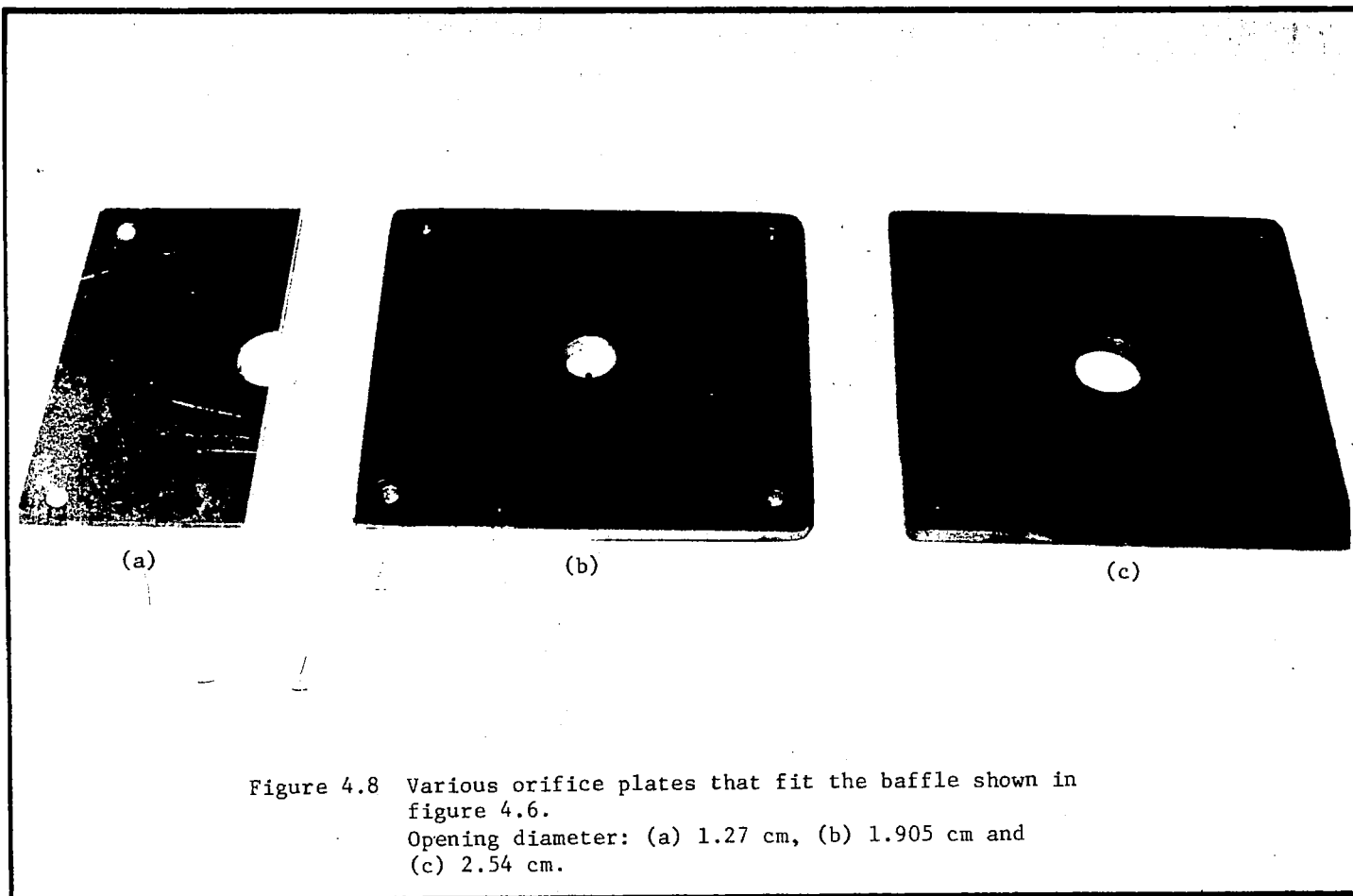


Figure 4.7 View of the 1.27 cm diameter nozzle upstream of the baffle.



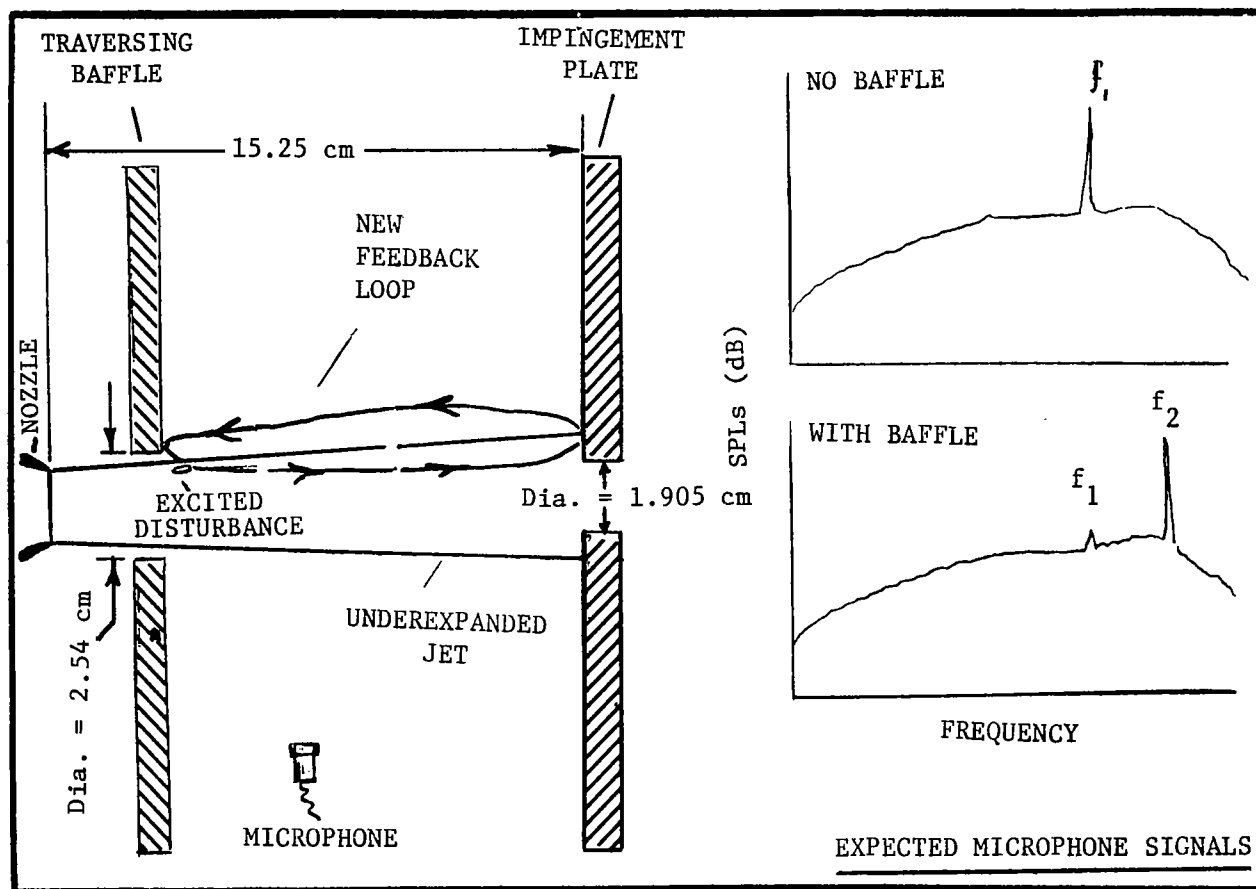


Figure 4.9 Configuration used for the impingement plate tests

(Frequency  $f_2$  produced through the new feedback loop and, if observed, should change with changing axial location of the baffle)

All of the flow visualization data presented here for the supersonic jet were taken with a vertical knife edge of the schlieren optics.

#### 4.2.3 Results

##### Feedback-Excited Instability Waves Identified in the Bare Jet First

Using the above-mentioned phase-averaging technique, the bare jet (i.e., without any baffles located downstream) at various supersonic conditions was visualized first. Once the operating jet pressure ratio exceeded a value of two, the instability waves were found to become extremely distinct. This is shown in figure 4.10. It was also found that as the pressure ratio was increased beyond a value of 2.4, the nature of the excited instability waves changed from planar to helical as seen in figure 4.10. Conditions corresponding to those of figure 4.10 (b) and (c) were then chosen for the tests with the baffle configurations. The corresponding pressure ratios were 2.197 and 2.62, respectively.

##### Drastic Changes Observed As a Function of the Baffle Location

Drastic changes were observed to take place in the jet as a function of baffle location. Typical results for the baffle with the 2.54-cm diameter opening are shown in figure 4.11. It was found that, at the lower pressure ratio of 2.197, a well defined planar instability wave structure vanished from the jet altogether by moving the baffle only by 0.16 cm (1/16 in). The nature of this instability wave at the higher pressure ratio appeared to change from helical to planar or part planar as a function of the baffle location as shown in figure 4.12. In fact, for the baffle with the 3.81-cm (1.5-in) center opening, the radial extent of the helical structure in the jet was found to increase considerably with respect to that obtained for the bare jet. This is shown in figure 4.13 for various arbitrary strobing phases. A closer inspection of these results shows that part of the structure is discontinuous indicating that there may be more than one continuous structure excited in the jet, possibly as a result of multiple feedback loops.

Similar results were obtained with the semi-circular baffle arrangement. Typical results for this arrangement are shown in figure 4.14 for two different axial locations of the baffle. Each column is for a given location of the baffle, and shows the ensemble-averaged flow structure for three



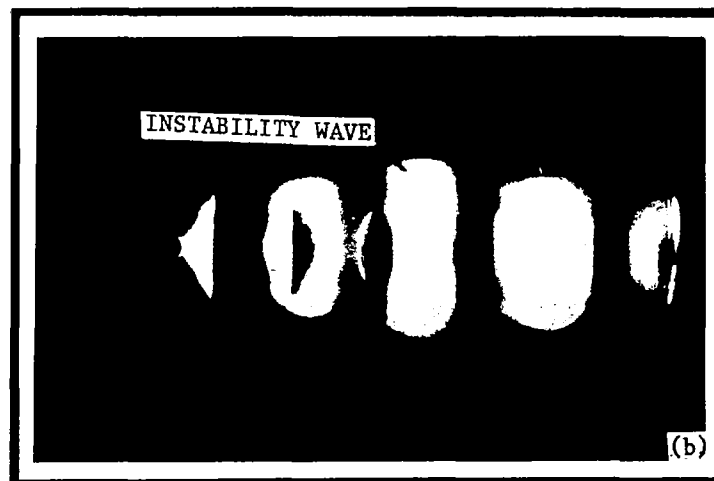


Figure 4.10 Ensemble averaged flow visualization of the supersonic jet at various pressure ratios, PR.  
 PR: (a) 2.035, (b) 2.197 and (c) 2.620.

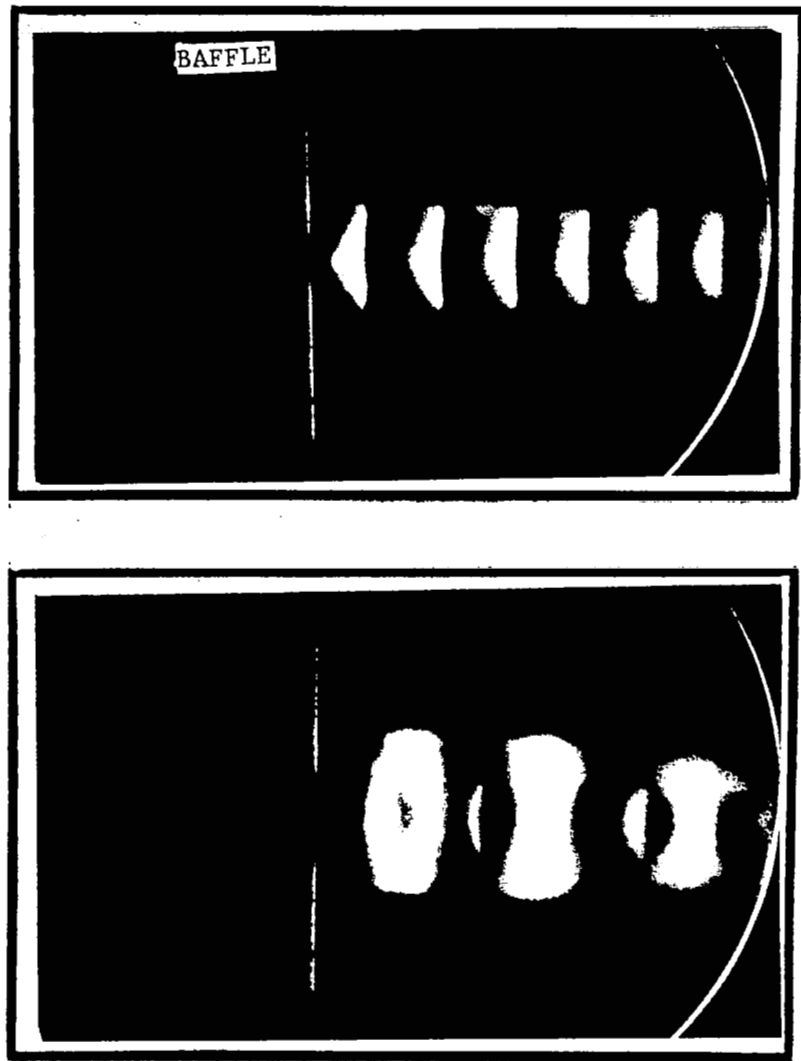


Figure 4.11 Changes produced in the jet flow structure by  
traversing the baffle by less than 0.16 cm (1/16 in).  
(PR = 2.197)

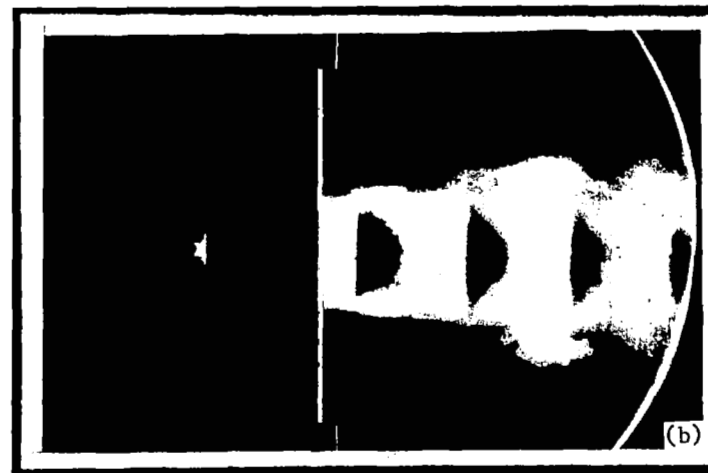
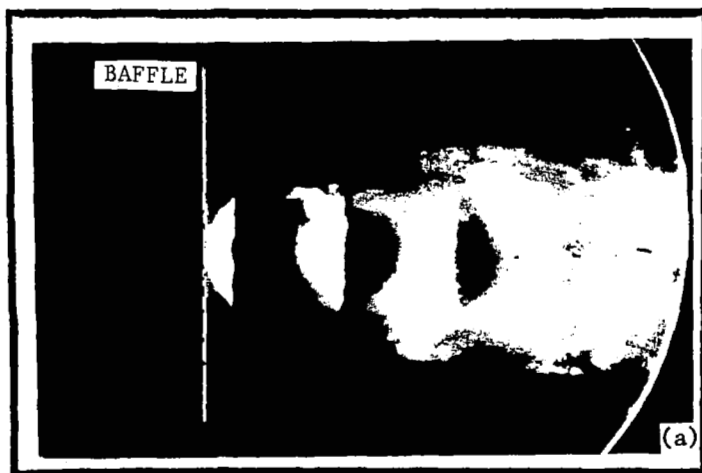


Figure 4.12 Changes in the nature of the instability weave, brought about by traversing the baffle, from (a) helical to (b) planar to (c) part helical and part planar. (Baffle opening diameter = 2.54 cm, PR = 2.69)

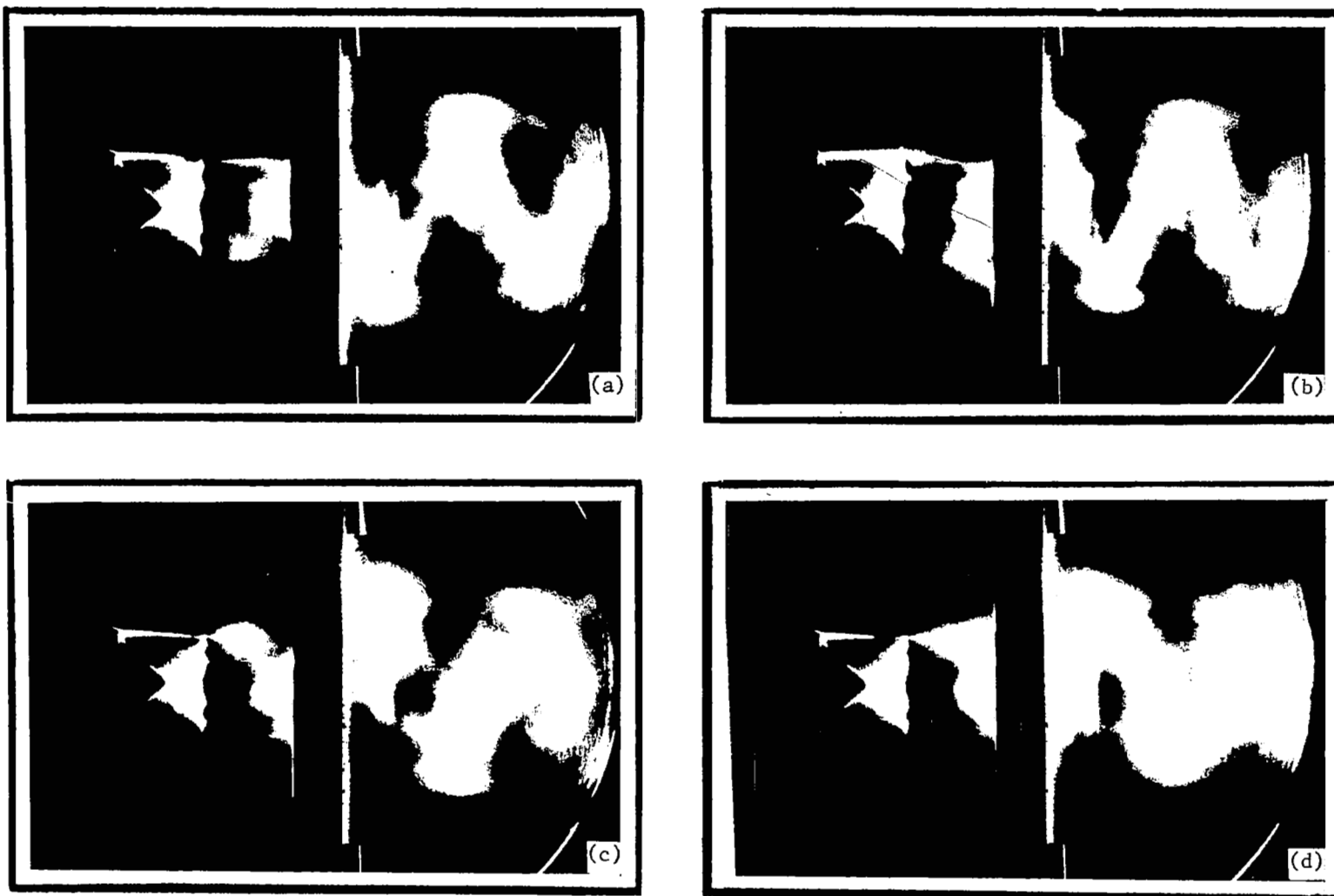
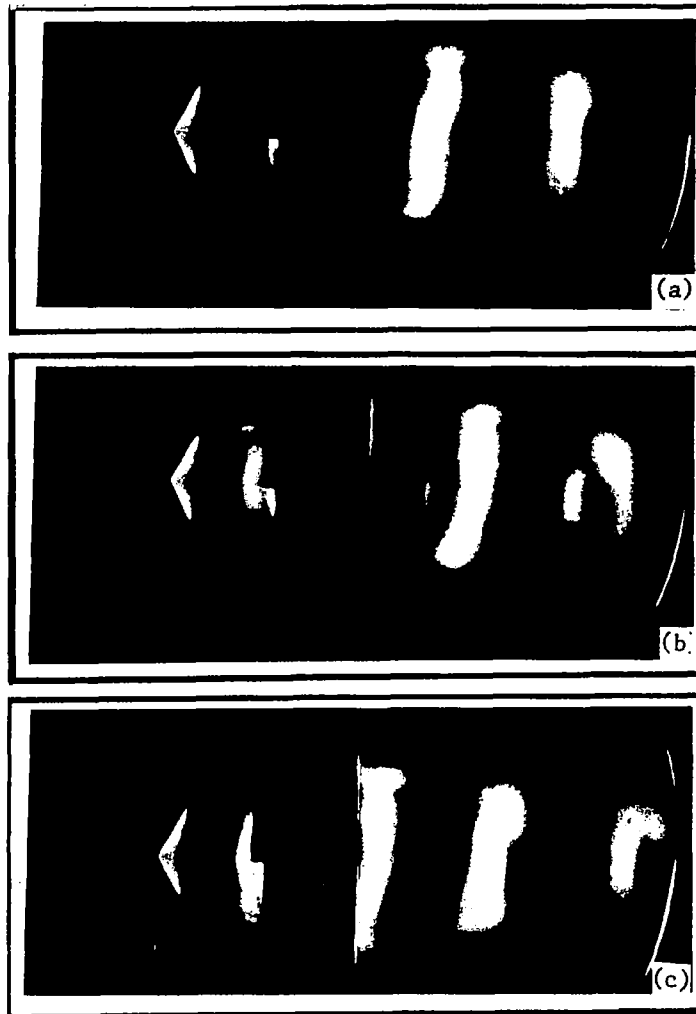


Figure 4.13 Instability wave at arbitrarily chosen different strobing phases (a thru d).

(Baffle diameter = 3.81 cm, PR = 2.549)

BAFFLE DISTANCE,  $X/D = 2.15$



BAFFLE DISTANCE,  $X/D = 2.58$

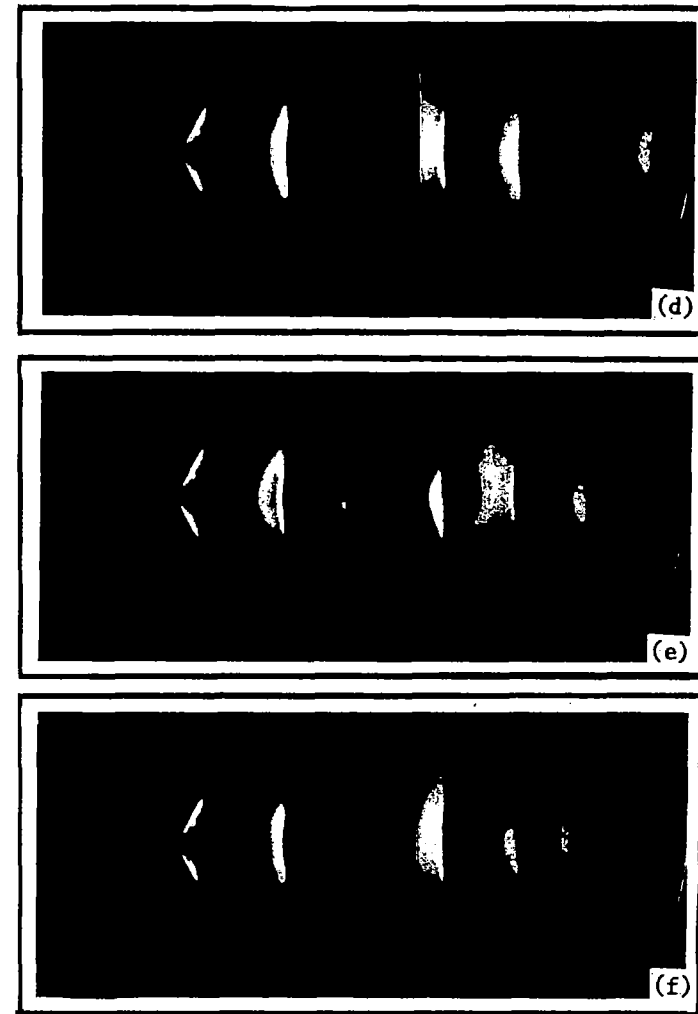


Figure 4.14 Instability waves for the semi-circular baffle for two axial locations of the baffle at different arbitrary strobing phases at  $PR = 2.197$ .

arbitrary strobing phases. The excited structure in the left column is much better defined than it is in the right hand side column. An additional important feature of the excited structure for this configuration is that the instability waves are tilted. This reflects the one-sided effect of the semi-circular baffle, close to which the feedback could be the strongest. At the higher pressure ratio, this baffle was also found to change the structure from planar to helical, or vice versa, as a function of the baffle location, as shown in figure 4.15.

#### Further Data Acquired with the Impingement Plate Located Downstream of the Baffle

Although the data presented above do indicate that the baffle positioned downstream of the nozzle exit had a strong influence on the behavior of the feedback instability wave, these data still suffered from the fact that it was not quite clear where the dominant feedback sound actually initiated. For this reason, further data were acquired with the impingement plate described above. With this configuration, it was known a priori that the feedback sound would, in all likelihood, initiate at the impingement plate. And a comparison between the measured and the calculated values of the feedback frequencies indeed indicated this to be true.

The flow visualization data for this configuration also showed that the feedback-excited instability waves were strongly affected by the presence of the baffle. As in the previous cases without an impingement plate, the nature of the excited instability waves was a function of the axial position of the baffle, as illustrated in figure 4.16. The spatial development of the instability wave corresponding to that seen in figure 4.16 (a) can be seen in figure 4.17 at various arbitrarily chosen strobing phases.

#### Acoustic Data Clears Confusion from the Flow Visualization Data

It should be noted that in almost all the flow visualization data presented above, it has not become clear if indeed the feedback instability wave is generated as a result of the receptivity near the baffle surface. This is because, when these waves are traced as a function of strobing phases, they still give the impression of originating near the nozzle exit, and somewhat upstream of the baffle for many cases. But an examination of the feedback frequencies measured by the microphones, however, indicates that the feedback loop length decreases as the baffle moves away from the nozzle exit. This was particularly so for the configuration with the impingement plate. The feedback frequencies for this configuration are plotted as a function of axial distance of the baffle from the nozzle exit plane in figure 4.18. Clearly, the feedback frequencies increase as the baffle is moved away from the nozzle exit, and

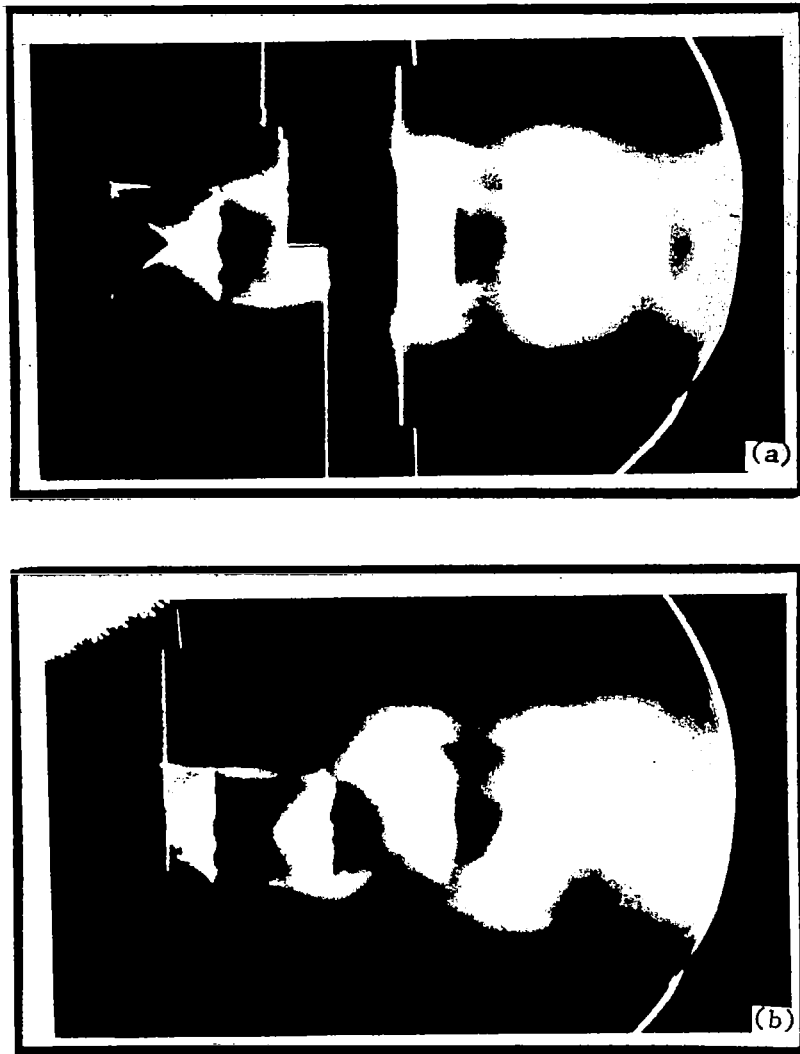


Figure 4.15 Changes in the modes of the instability waves as a function of the axial location of the semi-circular baffle  
(a) planar mode, (b) helical mode (PR = 2.549)

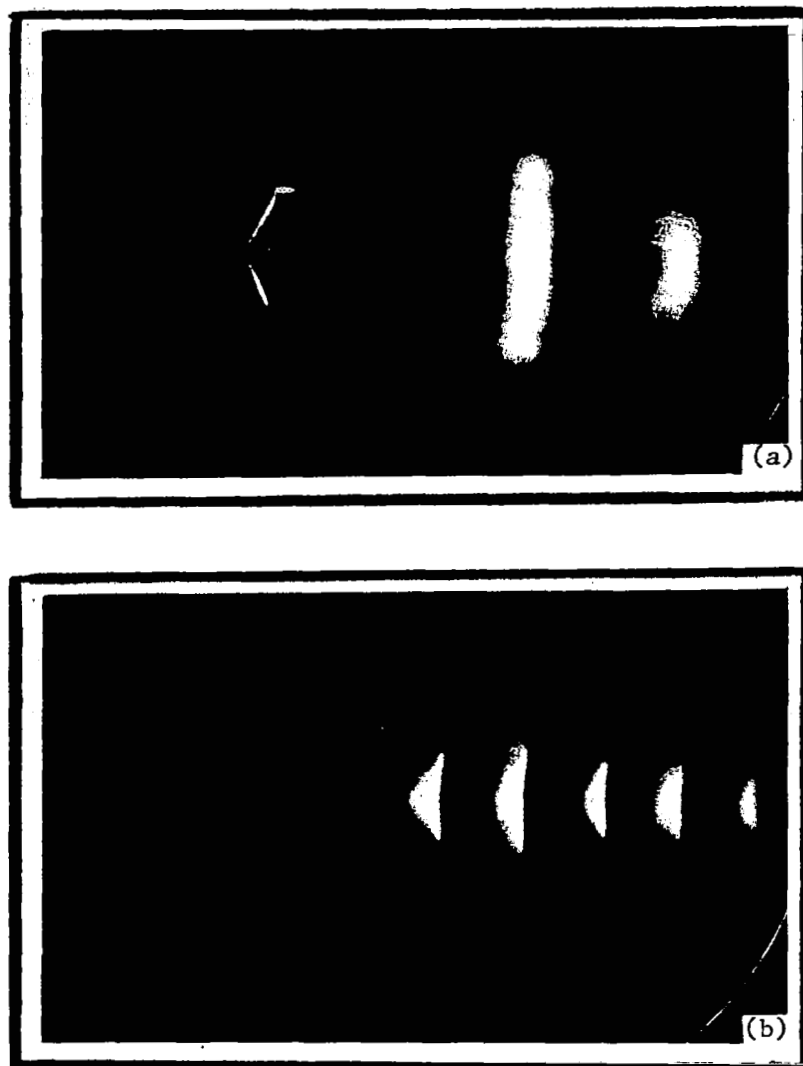


Figure 4.16 Effect of traversing the baffle with the impingement plate located 15.25 cm downstream of the nozzle lip.  
(PR = 2.197)



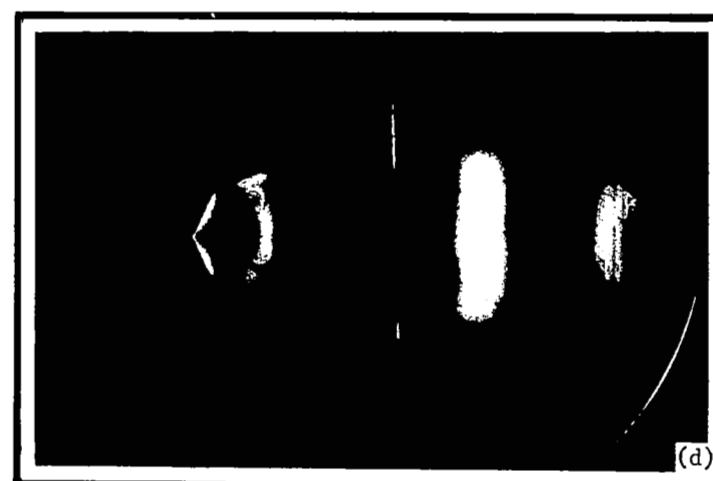
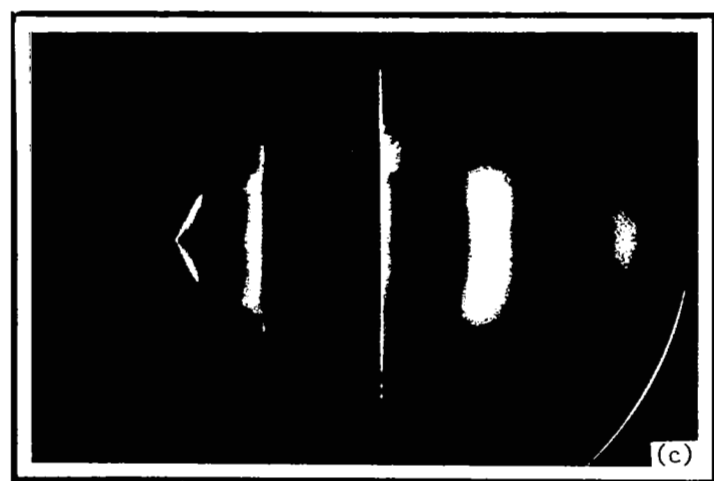
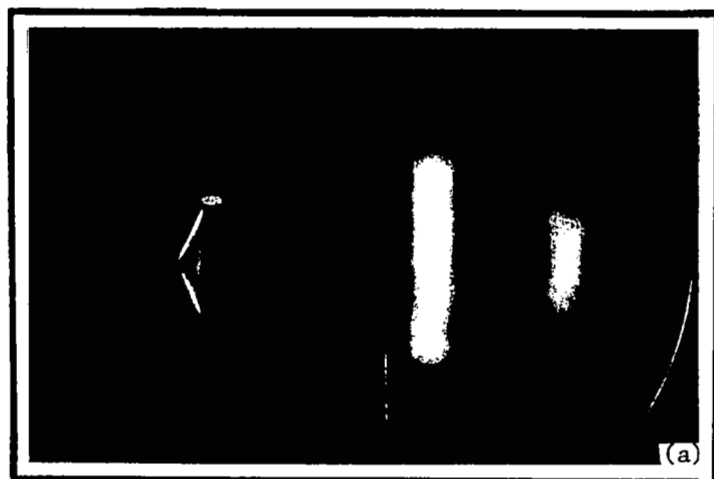


Figure 4.17 Spatial development of the instability wave corresponding to figure 4.16 (a) data. (each successive photograph taken at arbitrarily chosen different strobing phase)

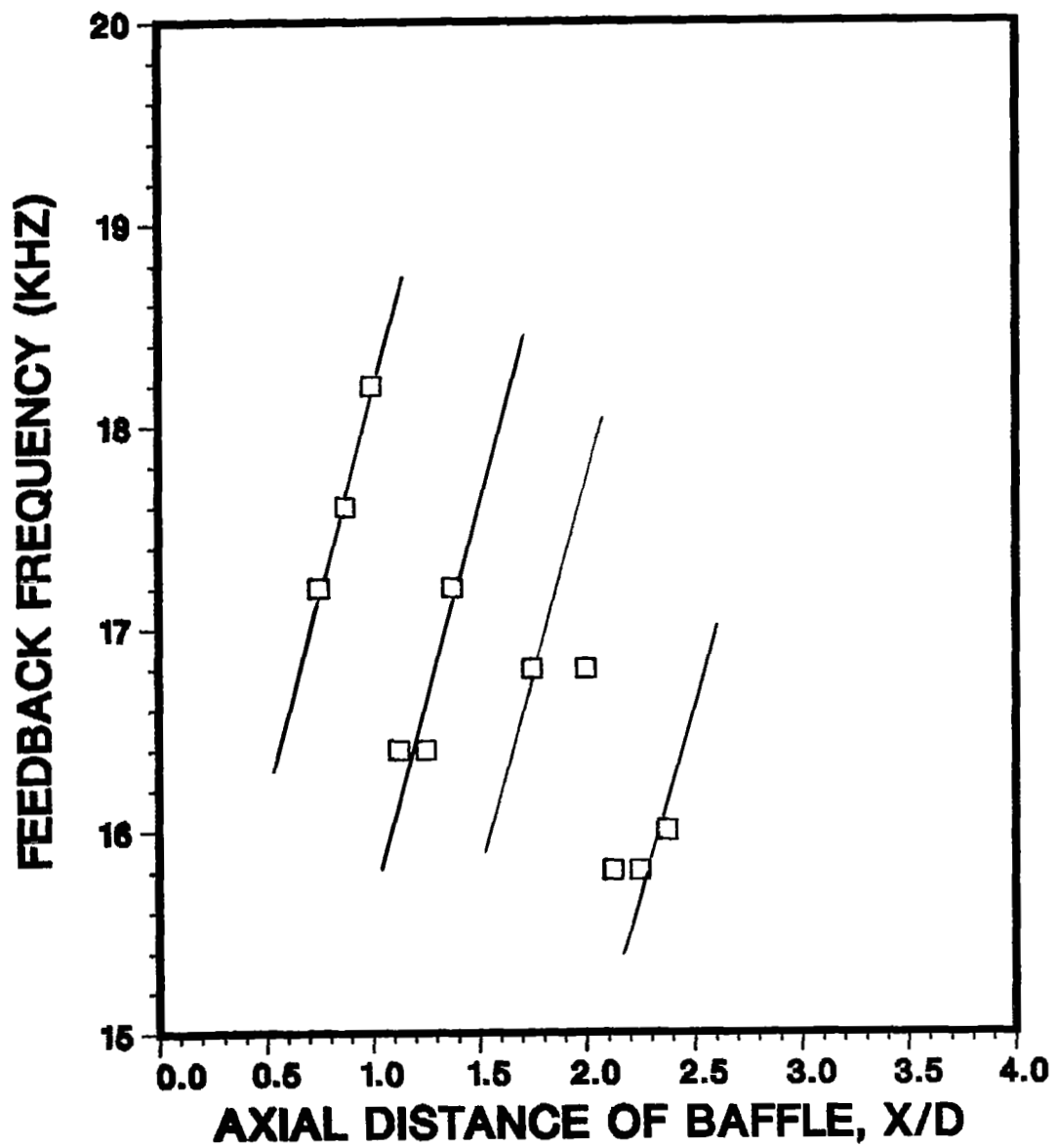


Figure 4.18 Increasing feedback frequencies with increasing distance between the baffle and the nozzle lip. (PR = 2.197)

they follow the multiple stage behavior typical of the feedback phenomenon.

If the changes in the feedback frequencies are being caused by the shifting of the local receptivity point, a valid reason must be found to explain why the instability waves still appear to originate from upstream of the baffle. It is possible that once the new feedback frequency sound is generated, it leaks through the annulus between the jet boundary and the baffle opening, and triggers large-scale structures at the exit at that frequency. Instability waves upstream and downstream of the baffle will then have the same wavelength and it will be difficult to distinguish them from each other. In addition, for those cases, where two frequencies were found to coexist, they were normally so large that the flow visualization would not be able to distinguish between the instability waves of one frequency from that of another, at least in the range of frequencies observed in the photographs presented above, because the difference in their wave length will be rather small. This is illustrated below.

For example, consider the case of the coexistence of two frequencies of 16 KHz and 18 KHz in the acoustic spectrum of the jet operated with a baffle and an impingement plate. The wave lengths for the conditions of figure 4.17 for the above two frequencies will be 1.34 and 1.19 cm, respectively. The difference in the wavelengths will thus be only 0.15 cm (0.06 in) which is considerably smaller than the thickness of each donut shaped large-scale structure visualized in the photographs presented here. Thus if the starting frequency without the baffle or the impingement plate is, 16 KHz, and after installing the baffle and/or the impingement plate, an additional frequency of 18 KHz is produced, then, even though the instability waves of two different frequencies have been excited, one at the nozzle lip and another at the baffle, it will be very difficult to distinguish them from the flow visualization data.

To make a real distinction between the two situations, further experiments should be conducted for larger diameter jets so that the screech frequencies of the bare jets will be rather low, whereas the frequency generated by the baffle-presence should be tuned to be as high as possible by suitably traversing the baffle. In this case, it may be possible to distinguish between the instability waves of two widely different frequencies.



## 5.0 CONCLUSIONS

### The Objective

The objective of this study was to show, by way of well controlled experiments, whether or not the coupling between a jet shear layer and sound incident upon it can be accomplished without the assistance of a trailing edge.

### Initial Results

The experiments required to accomplish the above-mentioned objective turned out to be extremely challenging, and at times very frustrating. The experiments were first performed using a 2.8-cm diameter round jet and also a planar jet with the sound source located outside the jet shear layer. In this configuration, it appeared as though the high frequency sound coupled closer to the jet exit much more efficiently than the low frequency sound which appeared to couple better at downstream distances. There was no categorical evidence, however, that this was indeed taking place because of the sound incident at regions of the shear layer downstream of the nozzle lip, or whether the sound reaching the nozzle exit itself was triggering the instabilities observed at downstream locations.

### Baffled-Jet Results

Further experiments were then conducted by attenuating the sound reaching the nozzle exit directly from the sound source by inserting barriers between it and the nozzle lip. Both the lead and aluminum barriers were tried. These barriers enabled the sound to be attenuated by more than 10 decibels. With this configuration also, it was found that the low frequency coupling appeared to take place at downstream distances. Nevertheless, since the levels of sound reaching the nozzle lip were always measurable, it made it very difficult to draw firm conclusions about the validity of the concept of the local receptivity.

### Screeching Supersonic Jet Results

After examining a plethora of flow-visualization data on instability waves

excited by the external sound source, it was decided that a different and novel experiment was needed to resolve the issue. At the suggestion of Professor C. K. W. Tam of Florida State University, it was decided to conduct tests on screeching supersonic jets by traversing a hard baffle, with an opening for the jet to pass through it, in the jet-flow direction.

The screech tones are known to result from the feedback loop consisting of sound arriving from a shock-cell at the nozzle lip and a feedback instability wave initiating at the lip by the sound and travelling down to the original source of sound to complete the feedback loop to start the process all over again. It was felt that if local receptivity has any merit, then a baffle located downstream of the nozzle lip may, for certain axial locations trigger instability waves close to its surface. If so, this should become evident by recording the screech frequencies, which will change as a result of the changes in the feedback loops. The advantage of this experiment was that, in this case even if some sound was leaking through the baffle opening to reach the nozzle lip, it would have a different feedback loop length and will have a different value for the recorded frequency. Thus, two or more frequencies could exist depending upon the locations of the receptivity regions of the jet shear layer. These effects were expected to produce even more positive results, if tested by letting the jet impinge on a plate located downstream of the traversing baffle, thereby fixing the distance of the sound producing source.

It was indeed found that the feedback frequencies changed drastically as a result of traversing the baffle axially. At times, more than one frequency were observed in the acoustic spectra for this configuration. For the majority of the test conditions, at least one of the measured screech tones was found to increase as the the baffle was moved downstream, indicating that the feedback loop length was decreasing. Flow visualization data showed that extremely well-defined large-scale structures were excited in the jet for those locations of the traverse that produced strong levels of the screech tone. However, such structures were not detected at all for some other locations of the baffle. In the latter case, the screech tones were also not detected. In addition, it was found that, for certain locations of the baffle, the nature of the large-scale structure changed from a planar to a helical mode.

These experiments certainly showed that unless valid reasons, other than local receptivity, are found to explain the observed results, one has to attribute the observed changes to the local receptivity as reasoned at the beginning of section 4.0.

## APPENDIX I - TERMINOLOGY

"Instability Wave" and "Large-Scale Structure" used interchangeably

$D_j$	Nozzle Diameter
$f$	Frequency
$f_e$	Excitation Frequency
$L_e$	Excitation Sound Pressure Level Measured at the Nozzle Exit
$L_s$	Excitation Sound Pressure Level Measured Just Beneath the Point Sound Source
PR	Pressure Ratio
$R_j$	Nozzle Radius
$r$	Radial Distance
SPL	Sound Pressure Level
$U$	Jet Exit Velocity
$u$	Local Velocity
$X$	Axial Distance
$\phi$	Phase Between the Acoustic Signal and the Timing of the Light Strobing

## REFERENCES

1. M. V. MORKOVIN 1969 Air Force Flight Dynamics Laboratory Technical Report AFFDL-TR-68-149. Critical evaluation of transition from laminar to turbulent shear layers with emphasis on hypersonically travelling bodies.
2. M. E. GOLDSTEIN 1981 *Journal of Fluid Mechanics*, Vol 104, 217-246. The coupling between flow instabilities and incident disturbances at a leading edge.
3. E. RESHOTKO 1976 *Annual Review of Fluid Mechanics*, Vol 8, 311-349. Boundary layer stability and transition.
4. P. J. SHAPIRO 1977 *Acoustics and Vibration Laboratory Report* No. 83458-83560-1, M.I.T.
5. C.K.W. TAM 1981 *Journal of Fluid Mechanics*, Vol 109, 483-501. The excitation of Tollmien-Schlichting waves in low subsonic boundary layers by free-stream sound waves.
6. J. W. MURDOCK 1980 *Proceedings of Royal Society of London*, Vol A372, 517-534. The generation of a Tollmien-Schlichting wave by a sound wave.
7. D. S. JONES and J. D. MORGAN 1972 *Proceedings of the Cambridge Philosophical Society*, Vol 72, 465-488. The instability of a vortex sheet on a subsonic stream under acoustic radiation.
8. D. G. CRIGHTON and F. G. LEPPINGTON 1974 *Journal of Fluid Mechanics*, Vol 64, 393-414. Radiation properties of the semi-infinite vortex sheet.
9. R. M. MUNT 1977 *Journal of Fluid Mechanics*, Vol 83, 609-640. The interaction of sound with a subsonic jet issuing from a semi-infinite cylindrical pipe.
10. C.K.W. TAM 1978 *Journal of Fluid Mechanics*, Vol 89, 357-371. Excitation of instability waves in a two dimensional shear layer by sound.



11. C.K.W. TAM and P.J.W. BLOCK 1978 *Journal of Fluid Mechanics*, Vol 89, 373-399. On the tones and pressure oscillations induced by flow over rectangular cavities.
12. S. W. RIENSTRA 1979 Ph. D. Thesis, Technische Hogenschool, Eindhoven Edge influence on the response of shear layers to acoustic forcing.
13. M. S. HOWE 1979 *Journal of Fluid Mechanics*, Vol 91, 209-229. Attenuation of sound in a low Mach number nozzle flow.
14. C.K.W. TAM 1979 IUTAM/ICA/AIAA-Symposium, Gottingen, 39-47. The effects of upstream tones on the large scale instability waves and noise of jets.
15. H. SCHLICHTING 1968 *Boundary Layer Theory*, New York: McGraw Hill, Inc.
16. K. K. AHUJA and C.K.W. TAM 1982 *Journal of Sound and Vibration*, Vol 83, 433-439. A note on the coupling between flow instabilities and incident sound.
17. M. C. WHIFFEN and K. K. AHUJA 1983 *Journal of Sound and Vibration*, Vol 86, 99-105. An improved schlieren system and some new results on acoustically excited jets.
18. K. K. AHUJA, J. LEPICOVSKY, C.K.W. TAM, P. J. MORRIS and R. H. Burrin 1982 *NASA-CR-3538*. Final Contract Report Submitted to NASA Lewis Research Center, Cleveland, Ohio. Tone excited jet - theory and experiments.
19. C. J. MOORE 1977 *Journal of Fluid Mechanics*, Vol 80, 321-367. The role of shear-layer instability waves in jet exhaust noise.
20. Z. MAEKAWA 1968 *Applied Acoustics*, Vol 1, 157-173. Noise reduction by screens.
21. J. LEPICOVSKY and K. K. AHUJA 1983, *American Institute of Aeronautics and Astronautics* Paper No. 83-0665. Some new results on edge-tone oscillations in high-speed subsonic jets.

1. Report No. NASA CR-3789		2. Government Accession No.		3. Recipient's Catalog No.	
4. Title and Subtitle Basic Experimental Study of the Coupling Between Flow Instabilities and Incident Sound				5. Report Date March 1984	
				6. Performing Organization Code	
7. Author(s)  K. K. Ahuja				8. Performing Organization Report No. LG83ER0137	
				10. Work Unit No.	
9. Performing Organization Name and Address Lockheed-Georgia Company Marietta, Georgia 30063				11. Contract or Grant No. NAS3-23286	
				13. Type of Report and Period Covered Contractor Report	
12. Sponsoring Agency Name and Address National Aeronautics and Space Administration Washington, D.C. 20546				14. Sponsoring Agency Code 505-31-3B (E-1896)	
15. Supplementary Notes Final report. Project Managers, Allen M. Karchmer and James R. Stone, Fluid Mechanics and Instrumentation Division, NASA Lewis Research Center, Cleveland, Ohio 44135.					
16. Abstract  The objective of the study described here is to determine whether or not a solid trailing edge is required to produce efficient coupling between sound and instability waves in a shear layer. The report starts out with a discussion on the differences found in the literature on the theoretical notions about receptivity, and a need to resolve them by way of well-planned experiments. Instability waves in the shear layer of a subsonic jet, excited by a point sound source located external to the jet, were first visualized using an ensemble averaging technique. Various means were adopted to shield the sound reaching the nozzle lip. It was found that the low frequency sound couples more efficiently at distances downstream of the nozzle. To substantiate the findings further, a supersonic screeching jet was tested such that it passed through a small opening in a baffle placed parallel to the exit plane. The measured feedback or screech frequencies and also the excited flow disturbances were found to change drastically on traversing the baffle axially. As argued in the report, this provided strong indication that a trailing edge is not necessary for efficient coupling between sound and flow.					
17. Key Words (Suggested by Author(s)) Flow-acoustic coupling; Receptivity; Jet excitation; Instability waves; Large-scale turbulence; Screech; Feedback phenomenon; Flow visualization; Separation control				18. Distribution Statement Unclassified - unlimited STAR Category 71	
19. Security Classif. (of this report) Unclassified		20. Security Classif. (of this page) Unclassified		21. No. of pages 100	
				22. Price* A05	